8-17-2016

Sorption of Organic Cations to Aluminosilicate Clay Minerals and Soils

William C. Jolin
University of Connecticut, william.jolin@uconn.edu

Sorption of Organic Cations to Aluminosilicate Clay Minerals and Soils

William C Jolin, PhD

University of Connecticut, 2016

With the increasing number of emerging contaminants that are cationic at environmentally relevant pH, there is a need for robust experimental methods and predictive models for organic cation sorption coefficients (K_d). Column chromatography was evaluated as a method to obtain organic cation sorption isotherms for environmental solids. A comparison of Freundlich isotherm parameters revealed isotherm linearity or non-linearity was not significantly different between column chromatography and traditional batch experiments. Importantly, skewness (a metric of eluting peak symmetry) analysis of eluting peaks can establish isotherm linearity for non-heterocyclic amines; thereby enabling a less labor intensive means to generate the extensive datasets of linear K_d values.

Current predictive models fail to account for the differences in the abundance and affinity of inorganic exchange ions naturally balancing negatively charged sites on environmental solids. To better understand how organic cation sorption is influenced by inorganic exchange ions, sorption coefficients of ten cationic pharmaceuticals were determined for six homoionic forms of the aluminosilicate clay mineral, montmorillonite. Regular trends in compound sorption coefficients across the clays were consistent with competition expected from inorganic cation selectivity sequence. Such regular changes in competition suggested that a probe compound, such as phenyltrimethylammonium, could capture soil-to-soil variations in inorganic cations for the prediction of organic cation

sorption to soils and soil minerals. Structure-affinity relationships from a literature model (Droge and Goss, ES&T 2013) allowed for the establishment of structural scaling factors which could be used to extrapolate from phenyltrimethylammonium K_d values for soils to those of different compound.

The use of a probe compounds is only valid if organic cations interact with all sites on clay minerals in the same manner. However, charge sites on clay minerals vary in the order of water molecules surrounding the site and the area over which the charge is spread. To understand the how differences in clay site structure influence sorption, a number of specific structural moieties were investigated from the base structure of benzylamine. The ordered hydration and increased charge focus of sites within a clay interlayer caused for large differences in the sorption coefficients of organic cations with polar moieties. These interactions where exemplified by deviations in quantitative trends in sorption coefficients of complex cationic pharmaceuticals, making organic cation sorption to clay minerals a function of water molecule order and charge focus.

Sorption of Organic Cations to Aluminosilicate Clay Minerals and Soils

William C Jolin

B.S., University of Connecticut, **2012**

A Dissertation

Submitted in Partial Fulfillment of the

Requirements for the Degree of

Doctor of Philosophy

at the

University of Connecticut

2016

APPROVAL PAGE

Doctor of Philosophy Dissertation

Sorption of Organic Cations to Aluminosilicate Clay Minerals and Soils

Presented by

William C Jolin, B.S.

Major Advisor

_____

Allison A. MacKay

Associate Advisor

_____

Dharni Vasudevan

Associate Advisor

_____

Timothy Vadas

Associate Advisor

_____

Alexander Agrios

University of Connecticut
2016

Acknowledgements

First and foremost, I would like to thank Dr. Allison MacKay. Without her unwavering support and instruction, I would never have been able to finish my dissertation. Her patience and guidance undoubtedly improved me as a researcher, for that she has my deepest gratitude.

I would like to thank Dr. Timothy Vadas for his guidance throughout my career. Conversations with him have considerably helped shape my research.

I thank Dr. Dharni Vasudevan for her collaboration over the past several years. Her input helped develop my understanding of chemical and sorption phenomena. I would also like to thank the members of her lab at Bowdoin College. The research performed there greatly aided this work.

I would like to thank Dr. Alexander Agrios for serving on my committee and his valuable input towards my dissertation.

I thank my parents for their support and encouragement. Finally, I would like to thank Chelsee Parker for her care and support throughout graduate school.

Table of Contents

1.0 Background

1.1 Organic Cations

Organic compounds that are positively charged at environmentally relevant pH (i.e. pH 3-8) are being released into the environment at an increased rate from industrial, anthropogenic, and veterinary activities.[1-4] Example sources of these organic cations include wastewater effluent discharges, veterinary antibiotic use, and land application of municipal biosolids.[1-4] Diphenhydramine (antihistamine), amphetamine (stimulant), trimethoprim (antibiotic), along with numerous other positively charged pharmaceuticals have been detected in nanogram per liter concentrations in natural water systems in the U.S.[1] Even at these low concentrations, there is still an increasing concern of adverse ecological and human health effects, which are directly related to both exposures levels and bioavailability of the compounds.[5] A crucial element of bioavailability is the contaminants' fate after being discharged or released. However, a number of important fate controlling mechanisms of these emerging pollutants still require further investigation.

1.2 Environmental Fate

When introduced into the environment, organic cations a subject to numerous, chemical, biological, and physical processes. These processes can be divided into two main groups: processes which alter the compound structure directly and those which affect the transport of the compound.[6] Altering the compound structure by biological or chemical means, results in a new compound which can be both more or less harmful to ecosystems and humans.[6] The extent in which a compound is available to these processes is dependent on the second group of processes, the physical transport and transfer of the compound. Physical transfer is largely dependent on an

organic cations behavior between different phases, such as water-air exchange and water-solid exchange.[6] Since organic cations are generally polar, exchange between the air and water phase is limited making the partition between the aqueous and solid phase a major factor in the transport of organic cations.[6] The process in which an organic cation in retained into soils and soils minerals is referred to as sorption.

1.3 Environmental Transport

The transport of a chemical within the natural environment determines chemical exposure, therefore controlling the risk to humans and ecosystems.[6,7] The transport velocity of contaminants is mainly determined by the velocity of water by both surface and subsurface flows.[6] Therefore, a contaminant that is only in the aqueous phase has a transport velocity that equals that of the water it is dissolved in. However, when a contaminate sorbs to the stationary, solid phase the transport velocity is effectively zero, which slows overall transport velocities, known as retardation.[8] A retardation factor (R_f, dimensionless) is calculated assuming the portion of the overall chemical mass moving in the water phase will have the same velocity as water itself and the portion interacting with the solid has a velocity of zero. The velocity of the contaminant (μ_c) is then determined by velocity of water (μ_w) and the retardation factor:

$$\mu_c = \frac{\mu_w}{R_f} \tag{1.1}$$

Taking into account the mass of the solid and volume of water, the retardation factor can be calculated[8]:

$$R_f = 1 + \frac{\rho_b}{n} \times K_d \tag{1.2}$$

Where ρ_b is the bulk density of the solid (kg L^{-1}) and n is the porosity of the solid (dimensionless). The sorption coefficient (K_d, L kg^{-1}) is defined by the ratio of the concentration on the sorbed phase (C_s, mol kg^{-1}) and in the aqueous phase (C_w, M):

$$K_d = \frac{C_s}{C_w} \tag{1.3}$$

The sorption coefficient is therefore exceedingly important in determining the fate of an organic cation once it is released in the environment. However, .

1.4 Sorption Prediction

With the ever-increasing number of cationic compounds utilized in industrial and anthropogenic practices, a robust model to predict the sorption coefficients for organic cations is needed.[6] Established sorption models, developed for neutral nonpolar compounds (e.g. EPISUITE[9]), greatly underestimate sorption of ionic compounds because those models do not account for electrostatic interactions between the sorbate and charged sorbents.[5,10,11] Recently, there has been encouraging progress in the development of new predictive models for ionic compounds sorption using polyparameter and computational methods.[10,12-16]

In the case of cationic organic compounds, empirical sorption models using molar volume and amine charge area contributions show promise for predicting sorption coefficients of non-heterocyclic amines of the form CxHyN to aluminosilicate clay minerals, organic matter, and soils.[10,12,13] However, cationic amine compounds with more complex structures require the use of corrective increments, derived from small sets of compounds sharing similar substructures (*e.g.*, aromatic rings, -Cl). Sorption of structurally complex cations can be described using molecular dynamics models that explicitly account for van der Waals and electrostatic energies of interaction between the sorbate and surface.[15] However, advanced computational tools are specialized and not widely available to practitioners. In the absence of comprehensive sorption

models for organic cations, there is a need for a robust, time-efficient technique to provide sorption isotherms for ionic contaminants of interest and to generate extensive datasets for predictive model development.[5,11,17,18]

1.5 Sorption Measurements

Currently, both batch and pulse input column techniques are used to determine equilibrium sorption coefficients (K_d) of ionic organic compounds. Batch experiments involve the mixing of sorbent and aqueous compound in a container, with K_d calculated from the removal of compound from the aqueous phase.[19] Batch experiments are simple, but can be time consuming and labor intensive to obtain replicates among large data sets. Column chromatography measures K_d using the difference of temporal first moments between compound and a non-retained tracer flowing through sorbent/SiC mixture packed column.[20] This technique employs a shorter column than its groundwater transport simulation counterpart, where the sorbent of interest is diluted in an inert substance and break through occurs quickly (minutes). Column chromatography experiments are more complex, generally requiring more extensive statistical analyses and careful packing of the column materials, but can be more time efficient. The differences in between these methods of K_d calculation and experimental set-up cause for concern when inter-comparing values obtained by opposing methods. Therefore, column chromatography must be validated as a method to obtain sorption isotherms of organic cations before it used to collect extensive data sets of organic cation sorption coefficients.

1.6 Sorption Isotherms

The ratio of sorbed concentration (C_s) to aqueous concentration (C_w) is not constant across different initial concentrations. Plots of the equilibrium relationships of organic cation concentrations on the solid and in the aqueous phase are known as sorption isotherms. Sorption

isotherms of organic cations to aluminosilicate minerals, organic matter, and soils are commonly non-linear.[13,21] Organic cation isotherms plateau when sorbed concentrations reach the full coverage of the CEC of the clay mineral, creating an "S" shaped isotherm. The Langmuir-Freundlich isotherm fit can be used to quantify isotherms that have sorbed concentrations up to or near the CEC the soil or clay mineral:[21]

$$C_s = \frac{C_{s,max}(K_{LF}C_w)^h}{1 + (K_{LF}C_w)^h} \quad (1.4)$$

Where $C_{s,max}$ is assumed to be the cation exchange capacity (CEC) of the clay, K_{LF} is the sorbate affinity, and the *h* reflects isotherm non-linearity, where h > 1 indicates convex isotherms and h < 1, concave relative to the x axis. When surface coverage does not exceed 10% of the CEC the paired C_s and C_w values may be fit with the general Freundlich equation:

$$C_s = K_f(C_W)^n \quad (1.5)$$

where K_f (mmol kg^{-1} mM^{-n}) is the Freundlich sorption coefficient and *n* is the Freundlich exponent. A sorption coefficient can be obtained for any paired measure of C_s and C_w and is defined as a single-point K_d (L kg^{-1}). In cases where $n \approx 1$, the Freundlich equation (Eq. 1.5) simplifies to the sorption coefficient. Single-point K_d values that are constant with C_w are indicative of a linear sorption isotherm.

1.7 Factors in Sorption

The magnitude of the sorption coefficient is influenced by both sorbent characteristics and compound structure. Some progress has been made into both qualitatively and quantitatively evaluating the influence of compound structural characteristics on sorption.[5,6] However the numerous possible differences in the solid phase have not be thoroughly studied in the context of organic cation sorption and an organic cation affinity for the surface.

1.7.1 Environmental Factors

Organic cations sorb to soils and sediments through electrostatic interactions between the compound's positively charged amine group with negative charge sites and hydrophobic forces driving the compound out of the aqueous phase.[5-8] Naturally occurring negatively charged sites are found on organic matter, aluminosilicate clay minerals, and metal oxides. On clay minerals, negative charge may arise from isomorphic substitutions of lower valance cations during crystal formation, creating a surplus of negative charge.[4] The negative charge of organic matter is pH dependent, and arises from the deprotonation of enolic, carboxyl, and phenolic groups.[3,7] Similarly, negative charge on aluminum and iron oxides is also pH dependent due to the dissociation of protons from surface bound hydroxyl groups, though at environmentally relevant pH these account for little of the total soil charge of since the point of zero charge is around 7.[4] Naturally occurring inorganic cations locally neutralize negatively charged sites and their exchange is a primary mechanism of organic cation adsorption.[7] These cations can include (in order of abundance) Ca^{2+}, Mg^{2+}, K^{+} , Al^{3+}, and Na^{+}, while in agricultural regions NH_4^{+} may also be present.[9,10] Therefore much importance is placed on how these inorganic cations can facilitate or suppress organic cation adsorption.

1.7.2 Exchange Affinity

Cation exchange is the process by which organic cations in the bulk solution replace the naturally occurring inorganic cations associated with negatively charged sites. Consequently, the affinity the inorganic cation displays for the surface is an important factor for sorption of cationic amines to negatively charged sites on aluminosilicates.[6,7] The differences in inorganic cation affinity to the montmorillonite surface is generally influenced by the valance charge and the

ionic radius of the cation.[4] Inorganic cations exhibit decreased attraction to negatively charged sites with decreased charge, such that adsorption affinity series or selectivity sequence is:[7,22]

$$Na^{+} < Ca^{2+} < Al^{3+}$$

An inorganic cation with an increased affinity for the surface would require more energy to replace, thus decreasing the sorption of organic cations vying for the same site. In agreement with this, Droge et al found that when ionic strength is kept constant, Ca^{2+} suppress organic cation sorption 10 times more than Na^{+} in a study of the cation exchange of 29 different organic cations to 3 aluminosilicate clay minerals, and organic matter.[8,16]

When extending the affinity sequence outside of beyond charge, the tendency for a cation to form inter-sphere complexes must also be considered. Generally, the relative affinity for a metal to shed it hydration shell and form inner sphere complexes is positively correlated with ionic radius.[4,13] This implies that a metal cation with a larger ionic radius will create a smaller electric field and will be less likely to remain solvated during interactions with a negatively charged surface.[13,17] The closer the ion is to the negative charge, the more energy it will take to exchange it with another cation (inorganic and organic). When included in the affinity series, the series is extended to the following:

$$Li^{+} \approx Na^{+} < NH_4^{+} \approx K^{+} < Mg^{2+} < Ca^{2+} < Al^{3+}$$

Whether sorption coefficients of organic cations to different homoionic clays are influences by this sequence has yet to be determined. Moreover, quantitatively accounting for the identity and abundance of each exchangeable cation - which can change drastically with soil type[23,24] - may be problematic, creating the need for a tractable method to quantify exchange affinities for soils with mixed cations.

1.7.3 Clay minerals

Exchange affinities for organic cations are also dependent on the surface chemistry of the negative site. Naturally occurring negative charge sites are predominantly found on organic matter and aluminosilicate clay minerals.[23] Clay minerals contain both permanent and pH dependent surface sites that are balanced with exchangeable cations.[7,24] pH dependent sites, resulting from the dissociation of protons of surface bound hydroxyl groups, are found on fully hydrated particle edges. [25] Permanent sites arise from isomorphic substitutions of lower valance cations into the crystal lattice (e.g. Mg^{2+} for Al^{3+}) during mineral formation, creating excess negative charge.[26,27] Substitutions can occur in both the tetrahedral (SiO_2) or octahedral (AlO_2) layers. Tetrahedral substitutions, which are closer to the surface, produce focused charges sites spread over 3 surface oxygen atoms.[26,28] Charge from isomorphic substitutions within the octahedral layer is distributed over a larger area on the surface.[26-28] Negatively charged surface sites arising from isomorphic substitutions can be fully hydrated (non-swelling clays) or found in the interlayer (swelling clays). The differences in site surface chemistry; both density (focused vs. defocused) and hydrated state can cause sorption coefficients of hydrophobic or polar organic cations to be very different.[10,13,29] However, the extent that prominent organic cation structural moieties are sensitive to variations in surface charge site chemistry has not been systematically evaluated.

1.8 Objectives

To advance the understanding of organic cation sorption, this research aims to complete the following objectives:

1. Validate column chromatography as a method to collect sorption isotherms of organic cations.
2. Determine an inorganic cation competition sequence for organic cations on exchanged montmorillonite and account for the identify and abundance of inorganic cations using the sorption of a simple cationic compound to access site energy
3. Determine the sensitivity of organic cations sorption to pure phase minerals with systematic variations in charge site chemistry.

These are detailed in the following chapters; Chapter 2 addresses Objective 1, Chapter 3 addresses Objective 2, and Chapter 4 addresses Objective 3.

2.0 Column Chromatography to Obtain Organic Cation Sorption Isotherms

2.1 Abstract

Column chromatography was evaluated as a method to obtain organic cation sorption isotherms for environmental solids while using the peak skewness to identify the linear range of the sorption isotherm. Custom packed HPLC columns and standard batch sorption techniques were used to intercompare sorption isotherms and solid-water sorption coefficients (K_d) for four organic cations (benzylamine, 2,4 dichlorobenzylamine, phenyltrimethylammonium, oxytetracycline) with two aluminosilicate clay minerals and one soil. A comparison of Freundlich isotherm parameters revealed isotherm linearity or non-linearity was not significantly different between column chromatography and traditional batch experiments. Importantly, skewness (a metric of eluting peak symmetry) analysis of eluting peaks can establish isotherm linearity, thereby enabling a less labor intensive means to generate the extensive datasets of linear K_d values required for the development of predictive sorption models. Our findings clearly show that column chromatography can reproduce sorption measures from conventional batch experiments with the benefit of lower labor intensity, faster analysis times, and allow for consistent sorption measures across laboratories with distinct chromatography instrumentation.

2.2 Introduction

Current sorption models, developed for neutral nonpolar compounds (*e.g.*, EPISUITE[9]), greatly underestimate sorption of ionic organic compounds because those models do not account for electrostatic interactions between the sorbate and charged sorbents.[5,10-12,30] Accurate sorption models are necessary because a growing number of environmental contaminants of interest are charged under environmental pH values, including surfactants, pesticides, antibiotics, and

pharmaceutical compounds.[1,5,31,32] Recently, there has been encouraging progress in the development of new predictive models for ionogenic compounds using polyparameter and computational methods.[10,12-16] In the case of cationic organic compounds, empirical sorption models using molar volume and amine type (*e.g.*, primary, secondary, or tertiary) show promise for predicting sorption of non-heterocyclic amines of the form C_xH_yN to aluminosilicate clay minerals, organic matter, and soils.[10,12,13,29] However, cationic amine compounds with more complex structures require the use of corrective factors, derived from small sets of compounds sharing similar substructures (*e.g.*, aromatic rings, -Cl). Sorption of structurally complex cations can be described using molecular dynamics models that explicitly account for van der Waals and electrostatic energies of interaction between the sorbate and the surface.[15] However, advanced computational tools are specialized and not widely available to practitioners. In the absence of comprehensive sorption models for organic cations, there is a need for a robust, time-efficient technique to obtain sorption isotherms for ionic contaminants of interest and to generate extensive datasets of sorption coefficients (K_d) for predictive model development.[5,11,17,18]

Sorption isotherms are obtained either by batch[11,21,33-35] or column techniques.[10,30,36] Batch isotherm measurements consist of mixing the sorbent with an aqueous solution of the compound in a closed reactor. Following sorptive equilibrium, the aqueous phase compound concentration is measured and the sorbed concentration is often calculated from the difference between the initial and final aqueous concentration with normalization to sorbent mass.[37] Reactor preparation with different initial solute concentrations allows the paired equilibrium sorbed (C_s, mmol kg^{-1}) and aqueous (C_w, mM) concentrations to be used to create an isotherm (a plot of C_s vs. C_w) for the sorbent. The paired C_s and C_w values may be fit with the general Freundlich equation:

$$C_s = K_f(C_W)^n \quad (1.1)$$

where K_f (mmol kg^{-1} mM^{-n}) is the Freundlich sorption coefficient and n is the Freundlich exponent. A sorption coefficient can be obtained for any paired measure of C_s and C_w and is defined as a single-point K_d (L kg^{-1}).

$$K_d = \frac{C_s}{C_w} \quad (1.2)$$

In cases where $n \approx 1$, the Freundlich equation (eq 1.1) simplifies to the sorption coefficient. Single-point K_d values that are constant with C_w are indicative of a linear sorption isotherm. Obtaining sorption isotherms with batch experiments is straightforward, but can be time-consuming and labor-intensive to include sufficient replicates and controls. These factors are particularly important for sorption studies with large compound sets and for studies of ionogenic compounds that require assessment under many different experimental conditions (*i.e.*, pH, ionic strength, competing inorganic solutes).

Sorption coefficients obtained from column techniques have the advantage of preserving solids in their native state.[38,39] Column experiments to measure compound sorption are typically employed to understand groundwater transport.[40] Columns packed with the solid of interest are flushed with synthetic groundwater at field flow rates. A step input of the compound of interest is introduced to the column and compound breakthrough at the outlet of the column is tracked over time. Sorption coefficients are derived from the retention time of the compound transported through the column.[41] Often, only one input concentration is utilized which can lead to discrepancies between sorption coefficient measurements from column and batch experiments,[42-44] particularly when isotherms for that sorbate-sorbent combination are nonlinear ($n \neq 1$).[45] For consistency between K_d values obtained from batch and column experiments, the experimental conditions must yield K_d values in the linear range of the sorption isotherm ($n = 1$) and

breakthrough curves should be appropriately integrated.[45] Further, the wide column diameters (> several cm) typically employed to simulate groundwater transport can lead to disequilibrium kinetics as diffusion times to sorption sites are long compared to advective transport through the column.[46-48] These factors, as well as the need for specialized equipment, have caused column studies to be less favored than batch techniques[19] for obtaining sorption isotherms.

Column chromatography, on the other hand, provides an effective means to overcome the disadvantages of both batch and column techniques for obtaining sorption isotherms.[20,49] Pulse injections of a compound of known concentration are made to short (several cm length), narrow diameter (10s mm) columns that are packed with a mixture of the sorbent of interest and an inert non-sorptive solid (*e.g.*, quartz[49], SiC[20]). Compounds are then eluted with a mobile phase of known composition using a high-pressure pump. The inert solid restricts movement of small sorbent particles within the column so that discrete sorbent particles contact the eluting phase, thereby minimizing solid matrix diffusion effects and improving compound access to sorption sites. As with large-scale columns, flowrates can still be varied to ensure equilibrium sorption conditions and to further minimize kinetic mass transfer effects.[49] Sorbent 'dilution' with the inert sorbent allows the solid-to-water ratio of the sorbent to be varied to balance compound separation from a non-retained tracer against dispersive effects which elongate compound breakthrough curves. Shorter duration experiments are possible through inline detection of compound breakthrough and automated calculation of retention times. Furthermore, the shape of the eluting compound peak can provide information about isotherm non-linearity through analysis of peak tailing or fronting.[36,46,50-52] Transport of compounds under equilibrium sorption conditions with non-linear isotherms will yield peak skewness values that differ from zero: tailing ($n < 1$) gives positive values and fronting ($n > 1$) gives negative values.[36,45] However,

skewness has not been validated as means of indicating isotherm non-linearity for column chromatography.

To date, column chromatography to obtain sorption coefficients has been used by a limited number of researchers.[20,30,51] Droge *et al* used column chromatography measurements to collect an extensive data set of organic cation sorption coefficients to organic matter, clay minerals and soils.[10,12,13,29] Although equilibrium conditions for sorption coefficient measurements have been assessed through the constancy of K_d values obtained under varied flow conditions[50], direct comparisons of isotherms obtained using column chromatography techniques with those from batch techniques have not been undertaken, nor have intercomparisons of column techniques across laboratories. Therefore, further validation is needed to ensure sorption coefficients from different collections means (batch to column, system to system) can be used in developing predictive models.

The purpose of this study was to validate the column chromatography technique for measuring sorption isotherms against conventional batch techniques. We examined four organic cations with varied extents of isotherm linearity and nonlinearity (n =, >, or < 1) using different environmentally relevant sorbents. Because we were interested ultimately to discern concentration ranges under which isotherm linearity could be assumed, we examined whether the shape of the compound peak eluting from the column chromatography technique (measured as skewness) showed regular trends with isotherm nonlinearity measures (*i.e.*, n). Further, transferability of the methodology and experimental findings were assessed across two labs with distinctly different HPLC systems (U. Connecticut and Bowdoin College).

2.3 Methods

2.3.1 Sorbents and chemicals

Texas Ca-montmorillonite (STx-1) and illite (IMt-1) were obtained from the Clay Minerals Society. SiC was from Alfa Aesar. Iredell soil was collected and characterized previously.[42] Sorbate compounds phenyltrimethylammonium (permanently charged), benzylamine (cationic, pK_a: 9.33), 2,4-dichlorobenzylamine (9.15), and oxytetracycline (zwitterionic, pKa_1: 3.27 (carboxylate, negative charge), pKa_2: 7.41 (amine, positive charge)) were from Sigma Aldrich. All other chemicals and reagents were ACS grade. Solutions were made with high purity 18.2 MΩ water (DI water) from a MilliQ system (Waters).

2.3.2 Batch sorption experiments

Batch sorption reactors were prepared with a solid-to-water ratio of 10 g/L for all sorbents. Homoionic clays were created by washing (24 h) montmorillonite or illite three times with 1 M sodium chloride, or 0.5 M calcium chloride, followed by three washes with DI water to remove excess salt solution. Initial test compound concentrations (1×10^{-5} to 1×10^{-4} M) were chosen to achieve an extent of equilibrium sorption between 5 and 95%, along with surface coverage equivalent to less than 5% of the sorbent's cation exchange capacity. For each test concentration, paired C_w and C_s values were obtained in triplicate and included a control set with no sorbent addition to infer initial compound concentration and to confirm the absence of other loss processes. Sorbent-containing and sorbent-free reactors were prepared with background solutions of either 5 mM $CaCl_2$, 20 mM NaCl or DI water, mixed for 24 hours in the dark, centrifuged, and filtered (0.45 µm PVTF) before analysis of the supernatant aqueous concentration. Aqueous compound concentrations from the batch studies were determined using high pressure liquid chromatography (Hewlett Packard HP 1050 outfitted with a C_{18} reverse

phase column (Ultra Aqueous, Restek) and a diode array detector). The system was operated with isocratic elution with a mixture of solvents: (A) 20 mM phosphate buffer adjusted to pH 2.5 containing 4 mM triethylammonium hydroxide and (B) acetonitrile. Mobile phase of (A: 90%, B: 10%) was used for phenyltrimethylammonium and benzylamine, (A: 60%, B: 40%) for 2,4 dichlorobenzylamine, and (A: 75%, B: 25%) for oxytetracycline. Absorbance wavelength of 205 nm was used for all compounds except oxytetracycline which was detected at 360 nm.

2.3.3 Column packing

Columns (30-mm length, 2.1-mm inner diameter, Restek #25118) were manually packed with a mixture of silicon carbide (SiC) and sorbent material for the 'sorbent-SiC' columns and with SiC for the 'SiC-only' columns. SiC-to-sorbent ratios (Table 1) were chosen so that the center of mass of the breakthrough curves for the test compounds was at least 1.5 times greater than for a non-retained tracer (NO_3^-) while minimizing peak spreading associated with extended compound retention times. Also, each column was designed to have a sorbent-to-water ratio (Table 1) that was within an order of magnitude of the 10 g/L used in the batch experiments. Dry SiC was passed through a 200 mesh sieve (74 µm) and wet-filtered through a 0.75 µm glass fiber filter to remove fines so particle sizes ranged from 0.75 to 74 µm. Montmorillonite was used as received. Illite and Iredell soil were ground using a motor and pestle and then passed through 200 mesh sieve. Fines were not removed from sorbent materials. Columns were packed without a column vibrator using a procedure adapted from Bi *et al.*[49] First, a mass of SiC and sorbent (typically 2 - 5 g of SiC, 10 - 50 mg sorbent) were combined together in a vial and vortexed for 2 minutes to blend the powders uniformly. An aliquot (10 – 20 mg) of the combined solid phase mixture was manually packed in a column using a spatula and tapping the column sides to limit mounding. Periodically, the flat end of a thin rod was inserted into the

column and used to lightly pack down material so that particles were not clumped. The mass of the solid mixture (sorbent + SiC) in the column was obtained from the difference in weights of the empty and packed sealed columns. After packing, the sealed column was oriented vertically and attached to the HPLC pump with flow directed vertically upward and discharging to waste. The column was slowly filled with DI water (10 µL/min) to remove all air. The flow rate was then increased gradually by 10 µL/min each hour to a final flowrate of 100 µL/min so that channeling within the packing material was minimized. Solid-to-water ratios assumed the column void space to be completely saturated. The difference in transport time of a non-retained tracer (NO_3^-) though the system with a column in place and the tubing with no column attached was used to calculate the column void space. The column void space was verified from the bulk density of the mixed column packing using the known mass ratio and solid phase densities of the SiC and the sorbent material. A comparative control column was packed entirely with SiC to verify that test compounds had no sorptive interactions with this inert solid.

Table 2.1. Experimental Conditions used in the test columns.

Column Name*	MMT-19	MMT-5	MMT-18B	ILL-53	IRE-23
Sorbent	Montmorillonite	Montmorillonite	Montmorillonite	Illite	Iredell Soil
Void Space (µL)	45	45	45	63	48
Sorbent Mass (mg)	0.86	0.215	0.80	3.3	1.1
Sorbent-to-water ratio (g/L)	19	5	18	53	23

* Number adjacent to the column name refers to the sorbent-to-water ratio; B refers to column packed at Bowdoin College; other columns were packed at U. Connecticut.

2.3.4 Column Operation

At U. Connecticut, packed columns were loaded into a standard HPLC system (Jasco PU-980 pump, AS-950 auto sampler, 40 □L injection loop, and MD-1510 multiwavelenth detector) with tubing lengths minimized to reduce peak spreading. Aqueous phase solution chemistry was fixed by the composition of column eluent solutions (Tab. 2.2). Aluminosilicate clay sorbents were converted to homoionic form (Ca- and Na-montmorillonite; Na-illite) by flushing the respective column with air-equilibrated (pH 6 ± 0.3) 5 mM $CaCl_2$ or 20 mM NaCl for 24 hrs before compound injection. Compound sorption to Iredell soil was determined with DI water adjusted to pH 5.2 (HCl); no pre-flushing was performed. The effect of flow rate on sorption was evaluated by varying flowrates between 50 and 200 μL min^{-1}. Subsequently, an operating flowrate of 100 μL min^{-1} was used for all experiments.

Compound or tracer solutions were introduced to the column using an injection volume of 40 μL and detected at the column outlet using wavelengths as indicated for the discrete sample analyses from the batch experiments. The concentration of test compound injected into the column was varied from 2.6×10^{-5} to 2.6×10^{-4} M to create sorption isotherms over a similar range of sorbate concentrations as used in the batch experiments. Triplicate injections of each concentration were made for both the SiC-only and the sorbent-SiC columns. Absorbance *vs.* time data collected following each injection were exported directly to a MATLAB routine to calculate the paired aqueous phase and sorbed concentrations from the eluted compound peak in the breakthrough curve.

A similar column packing and operation procedure was used for the Bowdoin College HPLC system (Agilent 1100 Series, Quaternary Pump, Diode Array Detector, and 100 μL injection loop). The Bowdoin College HPLC system was more sensitive to the operating

conditions for obtaining sorption isotherms. The low eluent pumping rate (100 µL min^{-1}), combined with a slow syringe withdraw and eject speed (50 µL min^{-1}) resulted in significant diffusional mixing of the compound with the mobile phase within the injection loop if it was partially filled. This issue, not typically observed under normal analysis conditions (*e.g.*, 1 mL min^{-1} flow rate), was resolved by employing an injection volume of 100 µL to completely fill the injection loop. Compounds with a single aromatic ring were detected at a wavelength of 210 nm (10 nm bandwidth) because of high signal-to-noise ratios at lower detector wavelengths.

2.3.5 Mass balance

Mass balance assessments for batch experiments were undertaken for benzylamine sorption on Ca-montmorillonite by adding $CaCl_2$ salt to achieve a final concentration of 1 M and facilitate competitive desorption. Samples were mixed for 24 hours in the dark, centrifuged, and filtered, and an aliquot of the supernatant was removed for analysis by HPLC. Mass balance in the column chromatography method was assessed by comparing the integrated compound peak areas obtained with the 'sorbent-SiC' column with those from a 'SiC-only' column. For both experimental approaches, mass balances within 5% were achieved, indicating the absence of any other compound loss mechanisms for either sorption measurement techniques.

2.3.6 Isotherms

Batch sorption experiments yielded equilibrium aqueous phase compound concentrations directly. Corresponding sorbed compound concentrations were calculated by difference as outlined earlier.

Column sorption experiments required that sorption coefficients be calculated first using eluted test compound peak characteristics, followed by the extraction of the corresponding aqueous and sorbed concentrations using a mass balance equation. Single-point K_d values were calculated

from the volume of eluent required to elute compounds from a column, V (L), and column sorbent mass, m (mg)[36]:

$$K_d = \frac{V}{m} = \frac{Q * \left[\left(t_{cmpd} - t_{tracer}\right) - \left(t_{cmpd-SiC} - t_{tracer-SiC}\right)\right]}{m} \quad (2.3)$$

where Q (L min^{-1}) is the eluent flow rate and the bracketed term is the effective travel time of the compound in contact with only the sorbent material in the 'sorbent-SiC' column. All times (t_i, min) were calculated by baseline-subtracting the pre-injection absorbance signal and then integrating the corresponding peak to obtain the center-of-mass: t_{cmpd} and $t_{cmpd\text{-}SiC}$ are the compound travel times through the sorbent-SiC and SiC-only columns, respectively, and t_{tracer} and $t_{tracer\text{-}SiC}$ are the nitrate tracer travel times through sorbent-SiC and SiC-only columns, respectively. Sorption coefficients obtained with Eq. 2.3 were converted to aqueous and sorbed concentrations[36]:

$$C_w = \frac{C_0 * V_i}{K_d * m + V_i} \quad (2.4)$$

$$C_s = \frac{C_0 * V_i - C_w * V_i}{m} \quad (2.5)$$

where C_0 (mM) is the concentration of the injected test compound solution and V_i (L) is the injection volume.

Paired C_w and C_s values were used to construct isotherms. For the purposes of evaluating isotherm linearity, single-point K_d values were calculated for every paired C_s and C_w value from batch experiments, or obtained directly from column experiments (Eq. 2.3).[21] Although single-point K_d values for potentially non-linear isotherms have received criticism when inter-comparisons between compounds are not undertaken at the same C_w value, here, we use single point K_d values to compare changes in slope *within* a single compound-sorbent isotherm. K_d values were considered to be in the linear range (n = 1 approximation valid) if the lowest two or

more consecutive aqueous concentrations yielded K_d values that were not significantly different from one another. Reported 'linear' K_d values (K_{d_Linear}) are the average of the individual, single-point K_d values in the linear range of the isotherm.

Variations in symmetry of eluted compound peaks were examined for all C_w values used to construct isotherms by comparing peak skewness, S[53]:

$$S = \sum \frac{(x-\mu)^3}{\sigma^3} \tag{2.6}$$

where μ and σ are the mean and standard deviation of the individual points, x, of the breakthrough curve.

2.4 Results and Discussion

2.4.1 Equilibrium Assessment in Column Studies

Evidence for equilibrium sorption conditions within the columns was obtained by examining the effect of flow rate on the sorption of benzylamine to a Na-montmorillonite column. It is known that organic cations sorb quickly to soils and aluminosilicate clay minerals in batch experiments, reaching equilibrium within eight hours;[54,55] however, these timescales are much greater than the 3- to 15-minute compound residence times observed in our columns. Sorption disequilibrium in flow-through columns has been evidenced by lower sorption coefficients and greater peak tailing as column flow rates are increased.[52] For the three eluent flow rates tested at U. Connecticut, benzylamine sorption to Na-montmorillonite (MMT-19, Table 1) showed no significant difference in K_d values: The 50 µL min^{-1} flow rate yielded a K_d value of 62 ± 1 L kg^{-1}, the 100 µL min^{-1} flow rate yielded a K_d value of 59 ± 1 L kg^{-1}, and the 200 µL min^{-1} flow rate yielded a K_d value of 57 ± 5 L kg^{-1}. Each of these values was not statistically different from the K_d value of 61 ± 4 L kg^{-1} that was obtained from batch

experiments, which had equilibrated for 24 hours (batch C_w values matched column conditions). Similarly, for the two eluent flow rates tested in the Bowdoin College set up, phenyltrimethylammonium sorption to Ca-montmorillonite (MMT-18B, Table 1) showed no significant difference in K_d values for flow rates of 50 µL min^{-1} (K_d = 126 ± 10 L/kg) and 100 µL min^{-1} (K_d = 124 ± 4 L/kg). These values were also close to the K_d value of 132 ± 6 L/kg obtained in batch experiments. Greater tailing at the highest flow rate (200 µL min^{-1}) increased the measurement error (standard deviation of triplicate K_d measurements) from 2% to 10%; therefore, 100 µL min^{-1} was used as the flow rate for all other experiments. Previous researchers have also used 100 µL min^{-1} as an operating flowrate in column chromatography to obtain sorption isotherms and sorption coefficients[29,30]; however, their validation of equilibrium column conditions had not included higher column flow rates.

3.4.2 Isotherm Comparisons between Batch and Column Studies

The isotherms obtained from the column chromatography method reproduced the results from conventional batch sorption experiments. Solid-to-water ratios of the sorbents in the column were adjusted with SiC to match batch ratios so that direct comparisons at similar C_w values could be made. Paired C_w and C_s values obtained from individual injections to the columns were nearly identical to values obtained from batch reactors assembled under the same experimental conditions (white *v.* black symbols, Fig. 2.1). In addition, paired C_w and C_s values obtained using column chromatography at U. Connecticut and Bowdoin College were also nearly identical (white squares without and with a plus, Fig 2.1A). Representative data shown in Fig. 2.1 includes compound-sorbent pairs chosen to validate the column chromatography method against batch experiments under a range of sorption scenarios. First, we examined isotherms with differing *n* values: Benzylamine sorption to Ca-montmorillonite (Fig. 2.1A) and

phenyltrimethylammonium sorption to Na-montmorillonite (Fig. 2.1B) exhibit Freundlich isotherms with (n > 1) because of potential compound-compound interactions in the clay interlayers.[21] Oxytetracycline sorption to Na-montmorillonite (Fig. 2.1C) exhibits a traditional non-linear (n < 1) isotherm. Benzylamine sorption to Iredell soil (Fig. 2.1D) and to illite (Fig. 2.S1) are best described with linear isotherms. Second, montmorillonite (Fig. 2.1A, B, C) and Iredell soil (Fig. 2.1D) both contain internal porosity that could create mass transfer limitations with the shorter contact times for sorptive equilibrium in column experiments, compared to batch reactors. The close match between column and batch isotherms in each of these cases, as well as for additional compound-sorbent pairs (Fig. 2.S1), further confirms that equilibrium conditions established during column chromatography in two different laboratory set-ups match those of conventional batch sorption experiments.

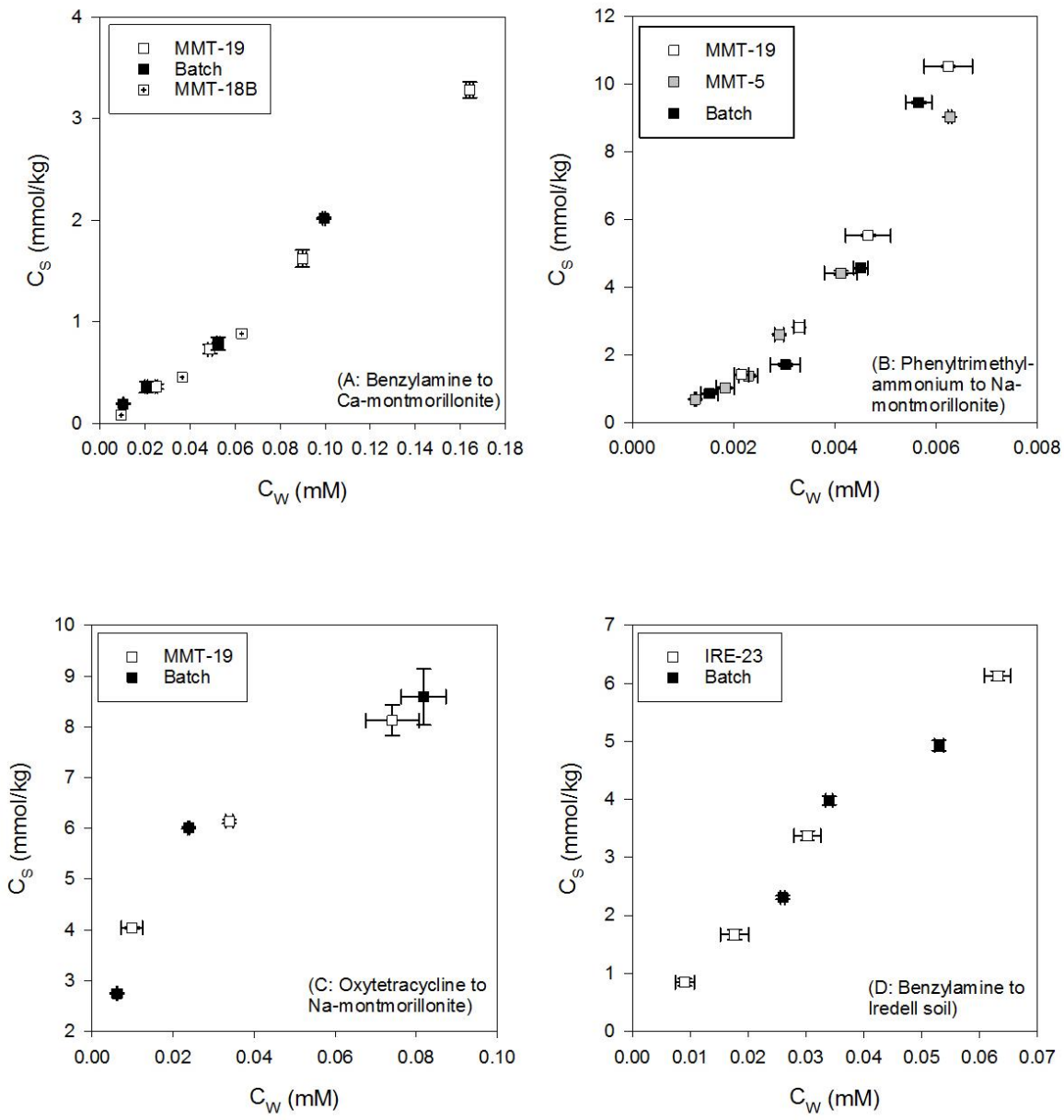

Figure 2.1. Sorption isotherms obtained from column experiments match those obtained from batch experiments for (A) benzylamine on Ca-montmorillonite, (B) phenyltrimethylammonium on Na-montmorillonite, (C) oxytetracycline on Na-montmorillonite and (D) benzylamine on Iredell soil. Black squares – batch data; white squares - column MMT-19 or IRE-23; white

squares with black "+" – column MMT-18B; grey squares - column MMT-5. Where not visible, error bars are smaller than the symbol size.

Agreement between column and batch methods was further supported by the observation that isotherm parameter values (e.g., K_f and n) derived from regression fits to experimental batch and column data were not statistically different (t-test, $p > 0.05$). Fitting the Freundlich equation to paired C_w and C_s values gave similar K_f and n values for both methods for each of the eight compound-sorbent pairs evaluated (Tab. 2.2). The one exception was oxytetracycline sorption to Na-montmorillonite for which the three data points gave fits that were sensitive to small variations in the sorbed concentration values. At low concentrations, where single point K_d values were constant with C_w, K_{d_Linear} values were not statistically different between the two methods either (Tab. 2.2). The standard deviation on isotherm parameters K_f and n or K_{d_Linear} values were similar between the two methods (Tab. 2.2), although replicates of individual concentration points showed greater reproducibility with the column chromatography method, compared to replicate batch reactors.

Table 2.2. Freundlich isotherm parameters (K_f and n exponent) and linear range sorption coefficients (K_{d_Linear}) obtained from batch and column chromatography methods. Values in parentheses indicate data collected with Bowdoin College system.

Compound	Solid	Background Solution	Batch K_f	Column K_f	Batch n	Column n	Batch K_{d_Linear}	Column K_{d_Linear}
Benzyl-amine	MMT	20 mM NaCl pH 6	98 ± 19[§]	105 ± 27	1.10 ± 0.05	1.14 ± 0.07	61 ± 4	59 ± 1
Benzyl-amine	MMT	5 mM $CaCl_2$ pH 6	18 ± 6	27 ± 3 (29 ± 2)	1.17 ± 0.03	1.10 ± 0.05 (1.26 ± 0.02)	15 ± 2	17 ± 2 (12± 2.5)
Benzyl-amine	IRE	DI pH 5.2	100 ± 60	115± 28	1.01 ± 0.41	1.01 ± 0.06	88 ± 8	96 ± 14
Benzyl-amine	ILL	20 mM NaCl pH 6	24 ± 3	27 ± 1	0.91 ± 0.03	0.93 ± 0.01	36 ± 3	38 ± 1
Phenyl-trimethyl-ammonium	MMT	20 mM NaCl pH 6	76800 ± 14700	65900 ± 4600	1.79 ± 0.16	1.74 ± 0.10	565 ± 62	556 ± 45
Phenyl-trimethyl-ammonium	MMT	5 mM $CaCl_2$ pH 6	232 ± 32	201 ± 64 (194 ± 24)	1.20 ± 0.05	1.12 ± 0.02 (1.11 ± 0.01)	132 ± 6	131 ± 4 (133± 16)
Oxytetra-cycline	MMT	20 mM NaCl pH 6.5	27 ± 9	19 ± 1	0.44 ± 0.08	0.34 ± 0.04	449 ± 10	415 ± 26
2,4-dichloro-benzylamine	MMT	20 mM NaCl pH 6	108 ± 21	120 ± 10	1.08 ± 0.04	1.10 ± 0.04	67 ± 4	72 ± 3

[§]represents average value and standard deviation based on triplicate analyses

2.4.3 Concentration ranges amenable to column chromatography

The range of concentrations over which isotherms can be obtained by column chromatography is set by physical limitations of the system detector. The lower concentration bound of an isotherm is set by the limit of detection of the instrument which can be as low as 5×10^{-7} M for modern absorbance detection. Low concentrations are also of concern for compounds that exhibit high extents of sorption and consequently, long retention times. Long retention times result in peak spreading that can lower compound absorbance to background levels. Such situations can be addressed by reducing the ratio of sorbent to inert packing material in a column. We evaluated isotherm consistency across columns with different sorbent ratios using phenyltrimethylammonium, the most sorptive compound of the test compounds examined here. Isotherm points obtained on a column with an effective solid-to-water ratio of 5 g/L of Na-montmorillonite (MMT-5, grey squares, Fig. 2.1B) compared well to those obtained with a Na-montmorillonite column packed with four times the mass of sorbent of 19 g/L (MMT-19, white squares, Fig. 2.1B). Individual data points for the MMT-19 column showed greater measurement errors as a result of greater peak spreading associated with the longer compound retention time (MMT-19: 8-15 min, MMT-5: 3–6 min). Thus, adjustments of the sorbent-to-SiC ratio in the chromatography columns will yield reproducible isotherms while enhancing peak detection via shorter column retention times.

Our primary interest in this study was to obtain sorption measurements under conditions of very low sorbent coverage (< 2% of cation exchange sites) that were within the linear range of the isotherm. For completeness, we used the column chromatography

method to examine benzylamine sorption to Na-montmorillonite up to 100% cation exchange site coverage. This compound, like other cationic aromatic amines, displays an 'S-shaped' non-linear isotherm that curves away from the *x*-axis at low concentrations due to sorbate-sorbate cation-π interactions on the surface, followed by curvature toward the *x*-axis as the sorbed concentration approaches the cation exchange capacity.[21] The complex S-shape isotherm for benzylamine sorption to Na-montmorillonite previously observed in batch studies[21] was successfully reproduced by our column chromatography method (Fig. 2.2). Quantitative comparisons with previous batch studies are not shown in Fig. 2.2 because of differences in clay mineral exchange ions (*e.g.* hetero vs. homoionic clay minerals) between the two studies. Nevertheless, the data in Fig. 2.2 demonstrates the ability of the column method to capture isotherm points up to full surface coverage without reaching detector saturation at the high concentrations injected.

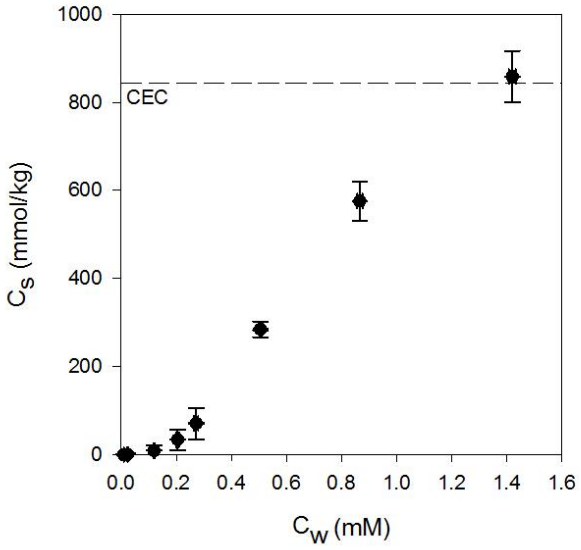

Figure 2.2. Isotherm ranging from 0.1 to 100 percent exchange site coverage for benzylamine on Na-montmorillonite using column chromatography displays complex "S" shape. Dashed line indicates cation exchange capacity of montmorillonite.

2.4.4 Breakthrough curve skewness as an indicator of non-linearity

We explored the use of compound peak symmetry measures to bound the range of C_w values over which isotherm linearity can be assumed (n = 1 valid). K_{d_Linear} values are often required for calibrating predictive models.[12,15,18] Such values are typically obtained by performing batch experiments to collect isotherms and comparing single-point K_d values (Eq. 2.2) across these extensive datasets. The labor-intensity of such an approach could be avoided if it were possible to assess whether a C_w and C_s pair falls within the linear isotherm range, independent of the full isotherm dataset. Accordingly, we investigated whether peak skewness measures might provide such insights. Under transport conditions with local sorptive equilibrium, peak symmetry is non-uniform when the Freundlich parameter deviates from n = 1.[36,45,48,50-52] We postulated that such a change in peak skewness might be observable across the set of points constituting an isotherm.

For our column operating conditions, the most appropriate comparative measure of peak symmetry was the fractional change in skewness, %ΔS:

$$\%\Delta S = \frac{Skewness_{sorbent-SiC} - Skewness_{SiC}}{Skewness_{SiC}} \times 100\%. \qquad (2.7)$$

where $Skewness_i$ is the calculated skewness for the compound peak on the respective 'sorbent-SiC' and 'SiC-only' columns. A difference measure was implemented because

peak asymmetry was observed for both tracer and test compound breakthrough on the non-sorptive 'SiC-only' column. This asymmetry likely originated from the injection volumes being greater than 1/6 of the column volume[56] and was the same for all compounds on the SiC-only column. Skewness measures for the non-retained tracer were the same for both the 'SiC-only' and the 'sorbent-SiC' columns, indicating column packing to be consistent between the two preparations. Further, for each compound, the same peak skewness was calculated at all injected concentrations less than 2 mM on the 'SiC-only' column. The only exceptions were the three highest concentrations (6 mM to 20 mM) used to obtain the benzylamine isotherm (Fig. 2.2). Thus, we concluded that variations in %Δ*S* across the isotherm for a given test compound could be ascribed to variations in equilibrium K_d thus be used to assess isotherm non-linearity.

The fractional change in peak skewness appears to be a robust indicator of single-point K_d linearity. Single-point K_d values were normalized to the average $K_{d\text{-}Linear}$ to assess the fractional deviation from linearity:

$$\%\Delta K_d = \frac{K_{d,point} - K_{d,linear}}{K_{d,linear}} \times 100\%. \quad (2.8)$$

Only paired C_w and C_s values that had a small fractional change in skewness less than |± 4%| were from the linear range of the sorption isotherm (*i.e.*, $\%\Delta K_d \sim 0$) (white symbols, Fig. 2.3). Although the absolute skewness values were distinct for measurements made at U. Connecticut (1.5) and Bowdoin (2.5), a $\%\Delta S$ less than an absolute value of 4% for experiments conducted at either location indicated that sorption was in the linear range of the isotherm (Fig. 2.3A). For high concentration points of compound-sorbent pairs from isotherms with Freundlich exponents $n > 1$ (i.e., $\%\Delta K_d > 1$), $\%\Delta S$ exhibited negative

values and fell in the upper left quadrant of Fig. 2.3B On the other hand, high concentration point for isotherms with $n < 1$ (i.e., $\%\Delta K_d < 1$), $\%\Delta S$ exhibited positive values and fell in the lower right quadrant (Fig. 2.3B). From this analysis it is clear that $\%\Delta S$ for a given concentration injection that is more positive, or more negative, than 4% is indicative of sorption in the non-linear range of the sorption isotherm. Therefore, relative change in skewness can be used to bound the linear range of a sorption isotherm. The indication of linear range sorption coefficients, coupled with the already reduced labor intensity compared to traditional batch experiments, makes column chromatography an efficient, robust tool to collect sorption coefficients of organic cations.

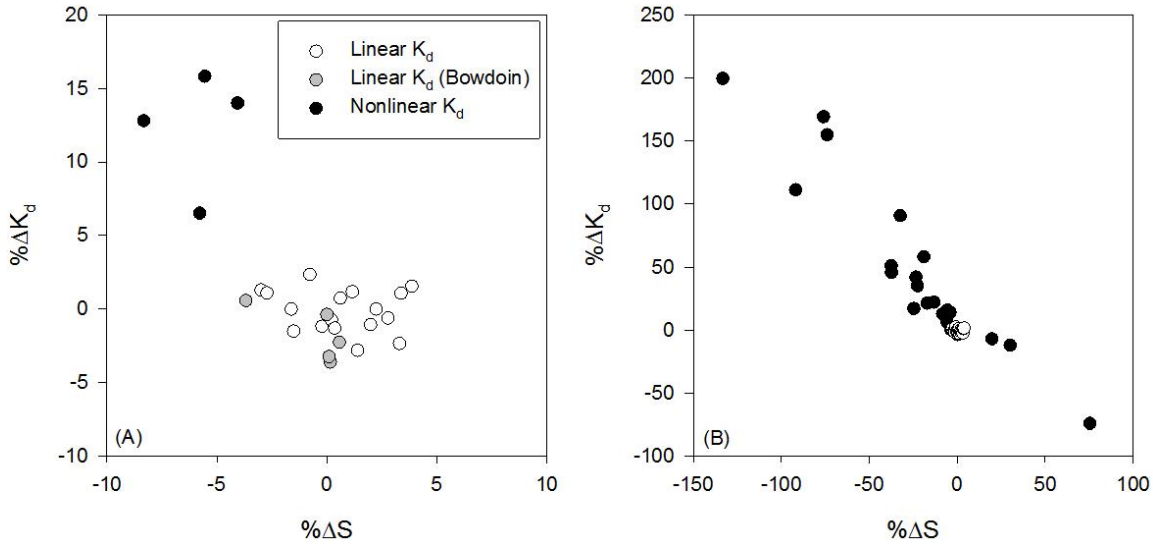

Figure 2.3. Relationship between $\%\Delta K_d$ and $\%\Delta S$ for (A) paired C_s and C_w values near the linear range of the sorption isotherm and (B) all sorbate-sorbent pairs in linear and non-linear range shows that changes in skewness of less than |± 4%| were associated with single-point K_d values that varied by 5% or less from independently assessed 'linear' K_d values (white circles, U. Connecticut; grey circles, Bowdoin College).

2.5 Supporting Information

2.5.1 Additional information on comparison of isotherms obtained from batch and column studies

Paired C_w and C_s values obtained from individual injections to the columns were nearly identical to values obtained from batch reactors assembled under the same experimental conditions (white *v.* black symbols, Fig. 2.4). Data shown in Fig. 2.4 includes compound-sorbent pairs that validate the column chromatography method against batch experiments for approximately linear isotherms where $n \approx 1$ of 2,4-dichlorbenzylamine to Na-montmorillonite (Fig. 2.S1A) and benzylamine to Na-montmorillonite (Fig 2.S1B). In addition, nonlinear isotherms for phenyltrimethylammonium on Ca-montmorillonite ($n > 1$, Fig. 2.S1B) and benzylamine to Na-illite ($n < 1$, Fig. 2.S1D) were also captured by column chromatography. The close agreement of this range in sorption scenarios indicates that isotherms collected by column chromatography reproduce those of traditional batch experiments.

We found that the column chromatography method is easily transferred between systems. Paired C_w and C_s values obtained using column chromatography at U. Connecticut and Bowdoin College were also nearly identical for phenyltrimethylammoiumn on Ca-montmorillonite (white squares without and with a plus, Fig 2.4B). Beyond the compounds examined in this study, K_{d_Linear} values for the cationic pharmaceuticals tramadol, propranolol, and trimethoprim, on Ca-montmorillonite were not significantly different between the two systems with K_{d_Linear} values of 530 ± 47, 1172 ± 102, and 1247 ± 108 L/kg respectively on the U. Connecticut system and 536 ± 35, 1325 ± 21, and 1174 ± 11 L/kg at Bowdoin College. Finally, both

setups showed that %ΔS of |± 4%| could be used to identify paired C_s and C_w values in the linear range of the sorption isotherm. With some optimization prior to use, we have clearly shown that this column method yields identical K_d measures across laboratories with distinct HPLC instrumentation.

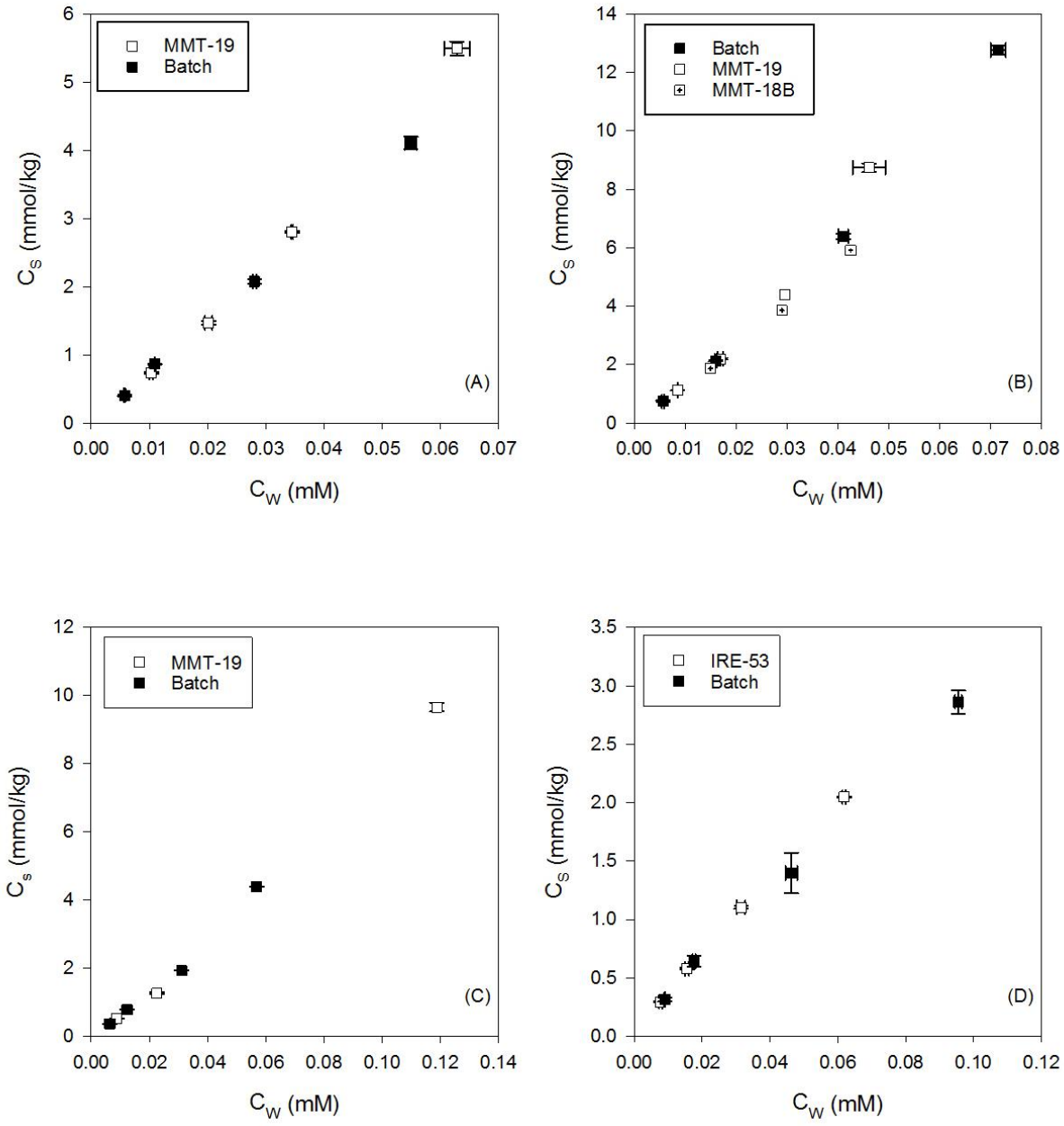

Figure 2.S1. Sorption isotherms obtained from column and batch experiments for (A) 2,4 dichlorobenzylamine on Na-montmorillonite, (B) phenyltrimethylammonium on Ca-montmorillonite, (C) benzylamine on Na-montmorillonite, and (D) benzylamine on Na-

illite. Both measurement methods capture the same trends in isotherm non-linearity. Black squares – batch data; white squares - column MMT-19 or ILL-53; white squares with black "+" – column MMT-18B; grey squares - column MMT-5. Where not visible, error bars are smaller than the symbol size.

2.5.2 Guide for method implementation

To implement column chromatography on an independent system, we recommend performing preliminary batch experiments or matching sorption coefficients from the literature. Matching sorption coefficients provides an increased level of accuracy when determining experimental conditions (i.e. flow rate, column packing ability). For new users interested in organic cations, we recommend starting with benzylamine or phenyltrimethylammonium sorption to Na- or Ca- montmorillonite at our experimental conditions.

To begin method implementation, start by packing a column with only SiC or another inert substance used to 'dilute' the sorbent of interest. To check the degree to which the column is packed, confirm that estimated column void space from the density and mass of the added solids matches that calculated by the difference in retention times of a tracer flowing through the system with and without a column attached. In addition, if multiple peaks or peak shoulders are present, the column may not be packed properly. Next, vary tracer and compound injection volume (by varying the injection loop) on the SiC-only column to find a volume that yields peaks with low skew without sacrificing detection limits due to compound solubility. A difference of note between the two systems of this study was the use of a larger injection volume used at Bowdoin College. It was found that if the injection volume did not match the volume of the injection loop in the HPLC,

then the skewness of the eluting peak increased, resulting in sorption coefficients that were distinctly different between the two set-ups. Finally, the higher sensitivity of the Bowdoin College detector required the using of 210 nm detection wavelength with a 10 nm bandwidth for detection. Therefore, we recommend optimizing the detector and obtaining robust signal-to-noise ratios prior to column operation.

Once optimization is complete on the SiC only column, proceed to packing a sorbent column. When packing a sorbent-SiC column when K_d values are known, pack the column with sorbents/SiC mixture that will provide separation of tracer and compound at least 50% greater than the compound retention time on SiC-only column. Again, check packing procedures by confirming estimated void space. On the sorbent-SiC column, multiple peaks or peaks with shoulders are caused by either channelization or a heterogeneous sorbent/SiC mixture. Finally, vary flow rate in the system to ensure equilibrium sorption is occurring. If K_d values are significantly higher at a lower flow rate, kinetic effects are present and the flowrate should be decreased until no changes in K_d are observed. We recommend performing experiments at the highest flow rate that does not cause for non-equilibrium sorption, decreased accuracy in sorption coefficients, or increased skew. Further optimization of the injection volume may be needed if flowrate is changed. Once sorption coefficients are matched, perform isotherms experiments for a compound with an isotherm where $n \neq 1$. Determine for the new system a range in %ΔS values that ensures linearity of the point sorption coefficients, decreasing future labor intensity. Once these optimization procedures are completed move onto more compounds and other solids. If more columns with the same solid are needed for detection limit reasons, we recommend overlapping sorbent loading of the columns so

that K_d values at the upper range of the established column are the low range of the new column. The overlap allows for a check of packing procedures of the new column.

If sorption coefficient data is not available and initial experiments must be performed using column chromatography, pack column with small ratio of sorbent to SiC (e.g (1-5) sorbent to 1000 SiC) and increase mass until separation is clear. Then perform optimization procedures detailed above.

3.0 Predicting organic cation sorption coefficients: Accounting for affinity and abundance of exchange ions using a simple probe molecule

3.1 Abstract

With the increasing number of emerging contaminants that are cationic at environmentally relevant pH values, there is a need for robust predictive models of organic cation sorption coefficients (K_d). Current predictive models fail to account for the differences in the identity, abundance and affinity of inorganic exchange ions naturally present at negatively charged receptor sites on environmental solids. To better understand how organic cation sorption is influenced by inorganic exchange ions, sorption coefficients of ten organic cations (including eight pharmaceuticals) were determined for six homoionic forms of the aluminosilicate mineral, montmorillonite. Organic cation sorption coefficients exhibited consistent trends across the various homoionic clays decreased as follows: $K_d^{Na+} > K_d^{NH4+} \geq K_d^{K+} > K_d^{Ca2+} \geq K_d^{Mg2+} > K_d^{Al3+}$. This trend for competition between organic cations and exchangeable inorganic cations is consistent with the inorganic cation selectivity sequence, determined for exchange between inorganic ions. Minor exceptions (Ca^{2+} vs Mg^{2+}) for organic cations with polar moieties were likely caused by interlayer hydration effects. Such consistent trends in competition between organic and inorganic cations suggested that a simple probe cation, such as phenyltrimethylammonium or benzylamine, could capture soil-to-soil variations in native inorganic cation identity and abundance for the prediction of organic cation sorption to soils and soil minerals. Indeed, sorption of two pharmaceutical compounds to 30 soils was better described by phenyltrimethylammonium sorption than by measures of benzylamine sorption, effective cation exchange capacity alone, or a model from the literature (Droge & Goss, *Environ. Sci. Technol.*, 2013, 47, 14224). Scaling factors derived from

existing models of organic cation sorption allowed for extrapolation of phenyltrimethylammonium K_d values to estimate K_d values for the sorption of more structurally complex organic cations to homoionic montmorillonites and to soils (root mean square error = 0.27 log units). Accordingly, the use of phenyltrimethylammonium as a probe compound was concluded to be a promising means to account for the affinity and abundance of natural exchange ions in the prediction of organic cation sorption coefficients for environmental solids.

3.2 Introduction

A growing number of environmental contaminants of interest, including pharmaceuticals, surfactants, and ionic liquids, are positively charged under environmentally relevant pH values, creating the need for accurate sorption models for organic cations.[1,5,31,32] Cation exchange, a process by which an organic cation replaces a naturally occurring inorganic cation balancing a negatively charge surface site, is a dominant mechanism of sorption to soils and sediments.[11,55,57] Traditional prediction approaches (*i.e.*, EPISUITE[9]), developed for neutral compounds, inaccurately predict sorption coefficients of organic cations because these models do not account for both the hydrophobic exclusion and the cation exchange interactions that organic cations undergo when sorbing to soils and soil minerals.[11,55,57] An empirical sorption model, recently proposed by Droge and Goss,[12] incorporates both hydrophobic and cation exchange contributions to organic cation interactions with clay minerals, organic matter, and soils. Organic cation sorption coefficients (K_d) are predicted from input parameters including molar volume, amine type (*e.g.*, primary, secondary, or tertiary) and corrective factors for structural moieties of the sorbate compound (*e.g.*, additional aromatic rings, -Cl), and cation exchange capacity of the solid (see SI for detailed model descriptions).[10,12,13,29] However, the predictive capacities of the Droge and Goss model are limited to homoionic calcium systems with an empirical correction (+1 log unit) to extrapolate to

homoionic sodium systems.[12] With the many inorganic cations that naturally balance negative charge sites on soils (*i.e.*, Na^+, Ca^{2+}, Mg^{2+}, K^+, Al^{3+}), accurate predictive models for organic cations must account for the different exchange affinities of inorganic cations that compete for the same sorption sites.[22,23,58] This study aimed to account for the distinct affinities of exchangeable inorganic cations on the sorption of organic cations and to evaluate whether the existing Droge and Goss models could be extended to account for sorbate structure effects.

While each inorganic cation has a distinct affinity for negative charge sites in soils, regular, predictable trends in cation exchange between inorganic cations have been observed. The selectivity series, a function of valence charge and hydrated radius, defines a sequence of increasing affinity of inorganic cations for soils:[22,23]

$$Li^+ \approx Na^+ < NH_4^+ \approx K^+ < Mg^{2+} < Ca^{2+} < Al^{3+} \qquad \text{(Sequence I)}$$

Thus, it is expected that increased affinity of the exchanging inorganic cation should cause increased competition, or reduced sorption coefficients, for organic cation sorbates. Trends consistent with this sequence of affinity have been observed for inorganic cation charge (*i.e.*, +1 vs. +2) in a study of cationic pyridine, purine and nucleoside sorption to homoionic Na^+-, Li^+-, Ca^{2+}- and Mg^{2+}-montmorillonite.[59] Ca^{2+}- and Mg^{2+}-montmorillonite showed lower sorption coefficients for these organic cations than did Na^+- and Li^+-montmorillonite. Such a trend between Ca^{2+}- and Na^+-saturated aluminosilicate clay minerals was also observed for a more extensive set of organic cations by Droge and Goss.[13] However, sorption coefficients for organic cations did not always decrease with increasing ionic radius of the saturating ion, as expected from the sequence of affinity.[59] While Li^+- and Na^+-saturated montmorillonite showed a similar extent of organic cation sorption (± 3%), sorption of organic cations to Mg^{2+}-montmorillonite was suppressed more so than for Ca^{2+}-montmorillonite.[59] This deviation from the anticipated sequence of inorganic cations (seq.

I) indicates that other properties, such as the hydration of the inorganic cation may contribute, along with cation exchange affinity, to influence trends in sorption of organic cations to homoionic montmorillonites. Therefore, identifying an affinity sequence of inorganic cations when being replaced with organic cations will greatly improve the understanding and predictive capability of organic cation sorption to soil components and, ultimately, soils.

Predictions of organic cation sorption to soils introduces the additional need to account for a heterogeneous distribution of exchangeable inorganic cations that varies across soil types.[23,24,60] Predictive models for cation sorption to soil that use soil cation exchange capacity (CEC) are only moderately successful because CEC only captures abundance of negatively charged receptor sites, providing a bulk measure not dependent on the composition of inorganic cations associated with the soil. In the absence of robust predictive models accounting for each individual exchange ion, it may be possible to account for complex variations in cation abundance through the use of a cationic probe compound.[61] Here, we propose that a cationic probe compound with a simple structure, such as benzylamine or phenyltrimethylammonium (PTMA) (Figure 3.S1), could account for abundance and affinity of naturally-occurring exchangeable cations by accessing the overall organic cation exchange affinity of a soil or soil mineral.[61] Further, sorption coefficients for organic cations, i, ($K^{i}_{d,pred}$) can be predicted from experimentally-determined sorption coefficient of the probe compound to that particular soil ($K^{probe}_{d,expt}$) and structural scaling factors (S^{i}_{soil}) that capture the free energy differences in sorption arising from structural differences between the organic cation of interest and the probe compound :

$$K^{i}_{d,pred} = K^{probe}_{d,expt} \times S^{i}_{soil} \quad (3.1)$$

Differences in structure manifest in both hydrophobic and electrostatic contributions to sorption interactions[15,35] and could be determined experimentally or using empirical predictive models.[12]

With the limited application to date of probe compounds for prediction sorption of other ionic organic compounds,[17,61] there is a need to evaluate whether probe compounds could be used to quantitatively account for the affinity and abundance of exchangeable inorganic cations using an extensive soil set. (Note that our emphasis herein are conditions of low sorbate surface coverage where linear isotherms are applicable.)

This study is aimed at improving the predictive capability of organic cation sorption to soils. To this end, we (i) identify the influence of exchangeable inorganic cation identity on the extent of organic cation sorption to homoionic montmorillonite and incorporate an additional parameter into the Droge and Goss model for sorption to aluminosilicate clays; (ii) establish measures of probe cation sorption ($K^{probe}_{d,expt}$) for heteroionic systems (aluminosilicate minerals and soils) that accesses overall organic cation exchange affinity of a soil or soil mineral, while accounting for the identity, abundance and affinity of naturally-occurring exchangeable inorganic cations; and (iii) leverage the Droge and Goss models for sorption to aluminosilicate minerals and organic matter to delineate scaling factors (S_i) and incorporate measures of probe sorption ($K^{probe}_{d,expt}$) to develop improved predictive models for organic cation sorption to aluminosilicate minerals and soils (Eq. 3.1).

3.3 Methods

3.3.1 Sorbents and chemicals

Texas Ca-montmorillonite (STx-1, CEC = 0.844 meq kg^{-1}) was obtained from the Clay Minerals Society. Silicon carbide (SiC) was from Alfa Aesar. Thirty soil samples were collected from 28 sites across the eastern United States as part of an earlier study by Jones *et al.*[54] Soils were previously characterized for native soil pH, effective cation exchange capacity (ECEC), and

concentrations of exchangeable Na^+, K^+, Ca^{2+}, Mg^{2+}, and Al^{3+} (Table S1). Sorbate compounds PTMA, benzylamine, serotonin, metoprolol, tramadol, propranolol, desipramine, atenolol, trimethoprim, and diltiazem (Fig. 3.S1) were from Sigma Aldrich. All other chemicals and reagents were ACS grade. Solutions were made with high purity 18.2 MΩ water (DI water) from a MilliQ system (Waters).

3.3.2 Sorption to Homoionic Montmorillonite: K_d Values Obtained by Column Chromatography

Pulse input column chromatography was used to obtain sorption coefficients for 10 organic cations (Figure S1) to six homoionic montmorillonite systems. Columns were carefully packed with mixture of montmorillonite (MMT) and inert SiC. Following methods detailed previously,[62] montmorillonite-to-water ratios of 19, 5, and 0.75 g L^{-1} were used in individual columns to balance compound retention against peak spreading. A comparative control column was packed entirely with SiC to verify that test compounds had no sorptive interactions with this inert solid. Packed columns were loaded into a standard HPLC system (Jasco PU-980 pump, AS-950 auto sampler, 40 µL injection loop, and MD-1510 multiwavelength detector). Montmorillonite was converted to homoionic Na^+-, NH_4^+-, K^+-, Ca^{2+}-, and Mg^{2+}-forms by flushing the respective column with air-equilibrated (pH 6 ± 0.3), 15 mM (NaCl, NH_4Cl, KCl) or 5 mM ($CaCl_2$, $MgCl_2$) solutions for 24 hrs before compound injection. Al^{3+}-montmorillonite (Al-MMT) was created by flushing with 2.5 mM $AlCl_3$ adjusted to pH 3 (HCl). Flushing solutions were designed to have identical ionic strengths, and also served as the experimental background solutions (eluent) for experiments on the respective clays. An operating flowrate of 100 µL min^{-1}, previously determined to allow sorptive equilibrium to montmorillonite,[62] was used for all experiments.

The concentration of test compounds injected into the column was varied from 4.3×10^{-6} to 2.6×10^{-4} M to create sorption isotherms. Triplicate injections of each concentration were made or

on both the 'SiC-only' and the 'montmorillonite-SiC' columns. Absorbance *vs.* time data collected following each injection were exported directly to a MATLAB routine to calculate retention times from the eluted compound peaks in the chromatograms.

Single-point K_d values (kg L^{-1}) were calculated from the eluent volume required to elute compounds from a column, V (L), and the column sorbent mass, m (mg)[20]:

$$K_d = \frac{V}{m} = \frac{Q * \left[\left(t_{cmpd} - t_{tracer}\right) - \left(t_{cmpd-SiC} - t_{tracer-SiC}\right)\right]}{m} \quad (3.2)$$

where V was calculated from Q (L min^{-1}), the eluent flow rate, and the effective travel time denoted by the bracketed term which represents the travel time of the compound in contact with only the montmorillonite in the montmorillonite-SiC column. All times (t_i, min) were calculated by integrating the corresponding peak to obtain the center-of-mass: t_{cmpd} and $t_{cmpd\text{-}SiC}$ are the compound travel times through the 'montmorillonite-SiC' and 'SiC-only' columns, respectively, and t_{tracer} and $t_{tracer\text{-}SiC}$ are the nitrate tracer travel times through the 'montmorillonite-SiC' and 'SiC-only' columns, respectively. Points were assumed to be in the linear range of the isotherm if two or more initial concentrations had similar K_d values (within 1 standard deviations of each other) and skewness values of runs on 'montmorillonite-SiC' columns matched (within 4%) those on the 'SiC-only' column.[62] All K_d values were determined to be in the linear range. Henceforth, $K_d^{X\text{-}MMT}$ will be used to specify sorption onto a particular homonionic montmorillonite, with X being either Na^+-, NH_4^+-, K^+-, Ca^{2+}-, Mg^{2+} or Al^{3+}.

3.3.3 Sorption to Soils: K_d from Batch Sorption Experiments

Sorption of four organic cations (benzylamine, PTMA, tramadol, and desipramine) to 30 soils was measured using standard batch experiments. Column chromatography was not utilized to evaluate sorption to soils because eluting columns with DI water or a background electrolyte (NaCl

or $CaCl_2$) would modify the identity and abundance of naturally occurring exchangeable inorganic cations on the soil. A predetermined mass of soil (see SI, *Batch Sorption and HPLC Methods*, for details) was placed in a 15-mL centrifuge tube and 10 mL of 5×10^{-5} M solution (pH 6-7) of the test compound prepared in deionized water was added. Soil-free reactors, which were prepared in the same manner, provided a measure of initial concentration and allowed us to confirm the absence of other loss processes. Soil-free and soil-containing reactors were rotated end-over-end for 18-24 hr (based on preliminary kinetic experiments) in the dark to allow sorption to reach equilibrium. Then, solutions from the soil-free reactors and supernatant from the soil-containing reactors were filtered with 0.45 µm nylon filers, dispensed into clean HPLC vials and centrifuge tubes for analysis of initial or equilibrium aqueous (C_w, mol L^{-1}) concentration and pH, respectively. Aqueous concentration values were measured by high performance liquid chromatography with diode array detector (HPLC-DAD) using an Agilent 1100 Series system (see SI for HPLC methods). Corresponding sorbed compound concentrations (C_s, mol kg^{-1}) were calculated by difference, and K_d values were then obtained as:

$$K_d = \frac{C_s}{C_w} \tag{3.3}$$

All experiments were performed in triplicate at native soil pH. Desorption experiments using $BaCl_2$ were used to confirm that loss from solution was primarily due to sorption phenomena.

3.4 Results and Discussion

3.4.1 Effect of cation identity on organic cation sorption to homoionic montmorillonite

To identify a sequence of exchangeable inorganic cation affinity when inorganic cations are replaced with organic cations, we evaluated the sorption of ten organic compounds (Fig. 3.S1), including eight pharmaceuticals, onto six homoionic montmorillonite clays. For most of the

organic cations examined, K_d values for sorption to homoionic montmorillonite saturated with monovalent cations (Na-MMT, NH_4-MMT, K-MMT) were greater than K_d values for divalent (Ca-MMT and Mg-MMT) and trivalent (Al-MMT) homoionic montmorillonite (Figure 3.1). The resulting K_d sequence is denoted below: :

$$K_d^{Na\text{-}MMT} > K_d^{NH4\text{-}MMT} \geq K_d^{K\text{-}MMT} > K_d^{Ca\text{-}MMT} \geq K_d^{Mg\text{-}MMT} > K_d^{Al\text{-}MMT} \quad \text{(Sequence II)}$$

Using $K_d^{X\text{-}MMT}$ as a measure of the extent to which exchangeable inorganic cation X^{n+} suppresses organic cation sorption, the following sequence of affinity for exchangeable inorganic cations when replaced with organic cations on the montmorillonite surface was indirectly defined:

$$Na^+ < NH_4^+ \leq K^+ < Ca^{2+} \leq Mg^{2+} < Al^{3+} \quad \text{(Sequence III)}$$

Sequence II and III suggest that increased affinity of inorganic cations results in lower sorption coefficients for the organic cation on the corresponding homoionic montmorillonite. Sequence I (exchange between inorganic cations) and Sequence III (replacement of an inorganic cation by an organic cation) are generally similar with exception of Ca^{2+} and Mg^{2+} affinities, discussed in later.

Sequence III is defined predominantly by the charge of the inorganic cation, as sorption coefficients decrease for montmorillonite exchanged with inorganic cations of increased charge (Fig. 3.1). The higher the charge of the exchangeable inorganic cation, the higher the energy required to remove it from negatively charged receptor sites on the montmorillonite surface.[13,22,25] For inorganic cations with the same charge, ionic radius (and the resulting influence on the hydration sphere) further influences the affinity sequence. The large ionic radii of NH_4^+ and K^+ lowers the energy required for these ions to shed hydrating water molecules, thereby allowing these ions to sit closer to the negatively charged sites of clay minerals, in comparison to hydrated Na^+.[22,63,64] This smaller distance of interaction between the exchangeable inorganic cation and a

negatively charged site increases the affinity of the inorganic cation for the site and consequently, the energy needed to replace it with an organic cation. As a result, decreased sorption coefficients were obtained for NH_4^+-and K^+-montmorillonite (Fig. 3.1), compared to Na^+-montmorillonite for all compounds except metoprolol. Since K^+ has a slightly larger ionic radius and a higher selectivity coefficient compared to NH_4^+,[65] sorption coefficients of all compounds to K^+-montmorillonite were lower than, or not significantly different (t-test $p > 0.05$) than sorption coefficients for NH_4^+-montmorillonite.

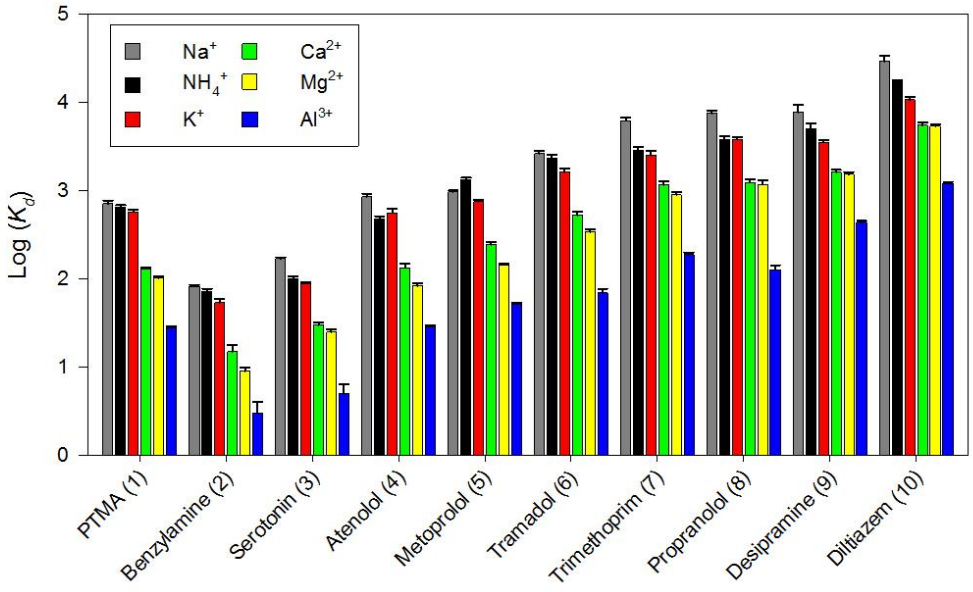

Figure 3.1. Sorption coefficients (Log K_d) of organic cations to Na^+ (grey), NH_4^+ (black), K^+ (red), Ca^{2+} (green), Mg^{2+} (yellow), and Al^{3+} (blue) exchanged montmorillonite follow a general pattern of decreased sorption with increased exchangeable inorganic cation charge. Compound numbers refer to structures found in Fig S1.

As noted earlier, Sequence I and III are distinct with respect to Ca^{2+} and Mg^{2+} affinities: for exchange between inorganic cations (Sequence I) the affinity of Mg^{2+} is less than Ca^{2+}, whereas Ca^{2+} exhibits a lesser affinity for the montmorillonite surface than Mg^{2+} with the exchange of an

organic cation (Sequence III). This trend is consistent with the hydration of the interlayer being an important factor in the sorption of organic cations, especially with respect to montmorillonite saturated with divalent cations. The smaller Mg^{2+} cation is more strongly hydrated, when balancing the charge within the montmorillonite interlayer, thereby causing water molecules within the interlayer to be more structured than for larger inorganic cations, such as Ca^{2+}.[66-68] This ordering of the water molecules within the interlayer appears to diminish the affinity of organic cations for the interlayer charge sites as lower sorption coefficients were seen for montmorillonite exchanged with Mg^{2+} than for Ca^{2+}-montmorillonite (Fig 3.1). This trend was apparent for most compounds (compounds 1-7, Fig 1) and may arise from either the increased energy required for an organic cation to exchange with the entire hydrated Mg^{2+} ion, or from the organic cation being hindered from entering the interlayer by the ordered water molecules.[68] This trend ($K_d^{Ca\text{-}MMT} > K_d^{Mg\text{-}MMT}$) was less evident for larger compounds with polycyclic ring structures (propranolol, desipramine and diltiazem, Fig. 1) which had sorption coefficients for Mg^{2+}-montmorillonite that were not significantly different (t-test, $p > 0.05$) than for Ca^{2+}-montmorillonite. The multi-ring, C-rich characteristics of compound 8-10 structures (Fig. S1) may to contribute to an increased driving force for these compounds to be excluded from the bulk solution, as compared to the more polar structures of compounds 1-7. Enhanced compound exclusion from bulk solution may either overcome the energy required to exchange with the entire hydrated ion or provide the energy required to disrupt the hydration shells of the Mg^{2+} ion.[6] Thus organic cation exchange to montmorillonite saturated with divalent cations is influence by both inorganic cation hydration and organic cation structure.

We obtained sorption isotherms for ten organic cations to six homoionic clays and found that most organic cation-montmorillonite combinations followed Sequence III. Therefore, the

unique contribution of this study is the knowledge that organic cations have a consistent sequence of affinity (*i.e.*, III) for the montmorillonite surface when being the replaced with an organic cation; this in turn indicates that, on average, exchange ions influence sorption of organic cations in a predictable manner.

3.4.2 Quantification of exchangeable ion contribution to K_d: Extension of the Droge and Goss Model for homoionic clays

Because inorganic cations showed a regular influence on organic cation sorption, we looked to extend the Droge and Goss model to homoionic clays. Our experimentally determined K_d values for the sorption of ten organic cations to six homoionic clays (Table 3.S3) were used to quantify exchange ion affinity, $Ex_{ion\text{-}X}$. Ca^{2+}-montmorillonite was used as the reference homoionic clay so that $Ex_{ion\text{-}Ca}$ was defined to be '0', in keeping with the Droge and Goss model being derived for Ca^{2+}-saturated montmorillonite. For the other five exchangeable cations (X^{n+}= Na^+, NH_4^+, K^+, Mg^{2+} and Al^{3+}), we defined $Ex_{\text{ion-X}}$ as follows:

$$Ex_{ion-X} = \frac{\log K_d^{X-MMT} - \log K_d^{Ca-MMT}}{CEC} \tag{3.4}$$

where $K^{X\text{-}MMT}_d$ (L/eq) is the experimentally determined K_d value for the montmorillonite homoionic is cations X and CEC (eq/kg) is the cation exchange capacity of the montmorillonite. For each individual cation, $Ex_{ion\text{-}X}$ values were remarkably similar across the ten test cations examined and the average $Ex_{ion\text{-}X}$ values were determined to be 0.85 ± 0.06 for Na^+, 0.65 ± 0.12 for NH_4^+, 0.58 ± 0.13 for K^+, -0.15 ± 0.09 for Mg^{2+} and 0.90 ± 0.13 for Al^{3+}. The empirically-derived $Ex_{ion\text{-}X}$ parameter was added to the structure-based model for organic cation sorption to Ca^{2+}-aluminosilicate minerals developed by Droge and Goss[13] to extend to other homoionic clays:

$$\log\left(\frac{K_{d,pred}^{X-MMT}}{CEC}\right) = 1.22Vx - 0.22NAi + 1.09 \pm CF_{clay} + Ex_{ion} \quad (3.5)$$

where V_x (L mol^{-1}) is the compound molar volume, *NAi* is the number of hydrogen atoms bonded to the cationic amine group, CF_{clay} are corrective factors for compound structural moieties (reproduced in Table 3.S5). Thus, the inclusion of the empirical correction term, Ex_{ion}, gives a resultant equation to account for competitive effects and distinct affinities of exchangeable cations . Notably, the empirically determined correction of +1 log unit recommended by Droge and Goss to extrapolate predictions to homoionic sodium clay minerals (15 mM NaCl) closely matches $Ex_{ion\text{-}Na}$ = 0.85 ± 0.06 determined in this study.

We compared the experimentally-determined K_d values using Eq. 3.5 and found good agreement (Fig. 3.2). The one exception using CF_{clay} values as defined by Droge and Goss occurred for compounds with ether moieties (-COC-). When CF_{clay} values were used as proposed by Droge and Goss[12], compounds that contained ether moieties gave predicted K_d values that were 2 to 10 times lower than measured values. Thus, no correction factor was used for ether groups in Eq. 3.5 (CF_{clay} for –COC- = 0, Tab. 3.S5). Our extension of the Droge and Goss model through incorporation of $Ex_{ion\text{-}X,}$ provided excellent correlation between the 60 experimental and predicted $K^{X\text{-}MMT}{}_{d,pred}$ values (Fig. 3.2). Further, predicted sorption coefficients of all compounds were within 0.3 log units (K_d factor of 2) of measured values for the homoionic systems studied (Fig. 3.2), making the use of the Ex_{ion} term a practical means to extrapolate predictive sorption coefficients from Ca^{2+}-aluminosilicate mineral systems to other homoionic systems.

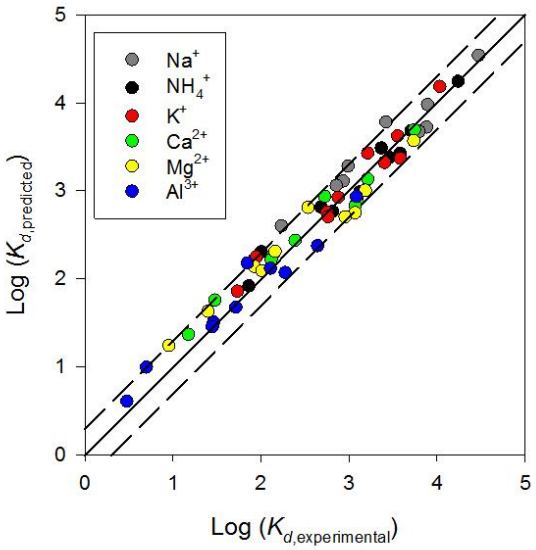

Figure 3.2. Predictions of sorption coefficients of cationic pharmaceuticals for homoionic Na^+ (grey circles), NH_4^+ (black circles), K^+ (red circles), Ca^{2+} (green circles) Mg^{2+} (yellow circles) and Al^{3+} (blue circles) montmorillonite are possible using the extended-Droge and Goss model[13] with empirical corrections ($Ex_{ion\text{-}X,}$ Eq. 3.5) for each exchange ion. Solid line is 1:1 and dashed lines represent ± 0.3 log units.

3.4.3 Probe organic cation sorption ($K^{probe}_{d,exp}$) to heteroionic aluminosilicate minerals and soils: accounting for the identity, abundance and affinity of exchangeable inorganic cations

We evaluated the potential for using sorption coefficients of simple organic cations (probe compounds) to establish an aggregate measure of inorganic cation identity, abundance and affinity on aluminosilicate mineral-containing soils. Soils are heteroionic systems with negative charge receptors sites locally neutralized by a variety of different inorganic cations. Measurements of soil CEC capture the abundance of negatively-charged receptor sites, and quantitative analysis of the inorganic cations displaced in the measurement of CEC ($f(Ex_i)$- Eq, 3.S1, SI) reveals the composition of inorganic cations associated with the soil. The distinct affinities of these inorganic

cations in the context of sorption competitiveness are not captured by CEC or its associated measurements. These shortcomings were highlighted by examining trends in experimentally-determined $K_{d,expt}$ values for two structurally-simple organic cations (benzylamine and PTMA) and two pharmaceuticals (desipramine and tramadol) for 30 soils. As expected, regressions of log $K_{d,expt}$ for benzylamine, PTMA, desipramine and tramadol versus log $ECEC_{soil}$ revealed correlations that were statistically significant ($p < 0.05$), but weak; R^2 values of were 0.60 (benzylamine), 0.48 (PTMA), 0.65 (desipramine), and 0.54 (tramadol) (Fig. 3.3, Fig 3.S3). The wide range in organic cation log $K_{d,expt}$ values for soils with the same, or similar, ECEC values (Fig. 3.3) indicated that soil ECEC values alone did not capture the heterogeneity factors of exchangeable inorganic cation identity and/or negative charge site location (*e.g.*, different clay types or organic matter). Consistent with this site heterogeneity, data points that fell below the best-fit correlation line corresponded to soils that tended to have higher relative abundances of exchangeable aluminum (*e.g.*, Adams and Peru soils, Tab. 3.S1). This trend suggested that exchangeable Al^{3+} may hinder sorption to soils more so than other cations, in agreement with our experimental results with homoionic montmorillonite systems. The existing soil-to-soil variations in native exchangeable inorganic cations are, therefore, exceedingly important for predicting sorption coefficients of organic cation.

We note that currently available models[12] for predicting organic cation sorption coefficients to soils were derived under conditions that Ca^{2+} was the primary exchange ion occupying soil negative charge sites. As such, this model (Eq. 3.S6, SI) was also not successful for predicting organic cation sorption in heteroionic soil systems (see Fig. 3.S2 and associated discussion in SI). Further, parameters such as $Ex_{ion\text{-}X}$ (Eq. 3.4) cannot be incorporated into existing soil organic cation sorption models (Eq. 3.S6, SI) because it is not possible determine whether the exchangeable inorganic cations balance negatively charged receptor sites on an aluminosilicate clay mineral or on

organic matter. Our observations (Fig. 3.3 and Fig. 3.S2), coupled with consistent $Ex_{ion\text{-}X}$ values across several organic cations, clearly show that an experimentally-determined aggregate parameter (such as $K^{probe}_{d,expt)}$ that accounts for the affinity, abundance and identity of exchangeable inorganic cations is required for the successful prediction of sorption coefficients for soils. Cationic sorbate and probe compounds should each respond similarly to the relative affinities of the distribution of inorganic cations that balance negative charge sites on heterionic sorbents and thus, sorbate sorption should be proportional to probe compound sorption.

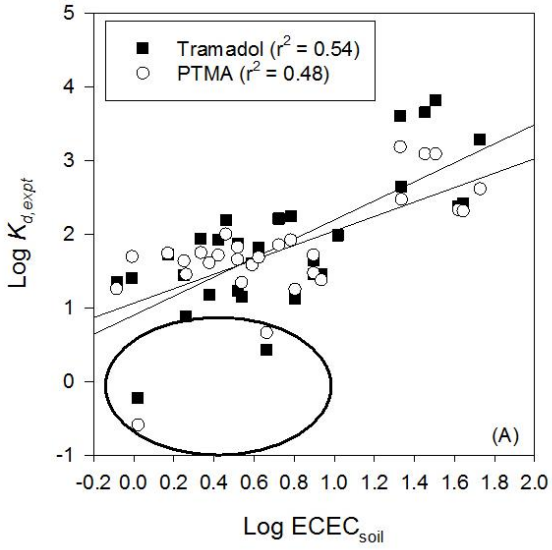

Figure 3.3. Correlation of sorption coefficients of tramadol (black squares) and PTMA (white circles) for 30 soils versus log ECEC for the soils. Solid lines represent best fit regressions. Points well below the best fit line are associated with soils containing high exchangeable Al^{3+} content (circled).

To identity an appropriate probe cation, we evaluated the correlation between soil $K_{d,expt}$ values for simple structures benzylamine and PTMA (potential probes) and more complex, organic

cations (desipramine and tramadol) (Figure 4). Indeed, $K_{d,expt}$ values desipramine and tramadol were better correlated with sorption coefficients of benzylamine and PTMA than Log ECEC (Fig. 3.4 vs Fig. 3.3). As such, the sorption of simple organic cations is better suited to providing an aggregate measure of exchangeable inorganic cation identity, abundance, and affinity. In addition, desipramine and tramadol $K_{d,expt}$ values were better correlated with $K_{d,expt}$ values for PMTA than with $K_{d,expt}$ values for the primary amine, benzylamine (Fig 3.4A vs 3.4B). PTMA, a quaternary amine, seemingly captures sorption trends of higher order amines better than the primary amine, benzylamine. PTMA offers some additional practical advantages as a probe molecule: it is available in a salt form making it easier to prepare solutions than the liquid benzyl amine and the permanent positive charge allows application of PTMA as a cationic probe under any soil pH conditions. Thus, PTMA was concluded to be better-suited as a probe compound than benzylamine which we had proposed earlier as a potential candidate.[17]

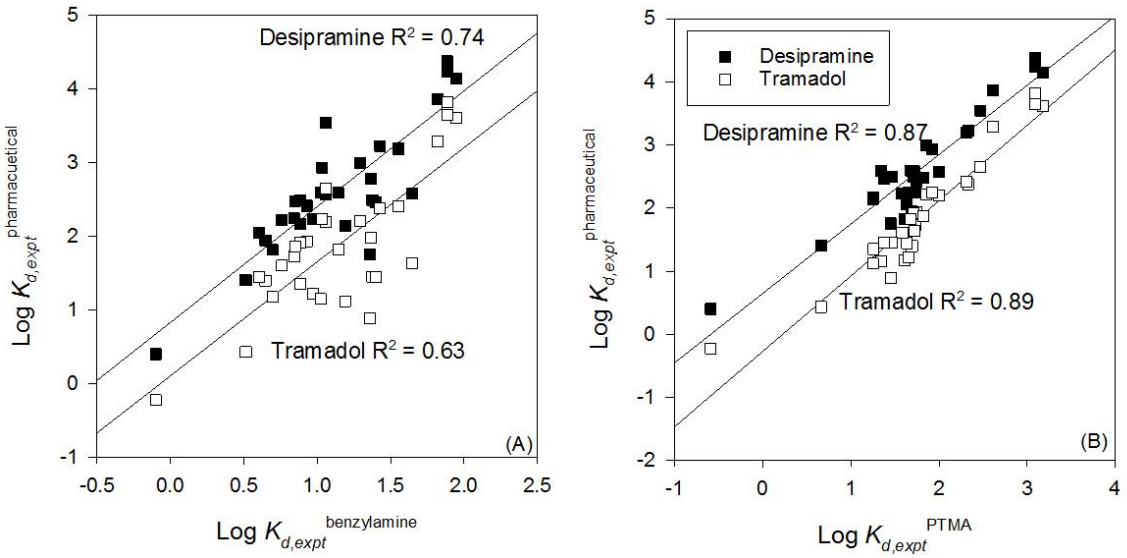

Figure 3.4. Correlations of soil Log $K_{d,expt}$ of desipramine (black squares) and tramadol (white squares) with (A) soil Log $K_{d,expt}^{benzylamine}$ and (B) soil Log $K_{d,expt,}^{PTMA}$. Solid lines represent best fit regression.

3.4.4 Delineation of scaling factors (Si) and incorporation ($K_{d,expt}^{probe}$) into a current predictive models for cation sorption

A probe cation can only be used in the prediction of sorption coefficients for other organic cation sorbates if scaling factors (S^i) can be determined for application in Eq. 3.1 after measurements of the probe compound sorption coefficients are obtained. Here, we utilize the structure-based models of Droge and Goss to estimate scaling factors.[10,12,13] Droge and Goss proposed empirical models for organic cation sorption to aluminosilicate mineral and organic matter components (Eq. 3.S3 and 3.S4) that utilizes parameters relevant to organic cation structure (*Vx, NAi,* and CF_{oc} or CF_{clay}) to estimate contributions to the overall soil K_d. Separate scaling factor are necessary to describe sorption interactions with these two soil components because organic cations interact with them differently, resulting in different multiplier sign and magnitude to describe structural contributions. We leveraged the Droge and Goss predictive models to delineate scaling factors (S^i) by considering the difference in parameter values between the organic cation of interest and our proposed probe compound, PTMA. We note that *NAi* PTMA is defined as 0 for quaternary amines. The resultant scaling factors when using PTMA as a probe compound are:

$$\log(S_{clays}^{i}) = 1.22(Vx_i - Vx_{PTMA}) - 0.22(NAi_i - NAi_{PTMA}) \pm (CF_{i,clay} - CF_{PTMA,clay}) \quad (3.6)$$

$$\log(S_{clays}^{i}) = 1.22(Vx_i - Vx_{PTMA}) - 0.22NAi_i \pm CF_{i,clay} \quad (3.7)$$

Note that Eq. 6 and 7 yield scaling factors that are normalized to the soil clay cation exchange capacity and soil fraction organic carbon sites, respectively.

We first validated the use of probe compound sorption with a scaling factor to predict K_d values for other compounds with our set of sorption data for homoionic montmorillonite. Sorption

coefficients for the nine test compound (all except PTMA) for the six homoionic clays were predicted with Eq. 3.1, using Eq. 3.6 to calculate scaling factors. Resultant $K^{X\text{-}MMT}_{d,pred}$ values were within 0.3 log units of the experimental values, indicating that PTMA could be used as a quantitative predictor of sorption coefficients for clay minerals (Fig. 3.5A). Estimation of clay sorption coefficients using a probe compound (Eq. 3.1) exhibits similar predicative capability for cation sorption as estimation with a structural model with direct adjustment for the inorganic cation identity by Eq. 3.5 (Fig. 3.2 vs. Fig. 3.5A). These results indicate that PTMA sorption implicitly accounted for influence of inorganic cation identify and affinity in these homoionic systems. With this proof of concept of probe compounds demonstrated for well-characterized sorbents, we then examined the same predictive capability in heteroionic soil systems.

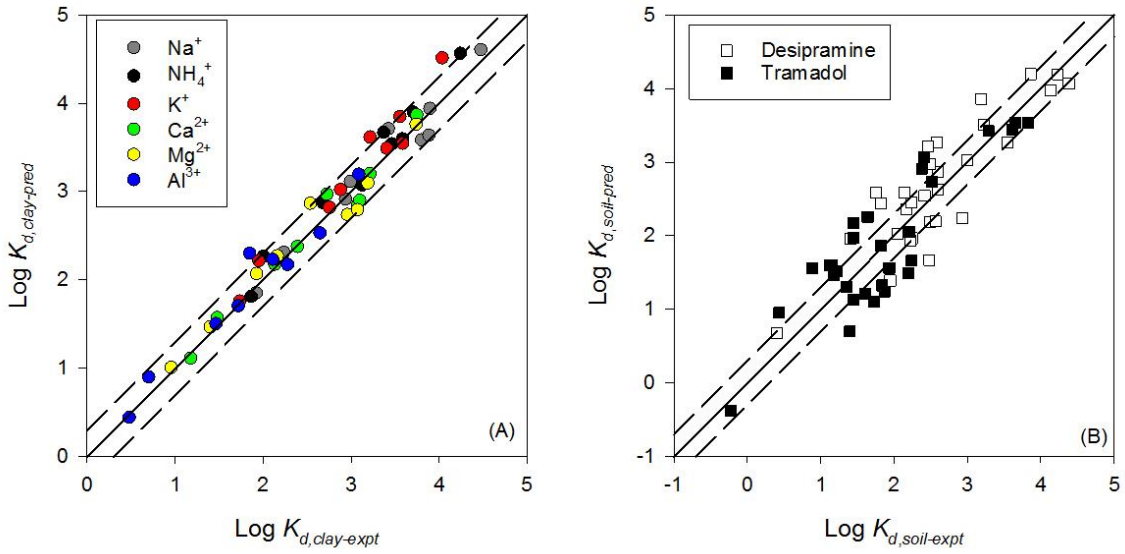

Figure 3.5. (A) The strong correlation between predicted and experimental clay K_d values (R^2 = 0.97, $p < 0.01$) indicate that $K_{d,expt}^{PTMA}$ and S^i_{clay} were able to account for different exchange ions without the use of empirical corrections ($Ex_{ion\text{-}X}$) for homoionic Na^+ (grey circles), NH_4^+ (black circles), K^+ (red circles), Ca^{2+} (green circles) Mg^{2+} (yellow circles) and Al^{3+} (blue circles) montmorillonite. (B) Soil K_d values for desipramine (white squares) and tramadol (black squares)

are well-predicted using $K_{d,expt}^{PTMA}$ with S^i_{clay} and S^i_{oc} . Solid line is 1:1 and dashed lines represent ± 0.3 log units.

Scaling factors for organic cation sorption to soils (S^i_{soil}) must be determined through the combination of individual scaling factors for both clay minerals (Eq. 3.6) and organic matter (Eq. 3.7). Since S^i_{clay} and S^i_{oc} were defined as normalized to the abundance of clay cation exchange capacity and organic carbon, respectively, the contributions of these components for a particular soil must be included. We followed the approach of the original Droge and Goss model development and calculated soil scaling factors, S^i_{soil}, according to:

$$S^i_{soil} = S^i_{clay} \times (CEC_{soil} - 3.4 f_{oc}) + S^i_{oc} \times f_{oc} \quad (3.8)$$

where the total clay CEC was obtained as the difference between the measured soil CEC and organic matter contributions, assuming a constant 3.4 meq of charge per fraction organic carbon.[12] For some of the soils studied, the value of (CEC_{soil} - 3.4 f_{oc}) was less than zero (Tab. 3.S3) so contributions of clay cation exchange capacity were assumed to be zero. Values of S^i_{soil} obtained by Eq. 3.8 were used in Eq. 3.1 with measured $K_{d,expt}^{PTMA}$ for PTMA on each of the soils to predict expected soil $K_{d,pred}$ values for tramadol, desipramine and benzylamine.

Predicted soil $K_{d,pred}$ values for tramadol and desipramine were well correlated to experimentally determined values on the 30 soils examined (Fig. 3.5B); the correlations are significantly stronger than correlation of experimental $K_{d,pred}$ values with soil ECEC (Fig. 3.3, Fig 3.S3) or with predicted values using the original Droge and Goss model for soils that does not account for varied inorganic cation affinity (Fig. 3.S2). Thus, the $K_{d,soil}$ for PTMA implicitly accounted for variations in native exchangeable inorganic cations identity, abundance and affinity. Our approach for estimating S^i_{soil} with Eq. 3.8 showed the greatest error (> 0.3 log units) for soils with (CEC_{soil} - 3.4 f_{oc}) < 0 such that scaling factors were determined from only organic carbon

contributions (data points with log $K_{d,expt}$ ~ 2 in Fig. 3.5). The assumption that there is no negatively charged receptor sites on clay minerals introduces error into our prediction, which was also seen in prediction of benzylamine sorption coefficients using PTMA as a probe (Fig 3.S4). Therefore, further work should focus on better estimation of CEC_{clay} for high organic matter soils

3.4.5 Outlook of PTMA as a cationic probe

The use of PTMA as an organic cationic probe compound is a promising option to account for the identity, abundance and affinity of exchangeable ions on environmental solids. Sorption of positively charged organic compounds depends on numerous environmental factors, including ionic strength, number of available sites, and identity of native exchange ions. These factors can by successfully captured by the soil $K_{d,pred}$ of a simple organic cation, PTMA, along with measures of soil CEC and f_{oc}. The permanent charge of PTMA allows for the quantification of cation exchange affinities at any pH, and the availability of PMTA as chloride salt from many suppliers makes solution preparation easy. Moving forward, advances in the determination of scaling factors between PTMA and complex organic cations using computational techniques will greatly improve sorption coefficient predictions.[15] Thus, the use of PTMA as a probe compound is a promising tool for the prediction of organic cation sorption coefficients for environmental solids.

3.5 Supporting Information

3.5.1. Sorbate structures

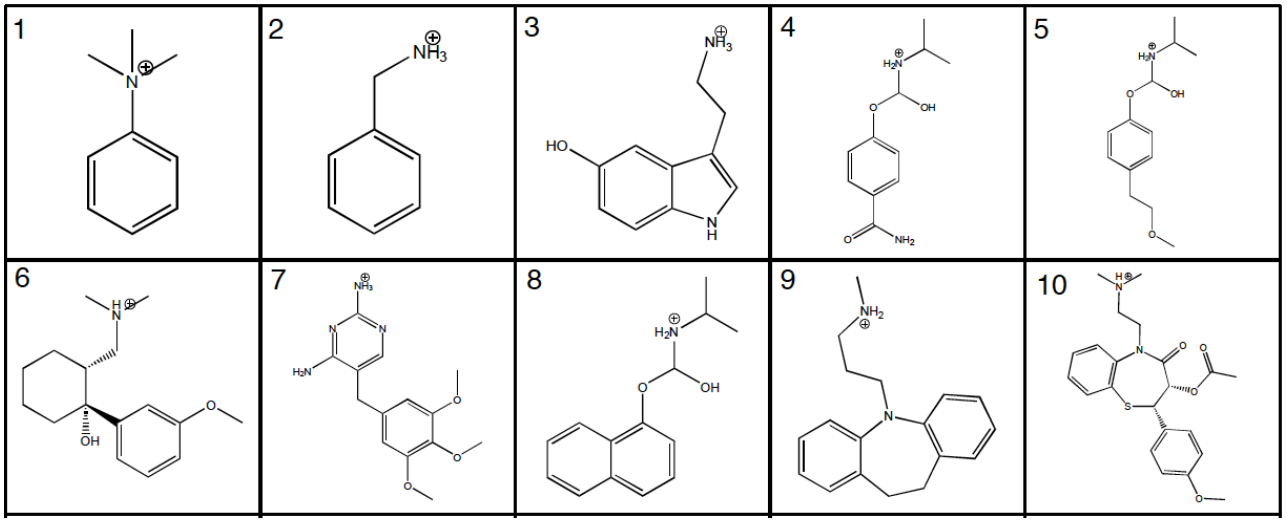

Figure 3.S1. Sorbate compound structures: (1) phenyltrimethylammonium, (2) benzylamine, (3) serotonin, (4) atenolol, (5) metoprolol, (6) tramadol, (7) trimethoprim, (8) propranolol, (9) desipramine, and (10) diltiazem

3.5.2. Soil Parameters

Thirty soil samples were collected from 28 sites across the eastern United States as part of an earlier study by Jones *et al.*[54] Soils were previously characterized for native soil pH, effective cation exchange capacity (ECEC), and concentrations of exchangeable Na^+, K^+, Ca^{2+}, Mg^{2+}, and Al^{3+} (Tab. S1). The fraction of exchange sites of which ion *i* was balancing (%Ex_i) was determined by:

$$f(Ex_i) = \frac{C_i * z_i}{ECEC_{soil}} \quad (3.S1)$$

where C_i (mol/kg) is the concentration of ion *i* on the soil and z_i is the cationic charge *(mol_c/mol)*.

Empirical predictive modeling required the determination of CEC contributed by clay minerals (CEC_{clays}). Following Droge and Goss (2013), it was assumed that that there is 3.4 meq of charge per fraction of organic carbon.[12] Therefore, CEC_{clays} was estimated as:

$$CEC_{clays} = (ECEC_{soil} - 3.4f_{oc}) \quad (3.S2)$$

However, for some of the soils studied, the assumption of 3.4 meq of charge per fraction organic carbon would result in a CEC_{clay} less than zero (Tab. 3.S3), for those soils, CEC_{clay} was assumed to be zero.

Table 3.S1. Soil Parameters

Soil	ECEC mol/kg	*f*oc	ECEC-3.4×foc	CEC_{clay}	*f*(Ex K)	*f*(Ex Na)	*f*(Ex Ca)	*f*(Ex Mg)	*f*(Ex Al)
Adams/SS	0.011	0.025	-0.07	0.00	0.02	0.02	0.06	0.01	0.89
Appling/SS	0.010	0.001	0.01	0.01	0.08	0.02	0.50	0.20	0.20
Ashe/SS	0.022	0.008	-0.01	0.00	0.05	0.01	0.35	0.23	0.36
Aycock/SS	0.026	0.004	0.01	0.01	0.12	0.01	0.54	0.12	0.22
Berryland/SS	0.008	0.017	-0.05	0.00	0.02	0.03	0.08	0.04	0.83
Burton/S	0.086	0.089	-0.22	0.00	0.02	0.00	0.05	0.02	0.90
Chewacla/SS	0.061	0.002	0.05	0.05	0.01	0.01	0.64	0.34	0.01
Codorus/SS	0.015	0.002	0.01	0.01	0.03	0.02	0.57	0.20	0.19
Colton/S	0.079	0.041	-0.06	0.00	0.01	0.00	0.89	0.10	0.00
Comus/S	0.035	0.025	-0.05	0.00	0.12	0.01	0.53	0.23	0.11
Enon/SS	0.029	0.002	0.02	0.02	0.01	0.02	0.05	0.16	0.75
Georgeville/S	0.024	0.008	0.00	0.00	0.06	0.01	0.09	0.37	0.48
Goldsboro/S	0.018	0.003	0.01	0.01	0.04	0.01	0.27	0.31	0.38
Hagerstown/S	0.104	0.031	0.00	0.00	0.05	0.00	0.82	0.12	0.00
Heiden/S	0.440	0.039	0.31	0.31	0.01	0.00	0.97	0.02	0.00
Heiden/SS	0.416	0.013	0.37	0.37	0.01	0.00	0.98	0.01	0.00
Iredell/SS	0.214	0.005	0.20	0.20	0.01	0.01	0.42	0.54	0.02
Kleinpeter/S	0.053	0.019	-0.01	0.00	0.03	0.01	0.79	0.17	0.01
Leon/S	0.018	0.018	-0.04	0.00	0.01	0.02	0.13	0.05	0.81
Moreland/SS	0.216	0.005	0.20	0.20	0.02	0.00	0.77	0.22	0.00
Orangeburg/SS	0.039	0.002	0.03	0.03	0.11	0.01	0.54	0.34	0.00
Peru/SS	0.046	0.026	-0.04	0.00	0.01	0.01	0.06	0.01	0.91
Pledger/S	0.533	0.042	0.39	0.39	0.02	0.00	0.89	0.09	0.00
Rains/S	0.079	0.046	-0.08	0.00	0.03	0.00	0.65	0.31	0.01
Rosman/S	0.064	0.028	-0.03	0.00	0.07	0.00	0.65	0.28	0.01
Sharkey/S	0.284	0.012	0.24	0.24	0.02	0.01	0.72	0.25	0.00
Sharkey/SS	0.321	0.007	0.30	0.30	0.01	0.01	0.74	0.24	0.00
Tunbridge/S	0.033	0.008	0.01	0.01	0.02	0.01	0.05	0.11	0.81
White	0.033	0.000	0.03	0.03	0.01	0.01	0.40	0.11	0.47
Wilkes/S	0.042	0.020	-0.02	0.00	0.03	0.01	0.48	0.37	0.11

1

3.5.3. HPLC Methods

Batch experiments were used to obtain sorption coefficients for soil sorbents used in this study. All batch experiments utilized an initial test compound concentration of 5×10^{-5} M. Preliminary experiments over a wider range of initial concentration values helped establish that the above-mentioned initial concentration yielded $K_{d,expt}$ values in the linear range of the sorption isotherm. A range of soil loading were selected to ensure that equilibrium aqueous concentrations were well within the detection limit of the instrument. For benzylamine, soil-to-water ratios of 10 g L^{-1} were used for soils with ECEC > 7 cmol_c kg^{-1} and 100 g L^{-1} for soils with ECEC < 7 cmol_c kg. For PTMA, soil-to-water ratios of 5 g L^{-1} were used for soils with ECEC > 7 cmol_c kg^{-1} and 50 g L^{-1} for soils with ECEC < 7 cmol_c kg. For tramadol and desipramine, soil-to-water ratios of 1 g L^{-1}, 10 g L^{-1}or 100 g L^{-1} were utilized to optimize equilibrium aqueous phase concentrations as mentioned above. Preliminary soil loading studies were used to establish these experimental conditions.

Aqueous compound concentrations from the batch studies were determined using high pressure liquid chromatography (Agilent 1100 Series, quaternary pump, and 100 µL injection loop outfitted with a diode array detector). Detection was performed by isocratic elution at 1 mL min^{-1} of solvents defined in Tab. 3.S2. A C_{18} reverse phase column (Ultra Aqueous, Restek) was used for benzylamine and desipramine, a phenyl-hexyl column (Eclipse, Agilent) for phenyltrimethylammonium, and an XDB-C18 reversed phase column (Eclipse, Agilent) for tramadol. Detection wavelengths were 205, 200, 251, and 271 nm for phenyltrimethylammonium, benzylamine, desipramine, and tramadol, respectively.

Table 3.S2. HPLC eluents used to compound detection

Compound	Eluent
Phenyltrimethylammonium	93% Triflouroacetic acid / 3% Acetonitrile
Benzylamine	70% 25 mM phosphate buffer with 2 mM trimethylamine (pH 7) / 30% methanol
Desipramine	10% 10 mM phosphate buffer with 10 mM triethylamine (pH 7) / 90% methanol
Tramadol	40% 25 mM phosphate buffer with 2 mM trimethylamine (pH 7) / 60% methanol

3.5.4. Experimental sorption coefficients

Table 3.S3. Sorption coefficients (L/kg) for homoionic montmorillonites.

Compound	K_d Na-MMT	K_d NH4-MMT	K_d K-MMT	K_d Ca-MMT	K_d Mg-MMT	K_d Al-MMT
Benzylamine	83 ± 3	73 ± 4.5	54 ± 5	15 ± 2.5	9 ± 0.9	3 ± 0.9
Serotonin	171 ± 5	101 ± 6	91 ± 3.5	30 ± 2	25 ± 2	5 ± 1.2
PTMA	718 ± 55	652 ± 36	579 ± 33	131 ± 4	103 ± 5	28 ± 1
Atenolol	858 ± 67	481 ± 35	565 ± 58	135 ± 15	84 ± 5	29 ± 1
Metoprolol	975 ± 33	1328 ± 82	753 ± 43	244 ± 19	145 ± 6	52 ± 2
Cimetidine	1731 ± 105	1001 ± 100	2136 ± 73	436 ± 27	255 ± 14	50 ± 2
Tramadol	2638 ± 179	2328 ± 203	1631 ± 150	530 ± 47	342 ± 28	70 ± 7
Trimethoprim	6273 ± 435	2897 ± 232	2525 ± 292	1172± 102	905 ± 64	189 ± 11
Propranolol	7599 ± 584	3804 ± 328	3842 ± 220	1247 ± 108	1179 ± 128	128 ± 14
Desipramine	7809 ± 1423	5055 ± 665	3565 ± 164	1629 ± 104	1540 ± 96	440 ± 20
Diltiazem	29603 ± 4315	17369 ± 568	10773 ± 941	5553 ± 393	5444 ± 242	1218 ± 40

Table 3.S4. Sorption coefficients (L/kg) for soils.

Soil Name	Benzylamine K_d (L/kg)	Desipramine K_d (L/kg)	Tramadol K_d (L/kg)	PTMA K_d (L/kg)
Adams/SS	0.6	2.5	0.6	0.3
Appling/SS	4.4	89	25	49
Ashe/SS	8.5	261	86	56
Aycock/SS	7.7	309	83	52
Berryland/SS	7.7	148	23	18
Burton/S	25	289	28	24
Chewacla/SS	11	862	174	83
Codorus/SS	6.9	176	53	55
Colton/S	24	313	28	30
Comus/S	11	391	14	22
Enon/SS	12	371	157	100
Georgeville/S	4.9	66	15	41
Goldsboro/SS	4.0	113	28	43
Hagerstown/S	23	610	96	267
Heiden/S	36	1560	259	206
Heiden/SS	27	1690	240	215
Iredell/SS	89	13900	4090	1540
Kleinpeter/S	20	986	162	72
Leon/S	23	57	7.7	28
Moreland/SS	12	3510	448	296
Orangeburg/SS	5.7	168	40	38
Peru/SS	3.3	26	2.7	4.6
Pledger/S	6	7300	1940	413
Rains/S	44	384	44	52
Rosman/S	15	139	13	18
Sharkey/S	78	17140	4490	1230
Sharkey/SS	77	24120	6660	1230
Tunbridge/S	9.4	174	17	45
White Store/SS	7.0	302	74	667
Wilkes/S	14	391	66	48

3.5.5. Description of the Droge and Goss models

Droge and Goss developed successful predictive models for cation sorption to aluminosilicate minerals (Eq. 3.S3) and organic matter (Eq. 3.S4) and combined them to build a predictive model for sorption to soils (Eq. 3.S5 and 3.S6).

$$\log\left(K_{CEC,clays}\right) = 1.22Vx - 0.22NAi + 1.09 \pm CF_{clay} \quad (3.S3)$$

$$\log(D_{oc}) = 1.52Vx + 0.32NAi - 0.27 \pm CF_{oc} \quad (3.S4)$$

where $K_{CEC,\ clays}$ (L/eq) is the sorption coefficient for organic cations on homoionic Ca^{2+}-aluminosilicate minerals normalized to the CEC of clay minerals (eq/kg), D_{oc} (L/kg$_{oc}$) is the sorption coefficient for sorption to homoionic Ca^{2+}-organic matter, *Vx* is the molar volume of the organic cation, *NAi* is the number of hydrogen atoms bonded to the cationic amine group and CF_{clay} or CF_{oc} refers to corrective factors for specific compound structural moieties (Table 3.S5). Sorption coefficients for soils ($K_{d,pred}$) were predicted from $K_{CEC,\ clay}$ and D_{oc}, while accounting for the cation exchange capacity of the clay (CEC_{clay}) and the fraction organic content (f_{oc}) of the soil as follows:

$$K_{d,soil} = K_{CEC,clays} \times CEC_{clay} + D_{oc} \times f_{oc} \quad (3.S5)$$

Since the CEC contribution from mineral phases in the soil cannot be determined independently, Droge and Goss assumed 3.4 meq of charge per fraction of organic carbon to estimate CEC_{clays} (as described in Eq. 3.S2). As such, their final equation for prediction of cation sorption to soils is delineated as follows:

$$K_{d,soil} = K_{CEC,clays} \times (CEC_{soil} - 3.4f_{oc}) + D_{oc} \times f_{oc} \quad (3.S6)$$

The strength of this model is that $K_{d,\ soil}$ can be predicted from four parameters pertaining to organic cation structure (*Vx*, *NAi*, CF_{oc} and CF_{clay}) and two parameters pertaining to the soil (CEC_{soil} and

f_{oc}). A shortcoming of this model is that is that it has only been tested for soils flushed with calcium, making them either homoionic or close to homoionic. As such, extension to soils of mixed exchangeable ionic composition (heteroionic systems) is difficult.

3.5.6. Predicting sorption coefficients using the published Droge and Goss model for soils

We predicted sorption coefficients using Eq. 3.S6 for PTMA, benzylamine, tramadol, and desipramine sorption for 30 different soils and compared them to experimental sorption coefficients determined for this study. For some of the soils studied, the assumption of 3.4 meq of charge per fraction organic carbon would result in a CEC_{clay} less than zero (Tab 3.S3). The CEC_{clay} of these soils was assumed to be zero. Since the Droge and Goss model was designed to predict sorption coefficients at a higher ionic strength than used in our experiments, the model was applied here to assess extent to which the model describes trends in our data, not absolute value of K_d values since ionic strength corrections would be required to compare absolute values.

Regressions of predicted and experimental K_d values showed poor correlations using the Droge and Goss model (Fig. 3.S2). Poor predictions of the sorption coefficients of PTMA, benzylamine, tramadol, and desipramine could potentially be caused by the differences in identities of the exchangeable ion content of the soils, as compared with the calcium-saturated soil sets used to calibrate predictive models (Fig. 3.S2). Differences in ionic strength between our systems and the experimental conditions used to calibrate the Droge and Goss model were expected to results in a regular offset between predicted and experimental K_d values. The lower ionic strength decreases competition for sorption sites on soil components, thus increasing experimental sorption coefficients. However, if a corrections for ionic strength was used by adding a $\Delta \log K_d$ term[12], data

points that significantly deviated from the 1:1 line would still be present, pointing to the influence of exchangea ion identify, abundance, and affinity. Experimentally determined measures such as fraction of exchange sites occupied by ion I, $f(Ex_i)$ (Eq. 3.S1), capture the identity and abundance of exchangeable cations for a soil, however, it is not possible determine whether the exchanged inorganic cation was balancing a negatively charged receptor site on organic matter or on a clay mineral. Therefore, parameters such as $Ex_{ion\text{-}X}$ (Eq. 3.4, manuscript) cannot be incorporated into this model for the prediction of $K_{d,\,soil}$. Our comparisons between predicted and experimental values clearly show that an experimentally determined aggregate parameter that accounts for the affinity, abundance and identity of exchangeable inorganic cations is required for the prediction of sorption coefficients for soils.

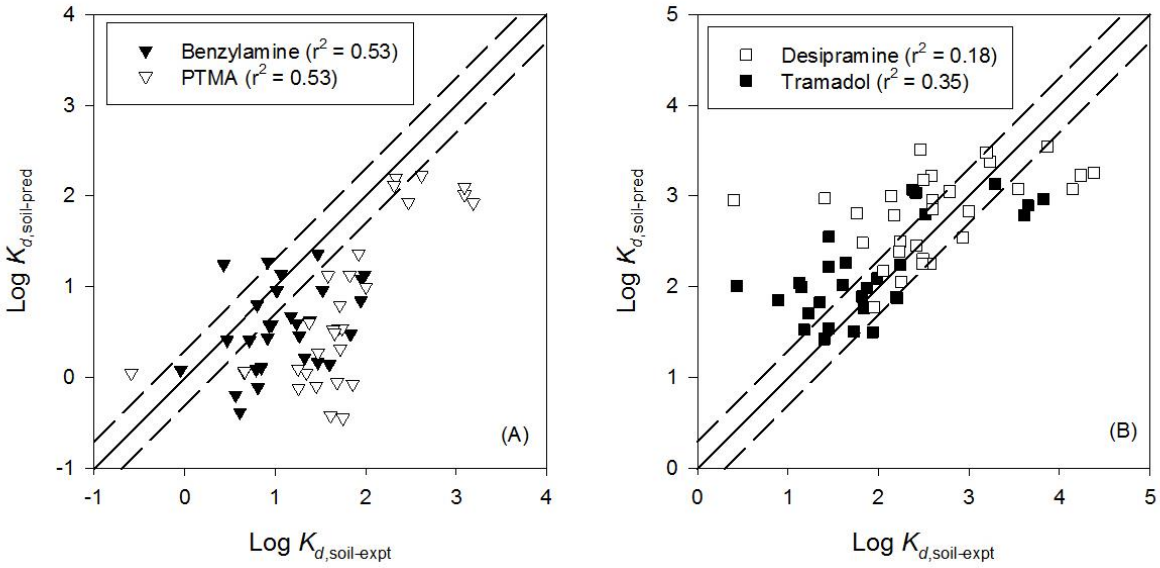

Figure 3.S2. Predicted sorption coefficients of PTMA (A, white triangles), benzylamine (A, black triangles), desipramine (B, white squares) and tramadol (B, black squares) using the published Droge and Goss model (Eq S6) for 30 different soils display scatter from the 1:1 line. Solid line is 1:1 and dashed lines represent ± 0.3 log units.

3.5.7. Compound modeling parameters

Parameters used in empirical models to predict sorption coefficients were obtained or adapted from Droge and Goss.[12] Parameters included the McGowan approximation of molecular volume (*Vx*) and the number hydrogens attached to the amine (*NAi*). Corrective factors for sorption to clays (CF_{clays}) and organic carbon (CF_{oc}) were used as defined by Droge and Goss with the exception of the ether moiety (-COC-) correction. Sorption coefficients were significantly under-estimated with the inclusion of corrective factors for ether moieties. Therefore, to improve predictive capability, a corrective factor for the -COC- group was not used. The sorption coefficients of all compounds which contained this group were well-predicted without the inclusion of this factor.

Table 3.S5. Parameters used to obtain scaling factors and predict sorption coefficients (obtained or adapted from Droge and Goss[12,13]).

Compound	Vx	NAi	CF_{clays}	CF_{oc}	Functional Groups for Corrective Factors
PTMA	1.26	0	N/A	N/A	
Benzylamine	0.98	3	N/A	N/A	
Desipramine	2.35	2	(+0.2)	(+0.6)	additional aromatic ring
Tramadol	2.39	1	(-0.3)	(-0.1)	[-OH]
Serotonin	1.51	3	(-0.3)		[-OH]
Metoprolol	2.32	2	(-0.3)		[-OH]
Propranolol	2.35	2	(-0.3,+0.1)		[-OH], polycyclic aromatic ring
Atenolol	2.24	2	(-0.4, -0.3)		[-C(=O)NH2], [-OH]
Trimethoprim	2.38	2	N/A		
Diltiazem	3.46	2	(-0.7,+0.2, -0.2)		[-C(=O)OC-], additional aromatic ring, [=O]

3.5.8. Additional $K_{d,soil}$ correlations with ECEC

As with PTMA and tramadol (Fig 3, manuscript), $K_{d,soil}$ for benzylamine and desipramine showed statistically significant, but weak, correlations with log $ECEC_{soil.}$ (Fig. 3.S3). Data points that deviated significantly from the best-fit line for benzylamine and desipramine corresponded to soils where similar deviations were observed for PTMA and tramadol (Fig. 3.3A).

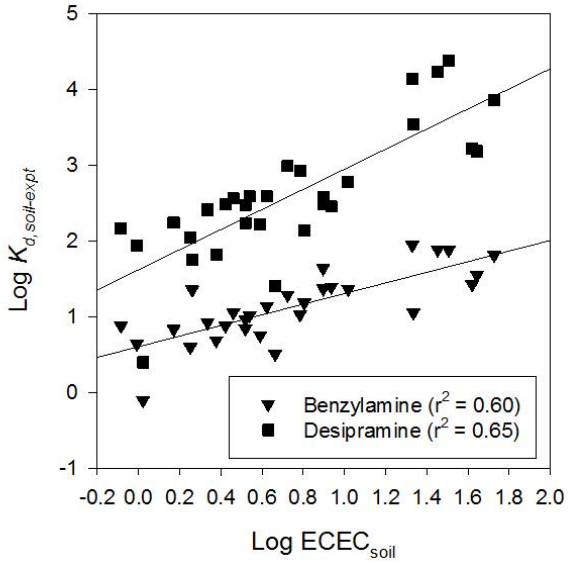

Figure 3.S3. The correlation of sorption coefficients of benzylamine (black triangles), and desipramine (black squares) with soil logECEC, soils well below the best fit line possessed high concentrations of exchangeable aluminum

3.5.9. Prediction of benzylamine sorption coefficients using PTMA as a probe

Benzylamine sorption coefficients were generally under-predicted using PTMA as a probe compound, and S^i values calculated using Eq. 3.6, 3.7, and 3.8 (manuscript). (Fig. 3.S4) The under-prediction of sorption coefficients for benzylamine, a small primary amine, generally occurred for soils for which organic matter was the dominant source of ECEC. Improvements in determining the source of CEC may improve predictions using a probe compound.

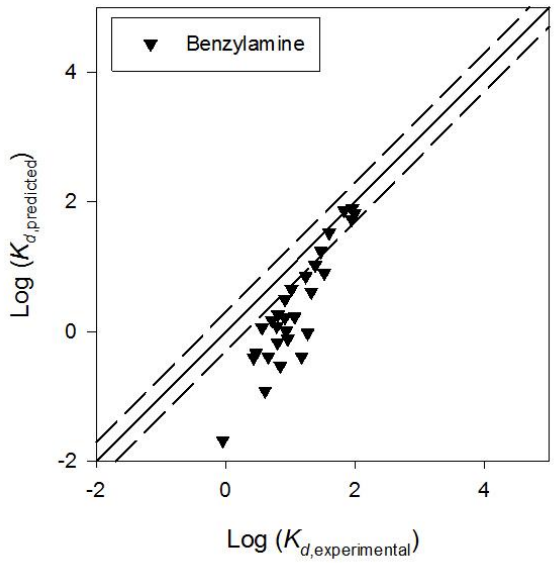

Figure 3.S4. Benzylamine sorption coefficients (black triangles) are under-predicted for lower sorption coefficients using PTMA as probe. Solid line is 1:1 and dashed lines represent ± 0.3 log units.

4.0 Beyond cation exchange: The effect of clay mineralogy on the sorption of organic cations

4.1 Abstract

Current predictive models assume that organic cations interact with all sites on clay minerals in the same manner. However, charge sites on clay minerals vary in hydration state and the area over which the charge is spread. As a means to isolate these changes in charge site chemistry, eight clay minerals were chosen to vary both the layer in which isomorphic substitutions occur and the presence of an interlayer. Sorption coefficients of nine structurally-complex organic cations for different clay minerals were not correlated directly with the cation exchange capacity. To understand the cause of the apparent deviations, a number of specific structural moieties were investigated from the base structure of benzylamine. The ordered water layers around the charge sites on the clay minerals with an interlayer caused for large differences in the sorption coefficients of organic cations with polar moieties. Furthermore, electron rich areas of sorbing compounds interacted with isomorphic substitutions located closer to the mineral surface and positively charged sites on the clay surface, which resulted in decreased sorption coefficients compared to non-polar compounds. These interactions where exemplified by deviations in quantitative trends in sorption coefficients of complex cationic pharmaceuticals. To account for these interactions predicting sorption coefficient of organic cations, clay minerals, more specially the fraction of charge sites within the tetrahedral layer of the clay mineral, was incorporated into and empirical predictive model.

4.2 Introduction

Organic contaminants that are positively charged at environmentally relevant pH values are released into natural systems through their increased use in agriculture and industry.[1,69-71] A key component of the fate and bioavailability of these organic cations is their extent of sorption to environmental solids.[6] An especially pertinent environmental sorbent for organic cations are clay minerals because of the permanent negative charge existing within the clay crystal lattice. Sorptive interactions between organic cations and clay minerals are the result of van der Waals and electrostatic interactions with the mineral surface.[15] The extent of these interactions is a function of both the clay mineralogy and sorbate structure.[13,17,35] With an emphasis on varied compound structure, previous studies conclude that structural effects may exert regular changes in sorption interactions regardless of sorbent mineralogy.[72,73] However, the limited number of observations under the same experimental conditions (*e.g.* exchangeable ions, ionic strength, etc.) prevents general conclusions from being drawn. As a result, there still exists a need to determine whether relative trends in organic cation coefficients are consistent across all negatively charged sites on clays, regardless of charge site chemistry.

Deviations in the qualitative ranks of sorption coefficients suggest that changes clay mineralogy may alter the affinity of compounds with certain structural characteristics. A common mineralogical difference in clay minerals is the presence of an interlayer. Charge sites balanced on the outer edges of the minerals are hydrated similar to the bulk solution (non-swelling clay, Fig 4.1A), while sites within in an interlayer are surrounded by ordered water molecules (swelling clay, Fig 4.1B).[6,74,75] Compounds with non-polar moieties may have an increased affinity for charge sites that are surrounded by ordered water molecules (represented by naphthylmethylamine (3), Fig. 4.1B).[6,13] In support of this claim, propranolol (polycyclic aromatic ring) had a larger sorption

coefficient for bentonite (hydrated interlayer) than alprenolol (single aromatic ring).[13] On illite, which has a collapsed interlayer thus making interlayer sites inaccessible, alprenolol had a larger sorption coefficient than propranolol. Since both compounds have the same base structure, the change in sorption coefficients is seemingly isolated to the presence of the polycyclic aromatic ring on propranolol.[13] The addition of polar moieties to a compound structure, may decrease the affinity of a compound for charged sites found within an interlayer, resulting in an increased affinity for sites found on the outer edge (represented by 4-nitrobenzylamine (2), Fig, 4.1A). A non-charged amine moiety on procaine likely caused procaine to have a higher sorption coefficient for illite compared to lidocaine on the same clay, while lidocaine has a higher sorption coefficient than procaine for bentonite.[13] The difference in the relative ranks procaine and lidocaine suggest that a polar amine moiety increases the affinity of a compound for the disordered hydration layers for non-swelling clays. However, the variations in the relative ranks of compounds are not definitive proof of charge hydration effects because of the limited number of comparisons and the lack of comparative values across multiple clays at the same experimental conditions. In the absence of systematic studies of compound trends on clay minerals with specific variations in charge characteristics, it is not possible to discern whether compounds structure is, in fact, the source of these differences in sorption coefficients.

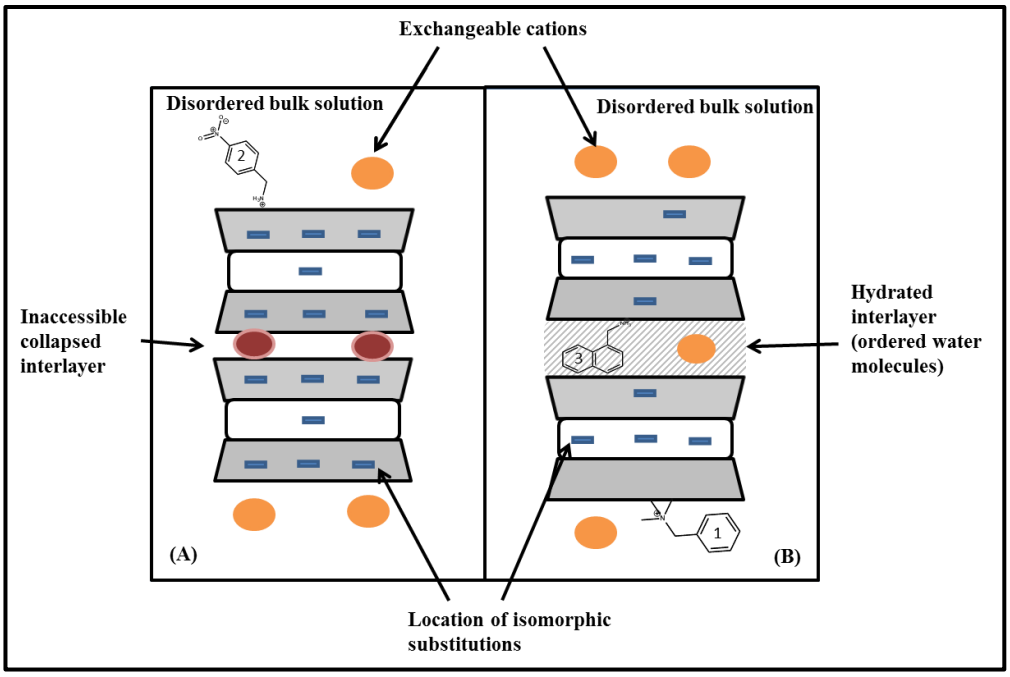

Figure 4.1. Representative clay structures to highlight possible effects that clay minerology may have on sorption of organic cations. (A) A clay with a higher percentage of tetrahedral (gray layer) substitutions and collapsed interlayer (similar to that of illite) makes all accessible negative sites hydrated similar to the bulk solution, increasing the affinity of primary amines with polar moieties (represented by 4-nitrobenylamine, "2"). (B) A swelling clay with a hydrated interlayer increases the affinity of non-polar compounds (represented by naphthylmethylamine, "3"), while more isomorphic substitutions in the octahedral layer (white) increases the affinity of higher order amines, (benzyltrimethylammonium, "1").

Many previous studies have shown that the methylation of the charged amine on an organic cation increases the affinity for the clay surface by increasing both van der Waals and electrostatic interactions.[13,15,35] Amine methylation has been indicated in both increasing[15] and decreasing[13,35] the area over which the +1 charge is spread, both of which increase electrostatic interactions. The increased size of a compound with more methyl groups also increases van der Waals interactions

with the clay surface.[15] However, there are limited comparisons amine methylamine effects across clay minerals with different minerology. For bentonite, the CEC-normalized sorption coefficients for a group of methylated quaternary amines are distinctly higher (factor of 10) for bentonite than for illite, even though both clays are 2:1 minerals.[13] The increased sorption coefficients for bentonite compared to illite of quaternary amines may be caused by the interlayer presence on bentonite, which increase van der Waals interactions, and/or the difference in the location of isomorphic substitutions within the crystal lattice between the clays. Illite has more tetrahedral substitutions, which are closer to the mineral-water interface, producing focused charges sites, where the charge spread over the 3 adjacent surface oxygen atoms (Fig. 4.1A).[26,28] The isomorphic charge of bentonite is from the octahedral layer and is distributed over a larger area on the surface (Fig. 4.1B).[26-28] If amine methylation indeed increases the area over which the +1 charge is spread, the result would increase the extent of electrostatic interactions between the defocused charge sites on bentonite, thus explaining the increase in affinity. However, without isolating the effects of isomorphic substitutions and interlayer presence, it is not possible to discern whether increased electrostatic effects or van der Waals interactions are the source of the increased affinity of quaternary amines to bentonite.

The purpose of this study was to systematically vary compound structure to probe how differences in clay minerals affect sorption of organic cations. Sorption coefficients were collected to eight different clay minerals, which varied the location of isomorphic substitutions (*i.e.* tetrahedral, octahedral layers) and hydration of the charge site (interlayer vs lack of an interlayer). We investigated specific variations in compound structure from the base structure of benzylamine to isolate the interactions of certain moieties have with various clays. The two main compound structure elements we aimed to examine were the addition of polar moieties and the methylation of

the amine. Both elements were affected by differences in the location isomorphic substitution within crystal lattice, while compounds with polar groups were also influenced by interlayer presence. Sorption coefficients of a group of nine pharmaceutical compounds for five of the clay minerals were then evaluated to determine how multiple moieties alter compound-surface interactions, and followed trends that corresponded to those seen for benzylamine derived compounds.

4.3 Methods

4.3.1 Sorbents and chemicals

Clay minerals (Tab. 1) were obtained from the Clay Minerals Society with the exception of vermiculite, which was from Grace Minerals (SC, USA). Nontrinite, chlorite, and illite were ground and passed through 200-grid mesh before use. All other clays were used as received. SiC was from Alfa Aesar. Sorbate compounds (structures: Fig. S1) were from Sigma Aldrich and Acros Organics. All other chemicals and reagents were ACS grade. Solutions were made with high purity 18.2 MΩ water from a MilliQ system (Waters).

Table 4.1. Properties and benzylamine sorption coefficients for the clay minerals studied, including Langmuir-Freundlich fit parameters (log K_{LF} and h; Eq 4.4) and linear range sorption coefficients (K_d). "O" refers to the octahedral layer and "T" the tetrahedral.

Sorbent	Layering	Charge Source[a]	CEC (eq/kg)[b]	Interlayer
Hectorite	TOT	Mostly O	0.44	Hydrated
Tx-Montmorillonite	TOT	66% O 33% T	0.84	Hydrated

Wy-Montmorillonite	TOT	66% O 33% T	0.76	Hydrated
Vermiculite	TOT	33% O 66% T	0.69	Hydrated
Nontronite	TOT	Mostly T	0.79	Hydrated
Chlorite	TOT	66% O 33% T	0.06	Iron Hydroxide Sheet
Illite	TOT	33% O 66% T	0.22	Collapsed
Kaolinite	TO	Deprotonated surface hydroxyl	0.02	None

[a] ref [26]

[b] CEC from the Clay Minerals Society, except vermiculite, which was from Ref [76]

4.3.2 Column Chromatography

Column chromatography was used to obtain sorption coefficients for compounds with a packing mixture of a single clay mineral and inert SiC. Following methods detailed previously,[62] solid-to-water ratios for individual columns (Tab. 4.S1) were designed to balance compound retention against peak spreading. A comparative control column was packed entirely with SiC to verify that test compounds had no sorptive interactions with this inert solid. Packed columns were loaded into a standard HPLC system (Jasco PU-980 pump, AS-950 auto sampler, 40 µL injection loop, and MD-1510 multiwavelenth detector). Clay minerals were converted to homoionic Ca-forms by flushing the respective column with 15 mM $CaCl_2$ (pH 6.7 ± 0.2) for 24 hrs before compound injection. The flushing solution also served as the experimental background solution (eluent) for experiments. Additional experiments were performed with 5 mM $CaCl_2$ at pH 8 (adjusted with NaOH) as the eluent for benzylamine, aniline, and 4-aminomethylbenzoic acid with Tx-montmorillonite and hectorite to understand sorptive behavior of compounds with pH dependent

charge. An operating flowrate of 100 µL/min was used for all experiments after previously determining sorptive equilibrium condition for clay minerals.[62]

The concentration of test compounds injected into the column was varied from 4.3×10^{-6} to 2.6×10^{-4} M to create sorption isotherms. For benzylamine, the isotherm range was extended to 0.5 M in order to evaluate isotherm shape as sorbed concentrations approached the CEC of the clay minerals. Triplicate injections of each concentration were made for both the SiC-only and the clay-SiC columns. Absorbance *vs.* time data following each injection were exported directly to a MATLAB routine to calculate a retention time from the eluted compound peak in the breakthrough curve.

4.3.3 Sorption Coefficient Determination

Single-point K_d values (kg/L) were calculated from the eluent volume required to elute compounds from a column, V (L), and column sorbent mass, m (mg)[20]:

$$K_d = \frac{V}{m} = \frac{Q * \left[\left(t_{cmpd} - t_{tracer}\right) - \left(t_{cmpd-SiC} - t_{tracer-SiC}\right)\right]}{m} \quad (4.1)$$

where Q (L min^{-1}) is the eluent flow rate and the bracketed term is the effective travel time of the compound in contact with only the sorbent in the clay-SiC column. All times (t_i, min) were calculated by integrating the corresponding peak to obtain the center-of-mass: t_{cmpd} and $t_{cmpd\text{-}SiC}$ are the compound travel times through the clay-SiC and SiC-only columns, respectively, and t_{tracer} and $t_{tracer\text{-}SiC}$ are the nitrate tracer travel times through clay-SiC and SiC-only columns, respectively. Points were assumed to be in the linear range of the isotherm if two or more initial concentrations had matching K_d values and skewness values of runs on clay-SiC columns matched (within 4%) those on the SiC-only column.[62] All reported K_d values were determined to be in the linear range.

4.3.4 Isotherms

For benzylamine, sorption coefficients obtained with Eq. 4.1 were converted to aqueous and sorbed concentrations[20]:

$$C_w = \frac{C_0 * V_i}{K_d * m + V_i} \tag{4.2}$$

$$C_s = \frac{C_0 * V_i - C_w * V_i}{m} \tag{4.3}$$

where C_0 (mM) is the concentration of the injected test compound solution and V_i (L) is the injection volume. Paired C_w and C_s values were used to construct isotherms. For the purposes of evaluating isotherm linearity, the Langmuir-Freundlich isotherm equation was used[77]:

$$C_s = \frac{C_{s,max}(K_{LF}C_w)^h}{1 + (K_{LF}C_w)^h} \tag{4.4}$$

Where $C_{s,max}$ is assumed to be the CEC of the clay, K_{LF} is the sorbate affinity, and h reflects isotherm non-linearity (h > 1 indicates convex isotherms and h < 1, concave). The Langmuir-Freundlich equation was log-transformed for fitting[21]:

$$\log\left(\frac{C_s}{C_{s,max} - C_s}\right) = h\log(C_w) + h\log(K_{LF}) \tag{4.5}$$

4.4 Results and Discussion

4.4.1 Nonlinearity

Identifying isotherm non-linearity is critical when establishing linear range sorption coefficients to clay minerals. We investigated sorption isotherms of benzylamine to each of the clay minerals to identify if any properties of the clay minerals influenced the shape of the isotherm. Organic cations displayed both concave and convex isotherms, relative to the x-axis, as concentration on the solid increases. Convex isotherms, which have increasing point sorption

coefficients (C_s/C_w) with increasing concentration on the surface, arose from compound-to-compound interactions.[21] Convex isotherm non-linearity ($h > 1$, eq 4) was seen for all clay minerals that contained an interlayer (hectorite, montmorillonite, vermiculite, and nontronite: white squares, Fig. 4.2). Convex isotherm non-linearity may have arisen from increased order of the water molecules in the interlayer allowing for compound-to-compound interactions and/or localized swelling. Localized swelling of the interlayer may create hydrophobic pockets. However, these pockets are not quantifiable in d-space XRD measurements due to low surface coverage at the low concentration range of the isotherm. Sorption isotherms for clays without an interlayer (illite, chlorite, and kaolinite: white squares, Fig. 4.2) had $h < 1$. The lack of an interlayer reduces the ordering of water molecules near the clay surface[6], which may not facilitate compound-to-compounds interactions. Values of h for clays that were not significantly different (ttest, $p > 0.5$) comparing clays of the same type, which indicates that CEC of the clay seemingly does not affect non-linearity (Fig. 4.2)

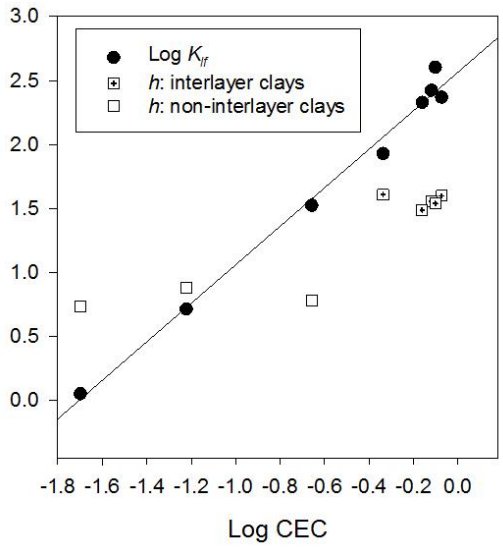

Figure 4.2. Log K_{lf} values of benzylamine (black circles) are correlated with the CEC of the clay minerals. "h" values > 1, corresponding to convex isotherms non-linearity, are seen for clays which contain an interlayer (white squares with "+"), while clays without an interlayer (white squares) display "h" values < 1 corresponding to concave isotherm non-linearity. Black line indicates best fit correlation of log K_{lf} with log CEC.

The affinity of benzylamine for the mineral surface (K_{lf}), on the other hand, was correlated with the CEC of the clay. Benzylamine, a primary amine which lacks polar moieties, is one of the simplest organic cations that contains an aromatic ring. As a result, sorption of benzylamine was dependent on the cation exchange capacity of the clay (Fig. 4.2). The magnitude of log K_{lf} is correlated with the log CEC of the clay (R^2 = 0.97; regression excel). Of note, benzylamine K_{lf} value for nontronite (CEC = 0.79 eq kg^{-1}) was slightly higher than that of Tx-montmorillonite (0.84 eq kg^{-1}). The predominantly tetrahedral isomorphic substitutions of nontronite increase the proximity of charge sites to the mineral surface, increasing the affinity of benzylamine for the charge site. A similar phenomenon was seen for linear range sorption coefficients (Fig. 4.3). Therefore, we chose to compare linear range sorption coefficients for the clay minerals, which served to limit labor intensity of data collection.

4.4.2 Sorption coefficient correlations with CEC

Benzylamine sorption coefficients (K_d) for clay minerals increased with increasing CEC of the clay, however this trend was not consistent across all organic cation structures. Sorption coefficients of benzylamine, followed the same trend as seen for K_{lf} values (Fig. 4.2 vs Fig. 4.3). However, sorption coefficients for tramadol and desipramine, two cationic pharmaceuticals which we have studied extensively (Chapter 3), were more wide spread from a best fit correlation (Fig. 4.3). Tramadol displayed higher sorption coefficients for hectorite and illite (CECs of 0.42 and 0.22

eq/kg respectively) than for nontronite and Tx-montmorillonite (0.79 and 0.84 eq/kg respectively). Tramadol, which is tertiary amine and has a number of polar moieties, may have a higher affinity for defocused charge groups and sites with disordered hydrating water molecules. Desipramine had lower sorption coefficients for nontronite compared to Tx-montmorillonite, hectorite, and illite (in that order), which may be caused by the lack of polar moieties for the secondary amine. These deviations could suggest a combination of effects, including whether the charge site is balanced within a hydrated interlayer and the focus of the charge site, may influence the magnitude of sorption coefficient of complex organic cations for clay minerals. To understand how specific moieties of complex organic cations effect sorption; we investigated specific variations in compound structure from the base structure of benzylamine.

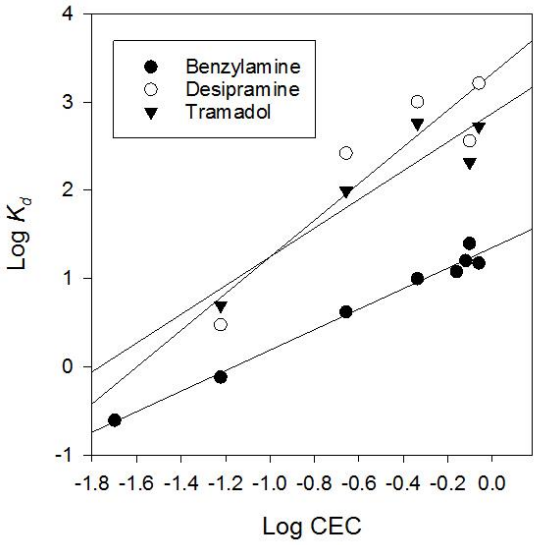

Figure 4.3. Sorption coefficients of benzylamine (black circles) are correlated with the CEC of the clay minerals; however sorption coefficients of desipramine (white circles) and tramadol (black triangles) display apparent scatter around the best fit line, possibly due to differences in clay mineral structure beyond CEC. Black lines indicate best fit correlation.

4.4.3 Defocusing effects

To investigate influence of compound structure on sorption to different clay minerals, sorption coefficients (log $K_{d,cmpd}$) were normalized to the sorption coefficient of benzylamine on the corresponding clay:

$$\Delta \log K_{d,cmpd} = \log K_{d,cmpd} - \log K_{d,benzylamine} \quad (4.4)$$

Which implicitly captures the clay-to-clay CEC variations through sorption coefficient of benzylamine. Comparing the relative extent of sorption for a compound ($\Delta \log K_{d,cmpd}$) across clay minerals gives insight into how certain structural components interact with different clay minerals. $\Delta \log K_{d,cmpd}$ values that are not zero and constant for all clay minerals suggest that structure moieties influence sorption and there are weak contributions from clay structure. Differences in $\Delta \log K_{d,cmpd}$ values could identify sorbate-structure combinations that give rise to deviations in tends seen for complex compounds.

Higher order amines displayed increased affinity for clays with a larger percentage of octahedral charge sites. $\Delta \log K_d$ values of quaternary (benzyltrimethylammonium, phenyltrimethylammonium) and tertiary amines (N,N-dimethylbenzylamine) for clays followed:

$$\text{Hectorite} > \text{Montmorillonite} \approx \text{Chlorite} > \text{Vermiculite} \approx \text{Illite} \geq \text{Nontronite} \quad (I)$$

Which corresponds, without exception, to an increase in $\Delta \log K_d$ with increased percent of isomorphic substitutions in the in the octahedral layer (Fig. 4.4). This phenomenon was also seen for the secondary amine, N-benzylmethylamine, though to a lesser extent (Fig. 4.4). Comparing chlorite with both montmorillonites (66% octahedral substitutions), and illite with vermiculite (33% octahedral substitutions) showed that interlayer effects are seemingly absent. This observation has two implications. The first is that van der Waals interactions are not the dominant source of

increased affinity of methylated amines to clay minerals. Second, the increase in affinity with increasing percent of isomorphic substitutions in the octahedral suggests that amine methylamine increases the areas over which the charge in spread[15], resulting in increased electrostatic interactions with clays that have defocused charges sites.

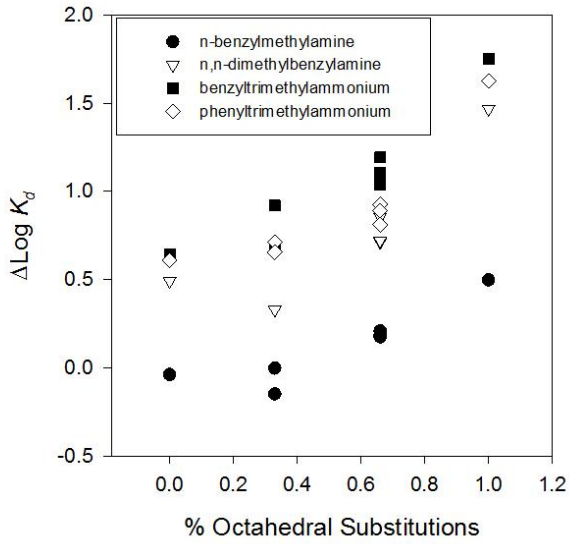

Figure 4.4. Higher order amines, benzyltrimethylammonium (black squares), phenyltrimethylammonium (white diamonds), and N,N-dimethylbenzylamine (white triangles display increasing $\Delta\log K_d$ values with a higher percent of isomorphic substitutions occurring in the octahedral layer. The secondary amine, N-benzylmethylamine (black circles), partially displays a similar phenomenon.

4.4.4 Interlayer Presence

Non-polar, napthylmethylamine had $\Delta\log K_d$ values that were constant across clays that had an interlayer, and lower $\Delta\log K_d$ values for clays without an interlayer (Fig. 4.5A). Since the addition of functional groups increases the molecular volume of a compound compared to benzylamine, we investigated $\Delta\log K_d$ values for naphthylmethylamine, which has an increased compound size without adding polar moieties. Napthylmethylamine had a higher affinity for the

ordered interlayer due to increased compound size, as $\Delta \log K_d$ values for illite, chlorite, and kaolinite, were lower than those for clays with an interlayer (Fig. 4.5A). The slightly lower $\Delta \log K_d$ values of naphthylmethylamine for hectorite compared to other clays with an interlayer may be the result of decreased order of the interlayer of hectorite. Within the hectorite interlayer, inorganic cations are less strongly bound to the defocused charge site allowing the cations to move more freely, disordering the hydrating water molecules.[78,79] Though differences in $\Delta \log K_d$ for napthylmethylamine, can be explained solely by the interlayer hydration, the deviations seen for other compounds, indicate focusing/defocusing of a charge site effects sorption (Fig. 4.5).

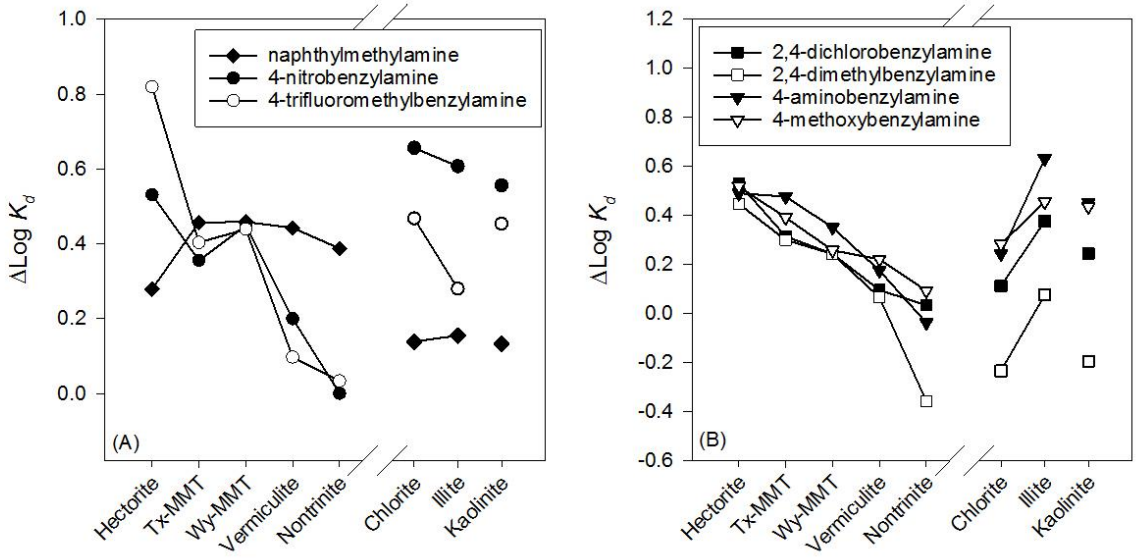

Figure 4.5. (A) $\Delta \log K_d$ values (Eq. 4) for non-polar naphthylmethylamine (black diamonds) are different between clays with and without and interlayer. $\Delta \log K_d$ values of 4-nitrobenzylamine (black circles) and 4-trifluoromethylbenzylamine (white circles) decrease with increased change focus on the clay mineral coupled with interlayer effects. (B) Compounds with more electron density near the charged amine display lower $\Delta \log K_d$ values for clays with an interlayer and focused charge sites, while the presence of partial positive charge for kaolinite and chlorite seemingly decreases $\Delta \log K_d$ values compared to illite: 2,4-dichlorobenzylme (black squares), 2,4

di-methylbenzylamine (white squares), 4-aminobenzylamine (black triangles), and 4-methoxybenzylamine (white triangles). Clays on the left of the break contain an interlayer, while clays without an interlayer are on the right.

Compounds with polar moieties had decreasing $\Delta \log K_d$ values for clays with lower percentage of octahedral substitutions (Fig. 4.5). If the addition polar functional groups only influenced sorption by increasing the molecular volume of a compound, trends in across clays $\Delta \log K_d$ values of compounds with polar moieties should be the similar to those seen for napthylmethylamine. However, compounds which contain polar functional groups have very different trends in $\Delta \log K_d$ values compared to napthylmethylamine. $\Delta \log K_d$ values of compounds which contained electron donating (4-nitrobenzylamine, 4-trifluoromethylbenzylamine, and 2,4-dichlorobenzylamine) and withdrawing moieties (4-methoxybenzylamine, 4-aminobenzylamine, and 2,4-dimethylbenzylamine) were affected in a similar way by the focusing of charge on clay minerals with an interlayer. For these compounds, $\Delta \log K_d$ values were distinctly lower for nontronite, where many compounds had sorption coefficients that were similar to benzylamine ($\Delta \log K_d = 0$) even with the increased size (Fig. 4.5A & B). For nontronite, which has isomorphic substitutions almost exclusively in the tetrahedral layer, the charge is focused and closer to the planar surface of the mineral. A negative charge closer to the surface is theorized to interact with electron rich area of the sorbing compounds. The higher proximity of negative charge may result in repulsion effects, which decreases the affinity of compounds with polar moieties. Compounds with areas of increased electron density (both on the ring and on functional groups) are either repulsed from the charge site itself or hindered from entering the interlayer. The opposite is seen for hectorite, which has almost exclusively octahedral substitutions. $\Delta \log K_d$ values for hectorite are

slightly larger than other interlayer clays for compounds that contain electron donating or withdrawing moieties (Fig 4.5A & B). Tx-montmorillonite, Wy-montmorillonite and vermiculite partially displayed these effects as the percent of octahedral substitutions shifts from 66% (both montmorillonites) to 33% (vermiculite).[26]

Compounds that contained electron donating groups had higher $\Delta\log K_d$ values for illite than for chlorite, while of compounds with electron withdrawing groups had higher $\Delta\log K_d$ values for chlorite. For non-interlayer clays, compounds with polar moieties had, on average, increased $\Delta\log K_d$ values compared to non-polar naphthylmethylamine (Fig. 4.5). The presence of polar moieties increases the affinity of a compound for the disordered hydrating water molecules of non-interlayer clays. Across non-interlayer clays, two trends were evident and corresponded to differences electron density on the sorbing molecule. For 4-nitrobenzylamine and 4-triflouromethylbenzylamine, $\Delta\log K_d$ values for chlorite were generally higher than those for illite (Fig. 4A), while the opposite trends was seen for 4-aminobenzylamine, 2,4-dimethylbenzylamine, 4-methoxybenzylamine and 2,4-dichlorobenzylamine (Fig. 4.5B). This difference in sorption trends for these compounds could be consistent with presence of a small amount of positive charge on kaolinite and chlorite. Some edge sites of kaolinite can be positively charged a neutral pH while the FeOH sheet residing in the interlayer of chlorite has a net positive charge.[80,81] The positive charge could attract compounds with compound with electronegative groups on the opposite end of the molecule that does not carry the +1 charge (4-nitrobenylamine, 4-trifluorobenzylamine), while electron donating groups do not facilitate these interactions (4-aminobenzylamine, 2,4-dimethylbenzylamine, and 4-methoxybenzylamine). Interestingly, 2,4-dichlorobenzylamine which has an electronegative group in the ortho position displays trends similar to compounds which have

electron donating groups. The presence of two electron withdrawing groups may cancel out effects seen for 4-nitrobenzylamine and 4-trifluoromethylbenzylamine.

4.4.5 Kaolinite

Compound $\Delta\log K_d$ values for kaolinite are generally similar to those for chlorite. Kaolinite is the only 1:1 (tetrahedral: octahedral) clay studied and the dominant source of charge is deprotonated surface hydroxyl groups. As such, comparing compounds trends of $\Delta\log K_d$ values for kaolinite to other clays does not isolate differences in clay structures. Many compounds, including 4-trifluoromethylbenzylamine, 2,4-dimethylbenzylamine, 2,4-dichlorobenzylamine, and 4-aminobenzylamine, had similar $\Delta\log K_d$ values for kaolinite as for chlorite (Fig. 4.5). It is possible that this is, in part, due to the small amount of positive charge on kaolinite is either repelling or attaching functional groups with differences in electronegativity, as some of the surface sites of kaolinite can be positively charged at pH 6.7. However, this trend did not hold for 4-nitrobenzylamine and 4-methoxybenzylamine, as both of these compounds had similar $\Delta\log K_d$ values for kaolinite as those for illite. However, without a comparison clay with the same layering as kaolinite, it is not possible to determine the cause of deviation.

4.4.6 Trends in compounds that contain a pH dependent charge group

4-aminomethylbenzoic acid (AMBA) and aniline displayed trends across clays that are consistent with lower pH values near the clay surface. The surface of clay minerals is generally at a lower pH (≈ 2 pH values) than the surrounding bulk solution due to electrical double layer effects.[82,83] To understand if this effect is influenced by differences in clay structure, we investigated sorption of AMBA (amine pKa: 9.53, carboxylate pKa: 3.87) and aniline (amine pKa = 4.87). At a bulk solution pH of 6.7, AMBA and aniline are zwitterionic and neutral respectively,

which should result in lower affinity for the surface than compounds that are strictly positively charged. In agreement with this, $\Delta \log K_d$ values for AMBA and aniline were generally negative (lower sorption than benzylamine), however $\Delta \log K_d$ values increased (less negative) as CEC of the clay increased (Fig. 4.6). This corresponds to an increase in the density of elective double layer, which decreases the pH near the surface. Both AMBA and aniline are then positively charged, increasing affinity of the compound for charged sites. As further evidence that AMBA and aniline are strictly positive near the surface of clay minerals, we collected sorption coefficients for aniline, AMBA, and benzylamine for hectorite (lowest interlayer CEC) and Tx-montmorillonite (highest CEC) at pH 8. Sorption coefficients of benzylamine were unchanged for both clays, while sorption coefficients aniline and 4-aminomethylbenzioc acid decreased by a factor of 2. Both aniline and 4-aminomethylbenzioic acid are expected to be neutral and zwitterionic compounds respectively, even with the decreased pH near the clay surface, decreasing affinity.

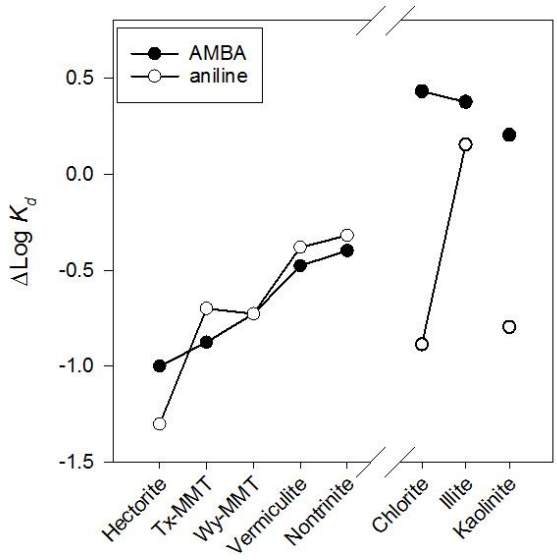

Figure 4.6. $\Delta \log K_d$ values at bulk solution pH of 6 for AMBA (black circles) and aniline (white circles) increase with increasing charge focus on clays with an interlayer. Clays on the left of the break contain an interlayer, while clays without an interlayer are on the right.

For clays that lack an interlayer, CEC also influences the extent of sorption for aniline, while AMBA displayed trends similar to cationic compounds with polar moieties. Increased affinity for the surface compared to benzylamine was seen for aniline with increased CEC of the clay. Aniline had a similar sorption coefficient as benzylamine for illite, which decreased to chlorite and kaolinite (Fig. 4.6). AMBA, on the other hand, displayed trends similar to 4-nitrobenzylamine and 4-trifluorobenzylamine (Fig. 4.5A), which corresponds to the removal of charge density from the aromatic ring for AMBA. Since the positive charge of AMBA is similar to that of benzylamine, AMBA likely sorbs by cation exchange to charge sites not residing in an interlayer, while the negatively charge carboxylate is not bound within the interlayer allowing more freedom in compound orientation to the surface, reducing repulsion interactions with the negative charged sites on clay minerals.

4.4.7 Trends in Sorption Coefficients of Pharmaceuticals

To investigate how interlayer and charge focus effects influence sorption of pharmaceuticals, we collected sorption coefficients of eight cationic and one zwitterionic pharmaceutical for five of the clay minerals (hectorite, Tx-montmorillonite, nontronite, illite, and chlorite). Sorption coefficients for pharmaceuticals were normalized to benzylamine for consistency with previous results (Eq. 4.4). Most pharmaceuticals contained polar moieties and/or had higher order amines (secondary or higher). The combination of these effects caused for trends similar to those seen in Fig. 4B, where $\Delta \log K_d$ values for seven of the nine pharmaceuticals generally displayed a trend defined by the hydration of the interlayer and the layer in which isomorphic substitutions occurred (Fig. 4.7):

$$\text{Hectorite} \geq \text{Tx-montmorillonite} > \text{Illite} > \text{Nontronite} > \text{Chlorite} \qquad \text{(II)}$$

However, some minor deviations from this trend were evident and corresponded to extremes in compound structure. $\Delta \log K_d$ values for hectorite were largest for triprolidine, clomipramine, tramadol, propranolol, metoprolol, and atenolol. Each of these compounds contains a secondary or tertiary charged amine which resulting in lower sorption coefficients to nontronite than the rest of the clays. Interestingly, propranolol and desipramine, secondary amines which lack polar components on the opposite side of the molecule which carries the charge, display $\Delta \log K_d$ values for hectorite that are not significantly different (ttest, $p > 0.05$) than those for Tx-montmorillonite. The slightly lower $\Delta \log K_d$ values for hectorite are similar to the slight decrease in $\Delta \log K_d$ value for hectorite seen for naphthylmethylamine (Fig. 4.5A) and correspond to the slightly more disordered interlayer of hectorite compared to other interlayer clays. All of the compounds that have at least two ring structures (heterocyclic or aromatic: desipramine, propranolol, triprolidine, clomipramine, and tramadol), had lower $\Delta \log K_d$ values to clays without an interlayer compared to hectorite and Tx-montmorillonite. Compounds with a single ring, atenolol and metoprolol, displayed higher $\Delta \log K_d$ values for illite compared to Tx-montmorillonite. The larger $\Delta \log K_d$ values for illite were likely caused by the higher affinity of these compounds for the disordered water molecules surrounding a site not residing in a clay interlayer. Since atenolol and metoprolol contain electronegative groups near the charged amine, $\Delta \log K_d$ values for chlorite were lower than those of Tx-montmorillonite and illite for all compounds, which corresponds to trends seen for benzylamine based compounds. Though, $\Delta \log K_d$ values for seven of the nine complex compounds studied agreed well with the general trend (II), two of the compounds displayed trends in $\Delta \log K_d$ values that were distinctly different.

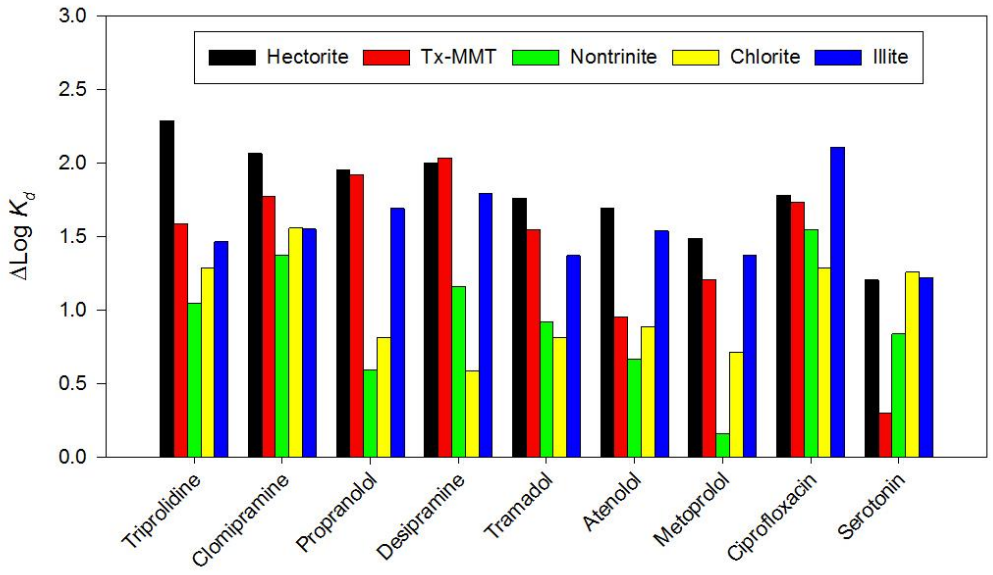

Figure 4.7. ΔlogK_d values of pharmaceuticals followed trend corresponding to the hydration and focus of charge sites on clay minerals.

Compound characteristics of serotonin and ciprofloxacin lead to large deviations from the trends seen for other compounds. Ciprofloxacin, which is zwitterionic at pH 6.7, displays the highest ΔlogK_d values for illite, similar to trends seen for AMBA. However, ciprofloxacin deviates from trends seen for AMBA, as the second highest ΔlogK_d values is to hectorite. The likely cause to this deviation is that ciprofloxacin is a tertiary amine, which has a higher affinity for the defocused charge sites on hectorite. Serotonin, which is the only primary amine studied, had a higher ΔlogK_d value for nontronite than that for montmorillonite, likely due to the increased affinity of primary amines for the focused charge sites on nontronite. The hydroxyl group on the end of the serotonin molecule increases the polarity of the compound, causing for increased sorption to disordered water molecules surrounding the charge sites on hectorite, illite and chlorite.

4.4.8 Quantitatively accounting for clay structure

Recently, we proposed the use of phenyltrimethylammonium (PTMA) as a probe compound to access the affinity of organic cations to negatively charged sites on montmorillonite. We demonstrated that prediction of organic cation sorption coefficients to montmorillonite with various exchange ions could be performed using the log K_d of PTMA and a scaling factor (S^i):

$$\log\left(K_{d,clay}\right) = \log\left(K_{d,PTMA}\right) + \log(S^i_{clays}) \tag{4.5}$$

with scaling factors, adapted from an empirical model by Droge and Goss,[13] for compound i empirically determined by:

$$\log(S^i_{clays}) = 1.22(Vx_i - Vx_{PTMA}) - 0.22NAi_i \pm CF_{i,clay} \tag{4.6}$$

Where Vx_i and Vx_{PTMA} are the McGowan molar volumes of the compound of interest and PTMA respectively, NAi is the number of hydrogen atoms attached to the amine of the compound since PTMA has a NAi value of zero. Both Vx_i and NAi are straightforward parameters to derive for a given compound of interest. An additional adjustment term (CF_i) is needed to improve prediction accuracy for compounds with certain functional groups (i.e. –Cl, -OH, etc.). The values of $CF_{i,clay}$ were obtained by averaging adjustment terms necessary for montmorillonite, illite and kaolinite.[13] That the magnitude of experimental adjustment terms varied across clays suggests differences in interactions between structural components and the individual clay surfaces across different clay minerals as the scaling factors were not constant for all clays. The importance of clay surface charge characteristics to compound sorption coefficients was demonstrated in our work here, which showed amine order and substituent polarity to be sensitive to charge focusing at the isomorphic

substitution sites. Thus, the assumed similarity of charge sites across clay minerals implicit to Eq. 4.5 could be problematic for compounds that differ greatly in structure from PTMA and requires integration of clay mineral structure characteristics into the approach for determining a compound scaling factor model.

We evaluated several strategies to incorporate clay mineral charge focus directly into the empirical prediction of S^i while also limiting the extent to which structure-specific adjustment terms were necessary. First, the fraction of charge sites, f_T, was included directly as an equation parameter. The sorption coefficients of benzylamine-based compounds were used as the training set because those compounds included a number of important characteristics (amine order, polar groups, and size effects); the pharmaceutical sorption coefficients were reserved as a test set. We limited the compound parameters to McGowan molar volume and amine order since both of these terms can be determined easily and have been shown to be a promising means to predict sorption of organic cations.[13] The values of the experimental scaling factors by rearranging Eq. 4.5 ($\log K_{d,cmpd} - \log K_{d,PTMA}$) were used (Regression, Excel) to determine the empirical modifiers of the parameters of NAi, ΔVx ($= Vx_i - Vx_{PTMA}$), and fraction of the charge sites in the tetrahedral layer (f_T) as separate terms in a multivariable linear regression (Excel). This approach was unsuccessful as the Vx term was not significant (error was larger than the value) and many sorption coefficients were not predicted accurately (average absolute error 0.7 log units).

Next, we examined f_T as an exponential correction because the $\Delta \log K_d$ values to clays between methylated benzylamine displayed an exponentiation decrease as the fraction of tetrahedral substitutions increased. The experimental S^i values were regressed against $NAi^{(1-f_T)}$ and ΔVx. For kaolinite, we assigned a f_T value of 0.9 since the primary source of charges are surface hydroxyl

groups that seemed to have similar interactions with organic cations as tetrahedral charge sites (Fig 4.5). The result of the regression analysis yielded a new empirical relationship for compound scaling factors as:

$$\log(S^{i}_{clays}) = 0.57\Delta Vx - 0.36NAi^{(1-f_T)} + 0.08 \quad (4.7)$$

Recalculation of sorption coefficients for the training set of benzylamine-based compounds using Eq. 1 with log S^i from Eq. 3 gave values that were well-predicted in comparison to measurements (Fig. 8). An important aspect of Eq. 3 is that no adjustments for structural moieties were needed, which is especially pertinent for compounds with the polar substituents that previously needed these factors. PTMA as a probe was likely able to predict sorption coefficients of compounds with polar moieties since the influence of interactions between polar moieties and the surface demonstrate are smaller compared to amine order (Fig 4.4 vs Fig 4.5).

Comparisons of the predicted and experimental values for the pharmaceutical compounds showed the need to account for additional aromatic rings for the case of montmorillonite clays. The accuracy of equations 1 and 3 to predict sorption coefficients was also seen for the test set (left out of the fitting procedure) of pharmaceutical compounds (Fig 4.8). However, with in this set, there were a few sorption coefficients that were under predicted. Sorption coefficients of all of the compounds that contained more than one aromatic ring were under predicted by more than 0.3 log units to montmorillonite. The predicted sorption coefficients of desipramine and propranolol to Tx-montmorillonite were almost one log unit lower than the experimental value, and the sorption coefficients of 1-naphthylmehtylamine, triprolidine, and clomipramine to Tx-montmorillonite were predicted 0.44, 0.75, and 0.66 log units under the experimental values, respectively. The sorption coefficient of 1-naphthylmethylamine was also under predicted by 0.41 log units to Wy-

montmorillonite. The interlayer of montmorillonite seemingly is able to accommodate larger compounds compared to other clays, increasing sorption coefficients of compounds with multiple aromatic rings more so than compounds with only one aromatic ring. This increase in sorption is beyond that predicted just by the increase in McGowan molar volume alone, however the cause of this increase to only montmorillonite was not evident. Therefore, a separate equation to predict scaling factors was developed for montmorillonite. To keep compounds characteristics simple, we defined the term "Aro" which is the number of aromatic rings within the compound structure and used the average difference between the predicted and experiment sorption coefficients (0.69) as the empirical modifier. For montmorillonite S^i was then calculated:

$$\log(S^i_{MMT}) = 0.57\Delta Vx - 0.36NAi^{(1-f_T)} + 0.69(Aro - 1) + 0.08 \quad (4.8)$$

Using equation 4.8 for montmorillonite and equation 4.7 for all other clays, the overall average absolute error between the experimental and predicted sorption coefficients was 0.19 and 0.21 for the training set and the test set, respectively.

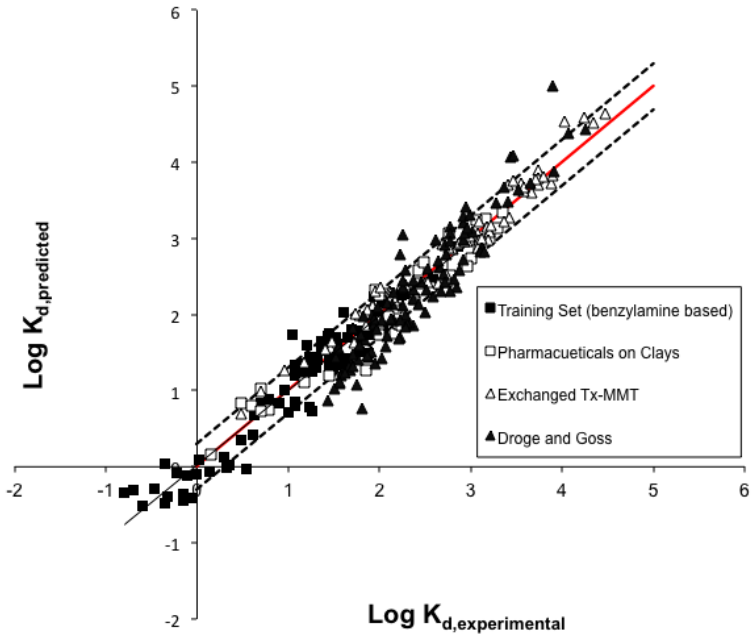

Figure 4.8. Experimental versus predicted sorption coefficients of the benzylamine based training set (black squares), the pharmaceutical compounds to various clay minerals (white squares), pharmaceuticals to exchanged montmorillonite (white triangles), and a set of 29 organic cations to kaolinite, illite and montmorillonite from Droge and Goss (black triangles). Red line is 1:1 and dashed lines represent ± 0.3 log units.

To further evaluate this method of prediction, we revisited data used to establish PTMA as a probe for six different exchanged homoionic montmorillonites (Chapter 3) and a published data set of sorption coefficients of 29 organic cations to kaolinite, montmorillonite, and illite from Droge and Goss which were the basis of the CF values.[13] For the first set, which consisted of sorption coefficients to exchanged montmorillonite, scaling factor determined by equation 4.8 predicted sorption coefficients with an average error of 0.15 log units (white triangles, Fig 4.8). Within this set, there were four compounds that contained more than one aromatic ring (desipramine, propranolol, trimethoprim, and diltiazem) all of which had sorption coefficients to the six

exchanged montmorillonites that were predicted within 0.3 log units (factor of 2) of experimental values. Sorption coefficients of the data set from Droge and Goss were also well predicted (black triangles, Fig 4.8). The accurate prediction of this set (average error = 0.29), which was the basis for the structural adjustment term, demonstrated that both equation 3 and 4 could accurately predict sorption without the use of structural adjustment terms. Therefore, incorporating the mineralogy of the clay in the determination of scaling factors increases the accuracy of prediction, further indicating that the use of PTMA as a probe compound is a robust means to predict sorption coefficients of organic cations to clay minerals.

4.4.9 Environmental Significance

The results presented in this work make it exceedingly evident that compound structural effects do not exert regular changes in sorption interactions regardless of sorbent mineralogy. $\Delta\log K_d$ values to common clays, including montmorillonite, illite, and kaolinite[7], are actually close in magnitude as the result of a combination of clay structural effects, which may have been cause of previous conclusions that quantitative ranks in compounds sorption coefficients are consistent across clay minerals. In the sense of clay mineral structure, the combination of charge focus and interlayer effects on clay minerals led to general trends in $\Delta\log K_d$ values. Accounting for the interactions between compound structural components and clay minerals was possible by the use of fraction of tetrahedral charge as a modifying exponent within the determination of scaling fractions to predict sorption coefficients of other compounds from the sorption coefficient of a probe compound. This method of prediction is a promising tool for prediction sorption coefficients to clay minerals. However, how this translates to soils, which also have charge from organic matter still requires exploration.

4.5 Supporting Information

4.5.1 Column Solid Loadings

Columns (30-mm length, 2.1-mm inner diameter, Restek #25118) were manually packed with a mixture of silicon carbide (SiC) and sorbent material for the 'sorbent-SiC' columns and with SiC for the 'SiC-only' columns. SiC-to-sorbent ratios (Table 4.S1) were chosen so that the center of mass of the breakthrough curves for the test compounds was at least 1.5 times greater than for a non-retained tracer ($NO3^-$) while minimizing peak spreading associated with extended compound retention times. An additional column with decreased solid loadings (denoted by parenthesis, Table 4.S1) were required for hectorite, Tx-montmorillonite, and nontrinite since sorption coefficients of pharmaceuticals were much higher and resulted in non-detectable peaks.

Table 4.S1. Experimental conditions used in the test columns. Values in parentheses indicate columns at lower solid loadings.

Sorbent	Hectorite	Tx-montmorillonite	Wy-montmorillonite	Vermiculite	Nontrinite	Illite	Chlorite	Kaolinite
Void Space (μL)	45 (45)	48 (45)	48	45	47 (48)	48	46	37
Sorbent Mass (mg)	1.5 (0.25)	0.71 (0.25)	0.80	0.5	0.9 (0.2)	2.9	8.2	27
Sorbent-to-water ratio (g/L)	35 (5.8)	15 (5.8)	18	13	19 (4.0)	61	177	712

4.5.2 Compound Structures

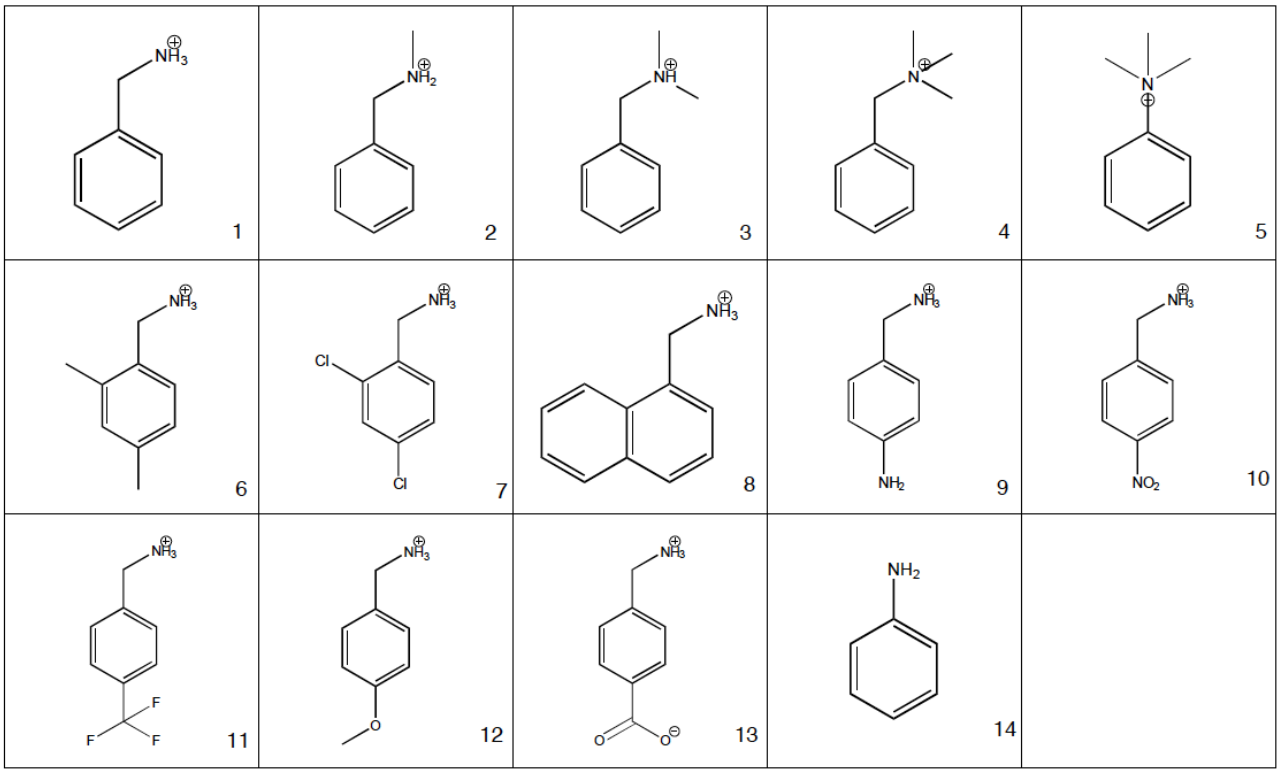

Figure 4.S1. Compounds structures of benzylamine based compounds: (1) benzylamine, (2) N-benzylmethylamine, (3) N,N-dimethylbenzylamine, (4) benzyltrimethylammonium (5) phenyltrimethylammonium, (6) 2,4-dimethylbenzylamine, (7) 2,4-dichlorobenzylamine, (8) naphthylmethylamine, (9) 4-aminobenzylamine, (10) 4-nitrobenzylamine, (11) 4-trifluoromethylbenzylamine, (12) 4-methoxybenzylamine, (13) 4-aminomethylbenzoic acid, (14) aniline.

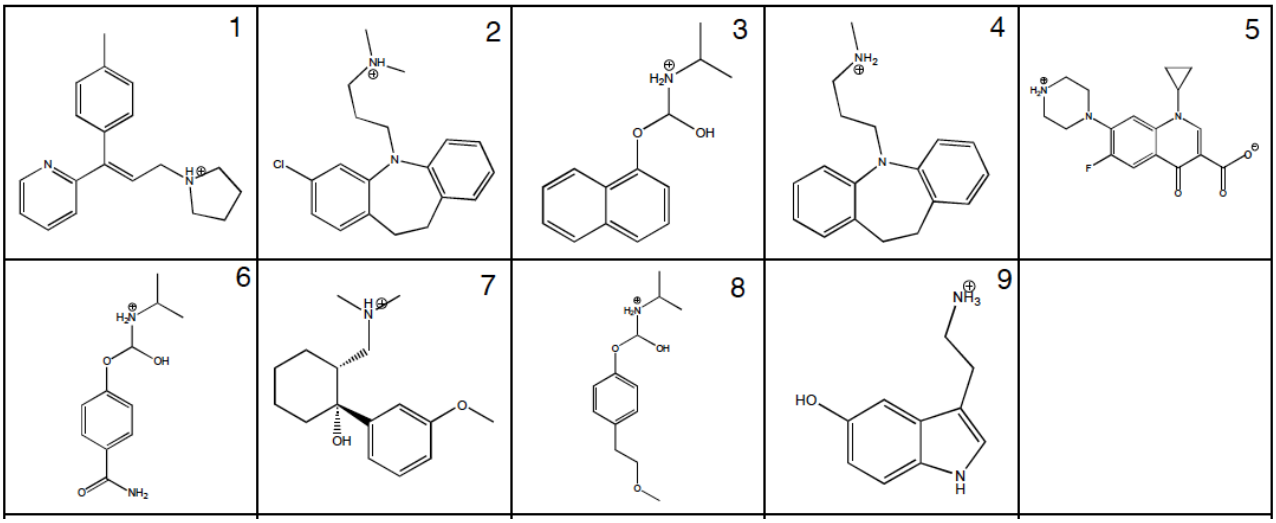

Figure 4.S2. Pharmaceutical compounds structures: (1) triprolidine, (2) clomipramine, (3) propranolol, (4) desipramine, (5) tramadol, (6) atenolol, (7) metoprolol, (8) ciprofloxacin, (9) serotonin.

4.5.3 Experimental Sorption Coefficients

Table 4.S2. Sorption coefficients (L/kg) of benzylamine based compounds for eight clay minerals

Compound	**K_d (L/kg) Hectorite**	**K_d (L/kg) Tx-montmorillonite**	**K_d (L/kg) Wy-montmorillonite**	**K_d (L/kg) Vermiculite**	**K_d (L/kg) Nontrinite**	**K_d (L/kg) Illite**	**K_d (L/kg) Kaolinite**	**K_d (L/kg) Chlorite**
Benzylamine	10 ± 1	15 ± 2	16 ± 2	12 ± 1	25 ± 2.5	4.2 ± 0.6	0.25 ± 0.07	0.77 ± 0.1
2,4-Dichlorobenzylamine	34 ± 2	31 ± 3	28 ± 4	15 ± 1	27 ± 3	10 ± 1	0.44 ± 0.07	1 ± 0.2
2,4-Dimethylbenzylamine	28 ± 4	30 ± 2	28 ± 4	14 ± 1	11 ± 1	5 ± 1	0.16 ± 0.06	0.45 ± 0.1
Naphthylmethylamine	19 ± 5	43 ± 3	46 ± 2	21 ± 1	61 ± 3	6 ± 1	0.34 ± 0.06	1.06 ± 0.2
n-benzylmethylamine	41 ± 6	23 ± 4	24 ± 2	12 ± 2	23 ± 6	3 ± 0.5	0.2 ± 0.04	1.25 ± 0.3
n,n-dimethylbenzylamine	382 ± 2	108 ± 9	83 ± 9	60 ± 5	78 ± 6	9 ± 0.5	0.6 ± 0.1	4.06 ± 0.4
Benzyltrimethylammonium	733 ± 57	191 ± 10	175 ± 9	100 ± 15	110 ± 2	20 ± 2	3.01 ± 0.37	12 ± 1.5
Phenyltrimethylammonium	550 ± 57	127 ± 8	125 ± 14	62 ± 3	102 ± 3	19 ± 2	1.55 ± 0.37	5 ± 0.6
4-aminobenzylamine	31 ± 2	45 ± 9	36 ± 3	18 ± 3	23 ± 2	18 ± 2	0.71 ± 0.1	1.35 ± 0.18
4-nitrobenzylamine	34 ± 3	34 ± 3	45 ± 4	19 ± 3	25 ± 3	17 ± 1.5	0.9 ± 0	3.49 ± 0.6
4-methoxybenzylamine	33 ± 3	37 ± 5	29 ± 4	20 ± 2	31 ± 3	12 ± 1	0.48 ± 0.1	2.1 ± 0.3
4-(triflouromethyl)benzylamine	66 ± 10	38 ± 5	44 ± 5	15 ± 3	27 ± 3	8 ± 1	0.71 ± 0.2	2.26 ± 0.4
4-Aminomethylbenzoic acid	1 ± 0.2	2 ± 0.4	3 ± 0.3	4 ± 1	10 ± 3	10 ± 1	0.4 ± 0.02	2.08 ± 0.1
Aniline	0.5 ± 0.1	3 ± 0.5	3 ± 0.5	5 ± 2	12 ± 1	6 ± 1	0.04 ± 0.01	0.1 ± 0.02
2-methoxy-5-nitroaniline	16 ± 1	9 ± 2	7 ± 1	10 ± 1	12 ± 2	6 ± 1	0.014 ± 0.01	0.45 ± 0.1

Table 4.S3. Sorption coefficients (L/kg) of benzylamine based compounds for five clay minerals

Compound	**K_d (L/kg) Hectorite**	**K_d (L/kg) Tx-montmorillonite**	**K_d (L/kg) Nontrinite**	**K_d (L/kg) Illite**	**K_d (L/kg) Chlorite**
Atenolol	493 ± 39	135 ± 15	117 ± 13	146 ± 9	6 ± 1
Desipramine	1004 ± 13	1629 ± 104	363 ± 6	264 ± 27	3 ± 0.4
Metoprolol	310 ± 53	244 ± 19	36 ± 8	100 ± 17	4 ± 0.6
Propranolol	905 ± 42	1247 ± 108	99 ± 20	207 ± 25	5 ± 1
Tramadol	577 ± 24	530 ± 47	208 ± 21	99 ± 11	5 ± 0.9
Ciprofloxacin	605 ± 44	821 ± 77	888 ± 88	540 ± 55	15 ± 2
Clomipramine	1166 ± 77	900 ± 45	598 ± 33	150 ± 17	28 ± 1
Serotonin	161 ± 28	30 ± 2	173 ± 13	70 ± 18	14 ± 1.5
Triprolidine	1953 ± 60	581 ± 44	279 ± 13	123 ± 31	15 ± 1

4.5.4 Compound Parameters and Predicted Sorption Coefficients

Table 4.S4. Parameters, experimental and predicted sorption coefficients (L/kg) of benzylamine based compounds used to derive equation 4.7

Compound	Clay	LogKd, expt	$LogK_d$, PTMA	Experimental Si	f(T)	Delta NAi	DeltVx	Log K_d Predicted
Benzylamine	Tx-montmorillonite	1.18	2.10	-0.93	0.33	3.00	-0.28	1.28
2,4-Dichlorobenzylamine	Tx-montmorillonite	1.49	2.10	-0.61	0.33	3.00	-0.23	1.31
2,4-Dimethylbenzylamine	Tx-montmorillonite	1.23	2.10	-0.87	0.33	3.00	0.00	1.44
Naphthylmethylamine	Tx-montmorillonite	1.93	2.10	-0.17	0.33	3.00	0.09	2.24
n-Benzylmethylamine	Tx-montmorillonite	1.36	2.10	-0.74	0.33	2.00	-0.14	1.54
n,n-dimethylbenzylamine	Tx-montmorillonite	2.03	2.10	-0.07	0.33	1.00	0.00	1.83
Benzyltrimethylammonium	Tx-montmorillonite	2.28	2.10	0.18	0.33	0.00	0.14	2.26
4-aminobenzylamine	Tx-montmorillonite	1.65	2.10	-0.45	0.33	3.00	-0.18	1.34
4-nitrobenzylamine	Tx-montmorillonite	1.53	2.10	-0.57	0.33	3.00	-0.11	1.38
4-methoxybenzylamine	Tx-montmorillonite	1.57	2.10	-0.54	0.33	3.00	-0.08	1.39
4-(trifluoromethyl)benzylamine	Tx-montmorillonite	1.58	2.10	-0.52	0.33	3.00	-0.03	1.43
Benzylamine	Illite	0.62	1.28	-0.66	0.66	3.00	-0.28	0.68
2,4-Dichlorobenzylamine	Illite	1.00	1.28	-0.28	0.66	3.00	-0.23	0.71
2,4-Dimethylbenzylamine	Illite	0.70	1.28	-0.58	0.66	3.00	0.00	0.84
Naphthylmethylamine	Illite	0.78	1.28	-0.50	0.66	3.00	0.09	0.89
n-Benzylmethylamine	Illite	0.48	1.28	-0.80	0.66	2.00	-0.14	0.83
n,n-dimethylbenzylamine	Illite	0.95	1.28	-0.33	0.66	1.00	0.00	1.00
Benzyltrimethylammonium	Illite	1.30	1.28	0.02	0.66	0.00	0.14	1.44

4-aminobenzylamine	Illite	1.26	1.28	-0.02	0.66	3.00	-0.18	0.74
4-nitrobenzylamine	Illite	1.23	1.28	-0.05	0.66	3.00	-0.11	0.78
4-methoxybenzylamine	Illite	1.08	1.28	-0.20	0.66	3.00	-0.08	0.80
4-(trifluoromethyl)benzylamine	Illite	0.90	1.28	-0.38	0.66	3.00	-0.03	0.83
Benzylamine	Chlorite	-0.11	0.70	-0.81	0.33	3.00	-0.28	-0.12
2,4-Dichlorobenzylamine	Chlorite	0.00	0.70	-0.70	0.33	3.00	-0.23	-0.10
2,4-Dimethylbenzylamine	Chlorite	-0.35	0.70	-1.05	0.33	3.00	0.00	0.04
Naphthylmethylamine	Chlorite	0.03	0.70	-0.67	0.33	3.00	0.09	0.09
n-Benzylmethylamine	Chlorite	0.29	0.70	-0.40	0.33	2.00	-0.14	0.13
n,n-dimethylbenzylamine	Chlorite	0.61	0.70	-0.09	0.33	1.00	0.00	0.42
Benzyltrimethylammonium	Chlorite	1.08	0.70	0.38	0.33	0.00	0.14	0.86
4-aminobenzylamine	Chlorite	0.13	0.70	-0.57	0.33	3.00	-0.18	-0.07
4-nitrobenzylamine	Chlorite	0.54	0.70	-0.16	0.33	3.00	-0.11	-0.02
4-methoxybenzylamine	Chlorite	0.32	0.70	-0.38	0.33	3.00	-0.08	-0.01
4-(trifluoromethyl)benzylamine	Chlorite	0.35	0.70	-0.34	0.33	3.00	-0.03	0.02
Benzylamine	Hectorite	1.20	2.74	-1.54	0.00	3.00	-0.28	1.59
2,4-Dichlorobenzylamine	Hectorite	1.53	2.74	-1.21	0.00	3.00	-0.23	1.62
2,4-Dimethylbenzylamine	Hectorite	1.45	2.74	-1.29	0.00	3.00	0.00	1.75
Naphthylmethylamine	Hectorite	1.70	2.74	-1.04	0.00	3.00	0.09	1.80
n-Benzylmethylamine	Hectorite	1.61	2.74	-1.13	0.00	2.00	-0.14	2.03
n,n-dimethylbenzylamine	Hectorite	2.58	2.74	-0.16	0.00	1.00	0.00	2.46
Benzyltrimethylammonium	Hectorite	2.87	2.74	0.12	0.00	0.00	0.14	2.90
4-aminobenzylamine	Hectorite	1.49	2.74	-1.25	0.00	3.00	-0.18	1.65
4-nitrobenzylamine	Hectorite	1.64	2.74	-1.10	0.00	3.00	-0.11	1.69
4-methoxybenzylamine	Hectorite	1.52	2.74	-1.22	0.00	3.00	-0.08	1.71
4-(trifluoromethyl)benzylamine	Hectorite	1.82	2.74	-0.92	0.00	3.00	-0.03	1.74
Benzylamine	Nontronite	1.40	2.01	-0.61	0.99	3.00	-0.28	1.57

2,4-Dichlorobenzylamine	Nontronite	1.43	2.01	-0.58	0.99	3.00	-0.23	1.60
2,4-Dimethylbenzylamine	Nontronite	1.04	2.01	-0.97	0.99	3.00	0.00	1.73
Naphthylmethylamine	Nontronite	1.79	2.01	-0.22	0.99	3.00	0.09	1.78
n-Benzylmethylamine	Nontronite	1.36	2.01	-0.65	0.99	2.00	-0.14	1.65
n,n-dimethylbenzylamine	Nontronite	1.89	2.01	-0.12	0.99	1.00	0.00	1.73
Benzyltrimethylammonium	Nontronite	2.04	2.01	0.03	0.99	0.00	0.14	2.17
4-aminobenzylamine	Nontronite	1.36	2.01	-0.65	0.99	3.00	-0.18	1.63
4-nitrobenzylamine	Nontronite	1.81	2.01	-0.20	0.99	3.00	-0.11	1.67
4-methoxybenzylamine	Nontronite	1.49	2.01	-0.52	0.99	3.00	-0.08	1.68
4-(trifluoromethyl)benzylamine	Nontronite	1.43	2.01	-0.58	0.99	3.00	-0.03	1.71
Benzylamine	Vermiculite	1.08	1.79	-0.71	0.66	3.00	-0.28	1.19
2,4-Dichlorobenzylamine	Vermiculite	1.18	1.79	-0.62	0.66	3.00	-0.23	1.22
2,4-Dimethylbenzylamine	Vermiculite	1.15	1.79	-0.65	0.66	3.00	0.00	1.36
Naphthylmethylamine	Vermiculite	1.32	1.79	-0.47	0.66	3.00	0.09	1.41
n-Benzylmethylamine	Vermiculite	1.08	1.79	-0.71	0.66	2.00	-0.14	1.34
n,n-dimethylbenzylamine	Vermiculite	1.78	1.79	-0.01	0.66	1.00	0.00	1.52
Benzyltrimethylammonium	Vermiculite	2.00	1.79	0.21	0.66	0.00	0.14	1.95
4-aminobenzylamine	Vermiculite	1.26	1.79	-0.54	0.66	3.00	-0.18	1.25
4-nitrobenzylamine	Vermiculite	1.28	1.79	-0.51	0.66	3.00	-0.11	1.29
4-methoxybenzylamine	Vermiculite	1.30	1.79	-0.49	0.66	3.00	-0.08	1.31
4-(trifluoromethyl)benzylamine	Vermiculite	1.18	1.79	-0.62	0.66	3.00	-0.03	1.34
Benzylamine	Wy-montmorillonite	1.20	2.10	-0.89	0.33	3.00	-0.28	1.27
2,4-Dichlorobenzylamine	Wy-montmorillonite	1.45	2.10	-0.65	0.33	3.00	-0.23	1.30
2,4-Dimethylbenzylamine	Wy-montmorillonite	1.45	2.10	-0.65	0.33	3.00	0.00	1.43
Naphthylmethylamine	Wy-montmorillonite	1.88	2.10	-0.21	0.33	3.00	0.09	1.48
n-Benzylmethylamine	Wy-montmorillonite	1.38	2.10	-0.72	0.33	2.00	-0.14	1.53
n,n-dimethylbenzylamine	Wy-montmorillonite	1.92	2.10	-0.18	0.33	1.00	0.00	1.82

Benzyltrimethylammonium	Wy-montmorillonite	2.24	2.10	0.15	0.33	0.00	0.14	2.26
4-aminobenzylamine	Wy-montmorillonite	1.56	2.10	-0.54	0.33	3.00	-0.18	1.33
4-nitrobenzylamine	Wy-montmorillonite	1.65	2.10	-0.44	0.33	3.00	-0.11	1.37
4-methoxybenzylamine	Wy-montmorillonite	1.46	2.10	-0.63	0.33	3.00	1.39	
4-(trifluoromethyl)benzylamine	Wy-montmorillonite	1.64	2.10	-0.45	0.33	3.00	-0.03	1.42
Benzylamine	Kaolinite	-0.60	0.19	-0.79	0.50	3.00	-0.28	-0.51
2,4-Dichlorobenzylamine	Kaolinite	-0.36	0.19	-0.55	0.50	3.00	-0.23	-0.48
2,4-Dimethylbenzylamine	Kaolinite	-0.80	0.19	-0.99	0.50	3.00	0.00	-0.35
Naphthylmethylamine	Kaolinite	-0.47	0.19	-0.66	0.50	3.00	0.09	-0.30
n-Benzylmethylamine	Kaolinite	-0.70	0.19	-0.89	0.50	2.00	-0.14	-0.31
n,n-dimethylbenzylamine	Kaolinite	-0.22	0.19	-0.41	0.50	1.00	0.00	-0.09
Benzyltrimethylammonium	Kaolinite	0.48	0.19	0.29	0.50	0.00	0.14	0.35
4-aminobenzylamine	Kaolinite	-0.15	0.19	-0.34	0.50	3.00	-0.18	-0.45
4-nitrobenzylamine	Kaolinite	-0.05	0.19	-0.24	0.50	3.00	-0.11	-0.41
4-methoxybenzylamine	Kaolinite	-0.32	0.19	-0.51	0.50	3.00	-0.08	-0.39
4-(trifluoromethyl)benzylamine	Kaolinite	-0.15	0.19	-0.34	0.50	3.00	-0.03	-0.36

Table 4.S5. Parameters, experimental and predicted sorption coefficients (L/kg) of pharmaceutical compounds

ompound	Clay	LogKd, expt	$LogK_d$, PTMA	f(T)	DeltaNAi	DeltVx	Log K_d Predicted
Atenolol	Tx-montmorillonite	2.13	2.10	0.33	2.00	0.94	2.15
Desipramine	Tx-montmorillonite	3.21	2.10	0.33	2.00	1.09	2.99
Metoprolol	Tx-montmorillonite	2.39	2.10	0.33	2.00	1.02	2.20
Propranolol	Tx-montmorillonite	3.10	2.10	0.33	2.00	0.91	2.89
Tramadol	Tx-montmorillonite	2.72	2.10	0.33	1.00	1.06	2.43
Chlopramine	Tx-montmorillonite	3.35	2.10	0.33	1.00	1.35	3.35
Serotonin	Tx-montmorillonite	1.48	2.10	0.33	3.00	0.21	1.56
Triloprime	Tx-montmorillonite	3.16	2.10	0.33	1.00	1.19	3.26
Atenolol	Illite	2.16	1.28	0.66	2.00	0.94	1.75
Desipramine	Illite	2.42	1.28	0.66	2.00	1.09	2.58
Metoprolol	Illite	2.00	1.28	0.66	2.00	1.02	1.79
Propranolol	Illite	2.00	1.28	0.66	2.00	0.91	1.73
Tramadol	Illite	2.00	1.28	0.66	1.00	1.06	1.91
Chlopramine	Illite	2.18	1.28	0.66	1.00	1.35	2.08
Serotonin	Illite	1.85	1.28	0.66	3.00	0.21	1.27
Triloprime	Illite	2.09	1.28	0.66	1.00	1.19	1.98
Atenolol	Chlorite	0.78	0.70	0.33	2.00	0.94	0.75
Desipramine	Chlorite	0.48	0.70	0.33	2.00	1.09	0.84
Metoprolol	Chlorite	0.60	0.70	0.33	2.00	1.02	0.80
Propranolol	Chlorite	0.70	0.70	0.33	2.00	0.91	0.73

Tramadol	Chlorite	0.70	0.70	0.33	1.00	1.06	1.03
Chlopramin	Chlorite	1.45	0.70	0.33	1.00	1.35	1.20
Serotonin	Chlorite	0.15	0.70	0.33	3.00	0.21	0.16
Triloprime	Chlorite	1.18	0.70	0.33	1.00	1.19	1.10
Atenolol	Hectorite	2.69	2.74	0.00	2.00	0.94	2.65
Desipramin	Hectorite	3.00	2.74	0.00	2.00	1.09	2.73
Metoprolol	Hectorite	2.49	2.74	0.00	2.00	1.02	2.69
Propranolol	Hectorite	2.96	2.74	0.00	2.00	0.91	2.63
Tramadol	Hectorite	2.76	2.74	0.00	1.00	1.06	3.07
Chlopramin	Hectorite	3.07	2.74	0.00	1.00	1.35	3.24
Serotonin	Hectorite	2.21	2.74	0.00	3.00	0.21	1.88
Triloprime	Hectorite	3.29	2.74	0.00	1.00	1.19	3.14
Atenolol	Nontronite	2.07	2.01	1.00	2.00	0.94	2.27
Desipramin	Nontronite	2.56	2.01	1.00	2.00	1.09	2.35
Metoprolol	Nontronite	1.96	2.01	1.00	2.00	1.02	2.32
Propranolol	Nontronite	2.00	2.01	1.00	2.00	0.91	2.25
Tramadol	Nontronite	2.32	2.01	1.00	1.00	1.06	2.34
Chlopramin	Nontronite	2.78	2.01	1.00	1.00	1.35	2.51
Serotonin	Nontronite	2.24	2.01	1.00	3.00	0.21	1.86
Triloprime	Nontronite	2.45	2.01	1.00	1.00	1.19	2.41

Table 4.S6. Parameters, experimental and predicted sorption coefficients (L/kg) of pharmaceutical compounds to exchanged montmorillonite

Compound	Clay	LogKd, expt	$LogK_d$, PTMA	f(T)	DeltaNAi	DeltVx	Log K_d Predicted
Benzylamine	Al-MMT	0.48	1.45	0.33	3.00	-0.28	0.70
Serotonin	Al-MMT	0.70	1.45	0.33	3.00	0.21	0.99
Atenolol	Al-MMT	1.46	1.45	0.33	2.00	0.91	1.56
Metoprolol	Al-MMT	1.72	1.45	0.33	2.00	1.02	1.63
Tramadol	Al-MMT	1.85	1.45	0.33	1.00	1.06	1.86
Trimethoprim	Al-MMT	2.28	1.45	0.33	2.00	1.06	2.40
Propranolol	Al-MMT	2.11	1.45	0.33	2.00	0.91	2.31
Desipramine	Al-MMT	2.64	1.45	0.33	2.00	1.09	2.41
Diltiazem	Al-MMT	3.09	1.45	0.33	1.00	2.15	3.23
Benzylamine	20 mM Na	1.79	2.74	0.33	3.00	-0.28	2.00
Serotonin	20 mM Na	2.12	2.74	0.33	3.00	0.21	2.28
Atenolol	20 mM Na	2.81	2.74	0.33	2.00	0.91	2.86
Metoprolol	20 mM Na	2.87	2.74	0.33	2.00	1.02	2.92
Tramadol	20 mM Na	3.17	2.74	0.33	1.00	1.06	3.16
Trimethoprim	20 mM Na	3.56	2.74	0.33	2.00	1.06	3.70
Propranolol	20 mM Na	3.66	2.74	0.33	2.00	0.91	3.61
Desipramine	20 mM Na	3.74	2.74	0.33	2.00	1.09	3.71

Diltiazem	20 mM Na	4.35	2.74	0.33	1.00	2.15	4.53
Benzylamine	Ca-MMT	1.18	2.12	0.33	3.00	-0.28	1.37
Serotonin	Ca-MMT	1.48	2.12	0.33	3.00	0.21	1.66
Atenolol	Ca-MMT	2.13	2.12	0.33	2.00	0.91	2.23
Metoprolol	Ca-MMT	2.39	2.12	0.33	2.00	1.02	2.30
Tramadol	Ca-MMT	2.72	2.12	0.33	1.00	1.06	2.53
Trimethoprim	Ca-MMT	3.07	2.12	0.33	2.00	1.06	3.07
Propranolol	Ca-MMT	3.10	2.12	0.33	2.00	0.91	2.98
Desipramine	Ca-MMT	3.21	2.12	0.33	2.00	1.09	3.08
Diltiazem	Ca-MMT	3.74	2.12	0.33	1.00	2.15	3.90
Benzylamine	K-MMT	1.73	2.76	0.33	3.00	-0.28	2.02
Serotonin	K-MMT	1.95	2.76	0.33	3.00	0.21	2.30
Atenolol	K-MMT	2.75	2.76	0.33	2.00	0.91	2.88
Metoprolol	K-MMT	2.88	2.76	0.33	2.00	1.02	2.94
Tramadol	K-MMT	3.21	2.76	0.33	1.00	1.06	3.17
Trimethoprim	K-MMT	3.40	2.76	0.33	2.00	1.06	3.71
Propranolol	K-MMT	3.58	2.76	0.33	2.00	0.91	3.63
Desipramine	K-MMT	3.55	2.76	0.33	2.00	1.09	3.73
Diltiazem	K-MMT	4.03	2.76	0.33	1.00	2.15	4.54
Benzylamine	Mg-MMT	0.95	2.01	0.33	3.00	-0.28	1.27
Serotonin	Mg-MMT	1.40	2.01	0.33	3.00	0.21	1.55
Atenolol	Mg-MMT	1.92	2.01	0.33	2.00	0.91	2.13
Metoprolol	Mg-MMT	2.16	2.01	0.33	2.00	1.02	2.19
Tramadol	Mg-MMT	2.53	2.01	0.33	1.00	1.06	2.42
Trimethoprim	Mg-MMT	2.96	2.01	0.33	2.00	1.06	2.96
Propranolol	Mg-MMT	3.07	2.01	0.33	2.00	0.91	2.88
Desipramine	Mg-MMT	3.19	2.01	0.33	2.00	1.09	2.98

Diltiazem	Mg-MMT	3.74	2.01	0.33	1.00	2.15	3.79
Benzylamine	Na-MMT	1.92	2.86	0.33	3.00	-0.28	2.11
Serotonin	Na-MMT	2.23	2.86	0.33	3.00	0.21	2.40
Atenolol	Na-MMT	2.93	2.86	0.33	2.00	0.91	2.97
Metoprolol	Na-MMT	2.99	2.86	0.33	2.00	1.02	3.03
Tramadol	Na-MMT	3.42	2.86	0.33	1.00	1.06	3.27
Trimethoprim	Na-MMT	3.80	2.86	0.33	2.00	1.06	3.81
Propranolol	Na-MMT	3.88	2.86	0.33	2.00	0.91	3.72
Desipramine	Na-MMT	3.89	2.86	0.33	2.00	1.09	3.82
Diltiazem	Na-MMT	4.47	2.86	0.33	1.00	2.15	4.64
Benzylamine	NH4-MMT	1.86	2.81	0.33	3.00	-0.28	2.07
Serotonin	NH4-MMT	2.00	2.81	0.33	3.00	0.21	2.35
Atenolol	NH4-MMT	2.68	2.81	0.33	2.00	0.91	2.93
Metoprolol	NH4-MMT	3.12	2.81	0.33	2.00	1.02	2.99
Tramadol	NH4-MMT	3.37	2.81	0.33	1.00	1.06	3.23
Trimethoprim	NH4-MMT	3.46	2.81	0.33	2.00	1.06	3.77
Propranolol	NH4-MMT	3.58	2.81	0.33	2.00	0.91	3.68
Desipramine	NH4-MMT	3.70	2.81	0.33	2.00	1.09	3.78
Diltiazem	NH4-MMT	4.24	2.81	0.33	1.00	2.15	4.59

Table 4.S5. Parameters, experimental and predicted sorption coefficients (L/kg) from Droge and Goss

Compound	Clay	LogKd, expt	$LogK_d$, PTMA	f(T)	Delta NAi	DeltVx	Log K_d Predicted
serotonin	*Ca-MMT*	*1.52*	*3.35*	*0.33*	*3.00*	*2.09*	*1.44*
tryptamine	*Ca-MMT*	*1.81*	*3.35*	*0.33*	*3.00*	*2.09*	*0.76*
naphylmethylamine	*Ca-MMT*	*1.93*	*3.35*	*0.33*	*3.00*	*2.09*	*1.99*
Prilocaine	*Ca-MMT*	*1.84*	*3.35*	*0.33*	*2.00*	*1.59*	*1.66*
metoprolol	*Ca-MMT*	*2.88*	*3.35*	*0.33*	*2.00*	*1.59*	*2.58*
propranolol	*Ca-MMT*	*2.66*	*3.35*	*0.33*	*2.00*	*1.59*	*2.61*
r-atenolol	*Ca-MMT*	*2.46*	*3.35*	*0.33*	*2.00*	*1.59*	*2.43*
alprenolol	*Ca-MMT*	*2.37*	*3.35*	*0.33*	*2.00*	*1.59*	*2.33*
n-benzylhexylamine	*Ca-MMT*	*3.12*	*3.35*	*0.33*	*2.00*	*1.59*	*2.87*
methamphetamine	*Ca-MMT*	*2.84*	*3.35*	*0.33*	*2.00*	*1.59*	*2.35*
ropivacaine	*Ca-MMT*	*2.92*	*3.35*	*0.33*	*1.00*	*1.00*	*3.21*
bupivacine	*Ca-MMT*	*2.77*	*3.35*	*0.33*	*1.00*	*1.00*	*3.15*
lidocaine	*Ca-MMT*	*1.98*	*3.35*	*0.33*	*1.00*	*1.00*	*2.09*
procaine	*Ca-MMT*	*2.92*	*3.35*	*0.33*	*1.00*	*1.00*	*2.99*
codiene	*Ca-MMT*	*2.72*	*3.35*	*0.33*	*1.00*	*1.00*	*2.91*
nicotine	*Ca-MMT*	*3.11*	*3.35*	*0.33*	*1.00*	*1.00*	*2.83*
3-dimethylaminopropiophenone	*Ca-MMT*	*2.91*	*3.35*	*0.33*	*1.00*	*1.00*	*2.73*
benzyltriethylammonium	*Ca-MMT*	*4.07*	*3.35*	*0.33*	*0.00*	*0.00*	*4.38*
benzyltrimethylammonium	*Ca-MMT*	*3.65*	*3.35*	*0.33*	*0.00*	*0.00*	*3.72*
benzyl(2-hydroxyethyl)dimethylammonium	*Ca-MMT*	*4.25*	*3.35*	*0.33*	*0.00*	*0.00*	*4.43*
benzylamine	*Na-Illite*	*1.75*	*2.64*	*0.66*	*3.00*	*1.45*	*1.07*
4-methylbenzylamine	*Na-Illite*	*1.95*	*2.64*	*0.66*	*3.00*	*1.45*	*1.35*
4-butylbenzylamine	*Na-Illite*	*2.59*	*2.64*	*0.66*	*3.00*	*1.45*	*2.23*

4-octylbenzylamine	*Na-Illite*	*3.91*	*2.64*	*0.66*	*3.00*	*1.45*	*3.88*
d-amphetamine	*Na-Illite*	*2.22*	*2.64*	*0.66*	*3.00*	*1.45*	*1.70*
phenylethylamine	*Na-Illite*	*2.02*	*2.64*	*0.66*	*3.00*	*1.45*	*1.42*
3-phenylpropylamine	*Na-Illite*	*2.37*	*2.64*	*0.66*	*3.00*	*1.45*	*1.85*
4-phenyl-1-butamine	*Na-Illite*	*2.32*	*2.64*	*0.66*	*3.00*	*1.45*	*1.88*
serotonin	*Na-Illite*	*1.88*	*2.64*	*0.66*	*3.00*	*1.45*	*1.45*
tryptamine	*Na-Illite*	*2.50*	*2.64*	*0.66*	*3.00*	*1.45*	*2.04*
naphylmethylamine	*Na-Illite*	*2.77*	*2.64*	*0.66*	*3.00*	*1.45*	*2.31*
Prilocaine	*Na-Illite*	*1.79*	*2.64*	*0.66*	*2.00*	*1.27*	*1.73*
propranolol	*Na-Illite*	*2.37*	*2.64*	*0.66*	*2.00*	*1.27*	*2.44*
r-atenolol	*Na-Illite*	*2.26*	*2.64*	*0.66*	*2.00*	*1.27*	*2.35*
alprenolol	*Na-Illite*	*2.53*	*2.64*	*0.66*	*2.00*	*1.27*	*2.61*
n-benzylethanolamine	*Na-Illite*	*2.30*	*2.64*	*0.66*	*2.00*	*1.27*	*1.88*
n-benzyl-n-buytylamine	*Na-Illite*	*2.29*	*2.64*	*0.66*	*2.00*	*1.27*	*2.00*
n-benzyl-n-ethylamine	*Na-Illite*	*2.29*	*2.64*	*0.66*	*2.00*	*1.27*	*1.84*
n-benzyl-n-methylamine	*Na-Illite*	*2.21*	*2.64*	*0.66*	*2.00*	*1.27*	*1.68*
fluoxetine	*Na-Illite*	*3.52*	*2.64*	*0.66*	*2.00*	*1.27*	*3.64*
methamphetamine	*Na-Illite*	*2.67*	*2.64*	*0.66*	*2.00*	*1.27*	*2.30*
n-benzyl-beta-alanine ethyl ester	*Na-Illite*	*2.37*	*2.64*	*0.66*	*2.00*	*1.27*	*2.21*
ropivacaine	*Na-Illite*	*2.78*	*2.64*	*0.66*	*1.00*	*1.00*	*3.07*
bupivacine	*Na-Illite*	*2.92*	*2.64*	*0.66*	*1.00*	*1.00*	*3.30*
lidocaine	*Na-Illite*	*2.25*	*2.64*	*0.66*	*1.00*	*1.00*	*2.36*
procaine	*Na-Illite*	*2.64*	*2.64*	*0.66*	*1.00*	*1.00*	*2.71*
n,n-dimethylbenzylamine	*Na-Illite*	*2.81*	*2.64*	*0.66*	*1.00*	*1.00*	*2.45*
methylephedrine	*Na-Illite*	*2.70*	*2.64*	*0.66*	*1.00*	*1.00*	*2.54*
codiene	*Na-Illite*	*2.77*	*2.64*	*0.66*	*1.00*	*1.00*	*2.96*

nicotine	*Na-Illite*	*2.71*	*2.64*	*0.66*	*1.00*	*1.00*	*2.43*
3-dimethylaminopropiophenone	*Na-Illite*	*2.51*	*2.64*	*0.66*	*1.00*	*1.00*	*2.33*
benzyltrimethylammonium	*Na-Illite*	*3.02*	*2.64*	*0.66*	*0.00*	*0.00*	*3.09*
acetylcholine	*Na-Illite*	*2.14*	*2.64*	*0.66*	*0.00*	*0.00*	*2.13*
3,4-dichlorobenzylamine	*Na-Kaolinite*	*2.06*	*2.20*	*0.90*	*3.00*	*1.12*	*1.57*
4-chlorobenzylamine	*Na-Kaolinite*	*1.68*	*2.20*	*0.90*	*3.00*	*1.12*	*1.26*
benzylamine	*Na-Kaolinite*	*1.43*	*2.20*	*0.90*	*3.00*	*1.12*	*0.87*
4-methylbenzylamine	*Na-Kaolinite*	*1.57*	*2.20*	*0.90*	*3.00*	*1.12*	*1.09*
4-butylbenzylamine	*Na-Kaolinite*	*2.16*	*2.20*	*0.90*	*3.00*	*1.12*	*1.92*
4-octylbenzylamine	*Na-Kaolinite*	*3.40*	*2.20*	*0.90*	*3.00*	*1.12*	*3.49*
d-amphetamine	*Na-Kaolinite*	*1.91*	*2.20*	*0.90*	*3.00*	*1.12*	*1.51*
phenylethylamine	*Na-Kaolinite*	*1.51*	*2.20*	*0.90*	*3.00*	*1.12*	*1.03*
3-phenylpropylamine	*Na-Kaolinite*	*1.86*	*2.20*	*0.90*	*3.00*	*1.12*	*1.46*
serotonin	*Na-Kaolinite*	*1.68*	*2.20*	*0.90*	*3.00*	*1.12*	*1.37*
tryptamine	*Na-Kaolinite*	*1.76*	*2.20*	*0.90*	*3.00*	*1.12*	*1.41*
naphylmethylamine	*Na-Kaolinite*	*1.67*	*2.20*	*0.90*	*3.00*	*1.12*	*1.32*
Prilocaine	*Na-Kaolinite*	*1.54*	*2.20*	*0.90*	*2.00*	*1.07*	*1.55*
metoprolol	*Na-Kaolinite*	*2.03*	*2.20*	*0.90*	*2.00*	*1.07*	*1.92*
propranolol	*Na-Kaolinite*	*2.93*	*2.20*	*0.90*	*2.00*	*1.07*	*3.07*
r-atenolol	*Na-Kaolinite*	*1.82*	*2.20*	*0.90*	*2.00*	*1.07*	*1.98*
alprenolol	*Na-Kaolinite*	*2.15*	*2.20*	*0.90*	*2.00*	*1.07*	*2.30*
n-benzylethanolamine	*Na-Kaolinite*	*1.59*	*2.20*	*0.90*	*2.00*	*1.07*	*1.24*
n-benzylhexylamine	*Na-Kaolinite*	*1.94*	*2.20*	*0.90*	*2.00*	*1.07*	*1.88*
n-benzyl-n-buytylamine	*Na-Kaolinite*	*1.70*	*2.20*	*0.90*	*2.00*	*1.07*	*1.48*
n-benzyl-n-ethylamine	*Na-Kaolinite*	*1.58*	*2.20*	*0.90*	*2.00*	*1.07*	*1.20*
n-benzyl-n-methylamine	*Na-Kaolinite*	*1.57*	*2.20*	*0.90*	*2.00*	*1.07*	*1.11*

3-methyl-n-methylbenzylamine	*Na-Kaolinite*	*1.62*	*2.20*	*0.90*	*2.00*	*1.07*	*1.24*
fluoxetine	*Na-Kaolinite*	*3.28*	*2.20*	*0.90*	*2.00*	*1.07*	*3.47*
methamphetamine	*Na-Kaolinite*	*2.22*	*2.20*	*0.90*	*2.00*	*1.07*	*1.92*
n-methyl-phenethylamine	*Na-Kaolinite*	*1.70*	*2.20*	*0.90*	*2.00*	*1.07*	*1.32*
n-benzylaminoecetoaldehyde diethyl acetal	*Na-Kaolinite*	*1.55*	*2.20*	*0.90*	*2.00*	*1.07*	*1.56*
ropivacaine	*Na-Kaolinite*	*2.29*	*2.20*	*0.90*	*1.00*	*1.00*	*2.58*
bupivacine	*Na-Kaolinite*	*2.61*	*2.20*	*0.90*	*1.00*	*1.00*	*2.99*
lidocaine	*Na-Kaolinite*	*1.71*	*2.20*	*0.90*	*1.00*	*1.00*	*1.82*
procaine	*Na-Kaolinite*	*2.08*	*2.20*	*0.90*	*1.00*	*1.00*	*2.15*
imipreamine	*Na-Kaolinite*	*3.37*	*2.20*	*0.90*	*1.00*	*1.00*	*3.68*
4-amino2-methylquinoine	*Na-Kaolinite*	*3.15*	*2.20*	*0.90*	*1.00*	*1.00*	*2.82*
n,n-dimethylbenzylamine	*Na-Kaolinite*	*2.08*	*2.20*	*0.90*	*1.00*	*1.00*	*1.72*
methylephedrine	*Na-Kaolinite*	*1.97*	*2.20*	*0.90*	*1.00*	*1.00*	*1.81*
verapamil	*Na-Kaolinite*	*3.90*	*2.20*	*0.90*	*1.00*	*1.00*	*5.00*
codiene	*Na-Kaolinite*	*2.25*	*2.20*	*0.90*	*1.00*	*1.00*	*2.44*
clonidine	*Na-Kaolinite*	*1.78*	*2.20*	*0.90*	*1.00*	*1.00*	*1.59*
nicotine	*Na-Kaolinite*	*2.42*	*2.20*	*0.90*	*1.00*	*1.00*	*2.14*
3-dimethylaminopropiophenone	*Na-Kaolinite*	*2.12*	*2.20*	*0.90*	*1.00*	*1.00*	*1.94*
2,2'(benzylamino)diethanol	*Na-Kaolinite*	*2.25*	*2.20*	*0.90*	*1.00*	*1.00*	*2.12*
benzyltributylammonium	*Na-Kaolinite*	*2.26*	*2.20*	*0.90*	*0.00*	*0.00*	*3.05*
benzyltripropylammonium	*Na-Kaolinite*	*2.23*	*2.20*	*0.90*	*0.00*	*0.00*	*2.78*
benzyltriethylammonium	*Na-Kaolinite*	*2.99*	*2.20*	*0.90*	*0.00*	*0.00*	*3.30*
benzyltrimethylammonium	*Na-Kaolinite*	*2.73*	*2.20*	*0.90*	*0.00*	*0.00*	*2.80*
benzyldimethylhexylammonium	*Na-Kaolinite*	*2.95*	*2.20*	*0.90*	*0.00*	*0.00*	*3.42*
benzyldimethyloctylammonium	*Na-Kaolinite*	*3.44*	*2.20*	*0.90*	*0.00*	*0.00*	*4.07*
benzyldimethyldecylammonium	*Na-Kaolinite*	*3.47*	*2.20*	*0.90*	*0.00*	*0.00*	*4.09*

benzyl(2-hydroxyethyl)dimethylammonium	*Na-Kaolinite*	*2.96*	*2.20*	*0.90*	*0.00*	*0.00*	*3.14*
acetylcholine	*Na-Kaolinite*	*1.94*	*2.20*	*0.90*	*0.00*	*0.00*	*1.93*

5.0 Concluding Remarks

The validation of column chromatography provided a means to collect the large data sets used throughout his project. Column chromatography provides a number of improvements on batch experiments for the collection of ionic organic compound sorption coefficients. It provides immediate determination of mass balance and varying flow rate can provide information on sorption kinetics. The use of SiC to dilute the sorbent of interest allows the solid to water ratio to be changed, which can improve limits of detection. In addition, SiC removes diffusion through the soil matrix as a limiting factor for flow through experiments. Column experiments capture isotherm non-linearity and provide a range of skewness values where linear range sorption occurs. Therefore, we conclude that the column technique is optimal for the collection of sorption coefficients of ionic compounds. The improvements in labor intensity and means to identify linear range coefficients through skewness value comparisons allowed for the collection of the vast number of sorption coefficients used to identity PTMA as a probe compound and the comparisons on of sorption coefficients for different clay minerals.

The use of PTMA as a cationic probe compound is a promising option to account for the abundance and affinity of exchangeable ions. The observation that on average the sorption of organic cations is influenced in the same manner by different exchangeable ions indicates PTMA can be used to aid the prediction of sorption coefficients. Furthermore, sorption of PTMA is better correlated with sorption of other organic cations than ECEC or the Droge and Goss model. The use of scaling factors determined from the Droge and Goss model was able to reproduce sorption coefficients of two complex

cationic pharmaceuticals to soils. The limitations in predicting the sorption of the primary amine, benzylamine, is likely caused by the difference between the amines orders. However, most cationic pharmaceuticals and pesticides are either secondary or tertiary amines[71] making higher order amines a main focus of predictive modeling. In addition, the improvement of the predictive capabilities to account for differences in structural components to homoionic systems using computations techniques[15] will improve the development of scaling factors. Therefore, we conclude that the use of a PTMA as a probe compound is a viable option to account for vast differences in natural exchange ions and their influence on the sorption of organic cations.

The deviation in quantitative trends seen throughout this study demonstrates that sorption to clay minerals is the result of complex interactions. These interactions where exemplified by deviations in quantitative trends in sorption coefficients of complex cationic pharmaceuticals, making organic cation sorption to clay minerals a function of hydration and charge focus. Therefore, accurate transport and bioavailability modeling for complex organic cations may still require the use of experimental data, especially for soils with high content of swelling clays. However, the most common natural clay minerals are illite and kaolinite, which generally display similar ΔlogKd values when normalized to the sorption of more simple compounds. Therefore, in a broad sense, sorption coefficients prediction may still be possible with the use of a probe compound.

The overall results from this study help identify the environmental factors most prevalent in the magnitude of organic cation sorption coefficients. For a specific compound, sorption coefficients are most dependent on the background conditions.

Background conditions include pH, which determines the charge of most organic cations, and the background concentrations of competing cations. A ten-fold increase in concentration (charge normal) decreases sorption coefficients by a factor of 10.[13,29] If backgrounds conditions are constant the next dominant factor in the magnitude of sorption coefficients is the CEC of the soil. Though deviations are present throughout this study, the CEC of the soil still dominates the magnitude of sorption coefficients. Following CEC, the identity and abundance of exchange ions greatly influences the magnitude of sorption coefficients. For instance, there was a 1.5 log unit decrease in sorption coefficients to Na-montmorillonite and Al-montmorillonite (Chapter 3). If exchange ions are constant (i.e. comparing homoionic systems), whether a charge site is on organic matter or clay mineral readily influences sorption coefficients. Higher order amines haves higher affinity for charge sites on clays minerals while lower order amines have higher sorption coefficients for organic matter.[13,29] Finally, the location of the charge site on the clay, as seen in Chapter 4, influences sorption for compounds with certain structural moieties. These numerous factors make predicting sorption coefficients of organic cation for soils and soil minerals a complex and difficult endeavor.

6.0 References

1. Kolpin, D.W.; Furlong, E.T.; Meyer, M.T.; Thurman, E.M.; Zaugg, S.D.; Barber, L.B.; Buxton, H.T. Pharmaceuticals, Hormones, and Other Organic Wastewater Contaminants in U.S. Streams, 1999−2000, A National Reconnaissance. *Environ. Sci. Technol.* **2002,** *36* (6), 1202-1211.

2. Kummerer, K. The Presence of Pharmaceuticals in the Environment due to Human Use - Present Knowledge and Future Challenges. **2009,** *90* 2354.

3. Lee, L.S.; Carmosini, N.; Sassman, S.A.; Dion, H.M.; Sepulveda, M.S. Agricultural contributions of antimicrobials and hormones on soil and water quality, In *Advances in Agronomy, Vol 93*, Elsevier Academic Press Inc: San Diego, 2007; Vol.93 pp. 1-68.

4. Radjenović, Jelena: Petrović, Mira: Barceló, Damià Fate and Distribution of Pharmaceuticals in Wastewater and Sewage Sludge of the Conventional Activated Sludge (CAS) and Advanced Membrane Bioreactor (MBR) Treatment. **2009,** *43* (3), 831-841.

5. Tolls, J. Sorption of Veterinary Pharmaceuticals in Soils: A Review. *Environ. Sci. Technol.* **2001,** *35* (17), 3397-3406.

6. Schwarzenbach, R.P.; Gschwend, P.M.; Imboden, D.M. *Environmental Organic Chemistry.* John Wiley and Sons Inc: Hoboken, New Jersey, 2003.

7. Sposito, G. *The Chemistry of Soils.* Oxford University Press, USA: Oxford, 2008.

8. Bouwer, H. Simple derivation of the retardation equation and application to preferential flow and macrodispersion. *Ground Water* **1991,** *29* (1), 41-46.

9. U.S. Environmental Protection Agency Estimation Programs Interface Suite for Microsoft Windows (EPISUITE), Washington, DC, 2012; Version 4.11.

10. Droge, S. and Goss, K. Ion-Exchange Affinity of Organic Cations to Natural Organic Matter: Influence of Amine Type and Nonionic Interactions at Two Different pHs. *Environ. Sci. Technol.* **2013,** *47* 798-806.

11. Williams, M.; Ong, P.L.; William, D.B.; Kookana, R.S. Estimating the Sorption of Pharmaceuticals Based on their Pharmacological Distribution. *Environ. Toxicol. Chem.* **2009,** *28* (12), 2572-2579.

12. Droge, S. and Goss, K. Development and Evaluation of a New Sorption Model for Organic Cations in Soil: Contributions from Organic Matter and Clay Minerals. *Environ. Sci. Technol.* **2013,** *47* (24), 14233-14241.

13. Droge, S. and Goss, K. Sorption of Organic Cations to Phyllosilicate Clay Minerals: CEC-Normalization, Salt Dependency, and the Role of Electrostatic and Hydrophobic Effects. *Environ. Sci. Technol.* **2013,** *47* (24), 14224-14232.

14. Jadbabaei, N. and Zhang, H. Sorption Mechanism and Predictive Models for Removal of Cationic Organic Contaminants by Cation Exchange Resins. *Environ. Sci. Technol.* **2014,** *48* (24), 14572-14581.

15. Samaraweera, M.; Jolin, W.; Vasudevan, D.; MacKay, A.A.; Gascon, J.A. Atomistic Prediction of Sorption Free Energies of Cationic Aromatic Amines on Montmorillonite: A Linear Interaction Energy Method. *Environ. Sci. Technol. Lett.* **2014,** *1* (6), 284-289.

16. Zhang, H.; Shields, A.J.; Jadbabaei, N.; Nelson, M.; Pan, B.; Suri, R.P.S. Understanding and Modeling Removal of Anionic Organic Contaminants (AOCs) by Anion Exchange Resins. *Environ. Sci. Technol.* **2014,** *48* (13), 7494-7502.

17. MacKay, A. and Vasudevan, D. Polyfunctional Ionogenic Compound Sorption: Challenges and New Approaches To Advance Predictive Models. *Environ. Sci. Technol.* **2012,** *46* 9209-9223.

18. Endo, S. and Goss, K. Applications of Polyparameter Linear Free Energy Relationships in Environmental Chemistry. *Environ. Sci. Technol.* **2014,** *48* (21), 12477-12491.

19. OECD *Test No. 106: Adsorption -- Desorption Using a Batch Equilibrium Method.* Organization for Economic Co-operation and Development: 2000.

20. Schenzel, J.; Goss, K.; Schwarzenbach, R.P.; Bucheli, T.D.; Droge, S.T. Experimentally Determined Soil Organic Matter–Water Sorption Coefficients for Different Classes of Natural Toxins and Comparison with Estimated Numbers. *Environ. Sci. Technol.* **2012,** *46* (11), 6118-6126.

21. Vasudevan, D.; Arey, T.; Dickstein, D.; Newman, M.; Zhang, T.; Kinnear, H.; Bader, M. Nonlinearity of Cationic Aromatic Amine Sorption to Alminosilicates and Soils: Role of Intermolecular Cation-pi Interactions. *Environ. Sci. Technol.* **2013,** *47* (24), 14119-14127.

22. Bourg, I. and Sposito, G. Ion Exchange Phenomena, In *Handbook of Soil Sciences, Properties and Processes,* 2nd ed.; Huang, P.M., Li, Y. and Sumner, M.E., Eds. CRC Press: New York, 2012; .

23. McBride, M.B. *Environmental Chemistry of Soils.* Oxford University Press: New York, 1994.

24. Sposito, G.; Skipper, N.T.; Sutton, R.; Park, S.; Soper, A.K.; Greathouse, J.A. Surface geochemistry of the clay minerals. *Proceedings of the National Academy of Sciences* **1999,** *96* (7), 3358-3364.

25. Bergaya, F.; Theng, B.K.G.; Lagaly, G. *Handbook of Clay Science.* Elsevier Science: Burlington, 2011.

26. Matocha, C.J. Clay: charge properties, In *Encyclopedia of Soil Science,* 2nd ed.; CRC Press: Boca Raton, FL, 2006; Vol.1 pp. 287-290.

27. Levy, R. and Shainberg, I. Calcium-magnesium exchange in montmorillonite and vermiculite. *Clays Clay Miner.* **1972,** *20* 37-46.

28. Ras, R.H.A.; Umemura, Y.; Johnston, C.T.; Yamagishi, A.; Schoonheydt, R.A. Ultrathin hybrid films of clay minerals. *Phys. Chem. Chem. Phys.* **2007,** *9* (8), 918-932.

29. Droge, S. and Goss, K. Effect of Sodium and Calcium Cations on the Ion-Exchange Affinity of Organic Cation for Soil Organic Matter. *Environ. Sci. Technol.* **2012,** *46* (11), 5894-5901.

30. Bi, E.; Schmidt, T.C.; Haderlein, S.B. Environmental factors influencing sorption of heterocyclic aromatic compounds to soil. *Environ. Sci. Technol.* **2007,** *41* (9), 3172-3178.

31. Sim, W.; Lee, J.; Oh, J. Occurrence and fate of pharmaceuticals in wastewater treatment plants and rivers in Korea. *Environ. Poll.* **2010,** *158* (5), 1938-1947.

32. Zuccato, E.; Castiglioni, S.; Bagnati, R.; Chiabrando, C.; Grassi, P.; Fanelli, R. Illicit drugs, a novel group of environmental contaminants. *Water Res.* **2008,** *42* (4), 961-968.

33. Chiou, C.T.; Peters, L.J.; Freed, V.H. A physical concept of soil-water equilibria for nonionic organic compounds. *Science* **1979,** *206* (4420), 831-832.

34. Chiou, C.T.; Porter, P.E.; Schmedding, D.W. Partition equilibriums of nonionic organic compounds between soil organic matter and water. *Environ. Sci. Technol.* **1983,** *17* (4), 227-231.

35. Carrasquillo, A.; Bruland, G.; MacKay, A.; Vasudevan, D. Sorption of Ciprofloxacin and Oxytetracycline Zwitterions to Soils and Soil Minerals: Influence of Compound Structure. *Environ. Sci. Technol.* **2008,** *42* 7634-7642.

36. Spurlock, F.C.; Huang, K.; van Genuchten, M.T. Isotherm nonlinearity and nonequilibrium sorption effects on transport of fenuron and monuron in soil columns. *Environ. Sci. Technol.* **1995,** *29* (4), 1000-1007.

37. Weber, W.J. and Usinowics, P. *Adsorption from aqueous solution.* American Chemical Society: 1968.

38. Holmén, B.A. and Gschwend, P.M. Estimating sorption rates of hydrophobic organic compounds in iron oxide-and aluminosilicate clay-coated aquifer sands. *Environ. Sci. Technol.* **1996,** *31* (1), 105-113.

39. Roberts, P.V.; Goltz, M.N.; Mackay, D.M. A natural gradient experiment on solute transport in a sand aquifer: 3. Retardation estimates and mass balances for organic solutes. *Water Resour. Res.* **1986,** *22* (13), 2047-2058.

40. Van Genuchten, M.T.; Wierenga, P.; Klute, A. Solute dispersion coefficients and retardation factors. In *Methods of Soil Analysis: Part 1—Physical and Mineralogical Methods,* American Society of Agronomy, Inc.: Madison, WI, 1986; pp. 1025-1054.

41. Relyea, J.F. Theoretical and experimental considerations for the use of the column method for determining retardation factors. *Radioact. Waste Manage. Nucl. Fuel Cycle* **1982,** 151-166.

42. Porro, I.; Newman, M.E.; Dunnivant, F.M. Comparison of batch and column methods for determining strontium distribution coefficients for unsaturated transport in basalt. *Environ. Sci. Technol.* **2000,** *34* (9), 1679-1686.

43. Fouquet, Y.; von Stackelberg, U.; Charlou, J.L.; Donval, J.P.; Foucher, J.P.; Erzinger, J.; Herzig, P.; Mühe, R.; Wiedicke, M.; Soakai, S. Hydrothermal activity in the Lau back-arc basin: Sulfides and water chemistry. *Geology* **1991,** *19* (4), 303-306.

44. Wang, T.; Li, M.; Teng, S. Bridging the gap between batch and column experiments: A case study of Cs adsorption on granite. *J. Hazard. Mater.* **2009,** *161* (1), 409-415.

45. Bürgisser, C.S.; Cernik, M.; Borkovec, M.; Sticher, H. Determination of nonlinear adsorption isotherms from column experiments: An alternative to batch studies. *Environ. Sci. Technol.* **1993,** *27* (5), 943-948.

46. Maclntyre, W.G.; Stauffer, T.B.; Antworth, C.P. A comparison of sorption coefficients determined by batch, column, and box methods on a low organic carbon aquifer material. *Groundwater* **1991,** *29* (6), 908-913.

47. Allen, H.E.; Chen, Y.; Li, Y.; Huang, C.; Sanders, P.F. Soil partition coefficients for Cd by column desorption and comparison to batch adsorption measurements. *Environ. Sci. Technol.* **1995,** *29* (8), 1887-1891.

48. Valocchi, A.J. Validity of the local equilibrium assumption for modeling sorbing solute transport through homogeneous soils. *Water Resour. Res.* **1985,** *21* (6), 808-820.

49. Bi, E.; Schmidt, T.C.; Haderlein, S.B. Practical issues relating to soil column chromatography for sorption parameter determination. *Chemosphere* **2010,** *80* (7), 787-793.

50. Bi, E.; Zhang, L.; Schmidt, T.C.; Haderlein, S.B. Simulation of nonlinear sorption of N-heterocyclic organic contaminates in soil columns. *J. Contam. Hydrol.* **2009,** *107* (1), 58-65.

51. Fesch, C.; Simon, W.; Haderlein, S.B.; Reichert, P.; Schwarzenbach, R.P. Nonlinear sorption and nonequilibrium solute transport in aggregated porous media: Experiments, process identification and modeling. *J. Contam. Hydrol.* **1998,** *31* (3), 373-407.

52. Altfelder, S.; Streck, T.; Maraqa, M.A.; Voice, T.C. Nonequilibrium sorption of dimethylphthalate—Compatibility of batch and column techniques. *Soil Sci. Soc. Am. J.* **2001,** *65* (1), 102-111.

53. MacGillivray, H. Skewness and asymmetry: measures and orderings. *Ann. of Stat.* **1986,** 994-1011.

54. Jones, A.D.; Bruland, G.L.; Agrawal, S.G.; Vasudevan, D. Factors influencing the sorption of oxytetracycline to soils. *Environ. Toxicol. Chem.* **2005,** *24* (4), 761-770.

55. Brownawell, B.; Chen, H.; Collier, J.; Westall, J. Adsorption of Organic Cations to Natural Materials. *Environ. Sci. Technol.* **1990,** *24* (8), 1234-1241.

56. Kromidas, S. *More practical problem solving in HPLC.* John Wiley & Sons: 2008.

57. Margulies, I.; Rozen, H.; Nir, S. Model for Competitive Adsorption of Organic Cations on Clays. *Clays Clay Miner* **1988,** *36* (3), 270.

58. Helfferich, F.G. *Ion Exchange.* Courier Corporation: New York, 1962.

59. Lailach, G.; Thompson, T.; Brindley, G. Adsorption of Pyrimidines, Purines, and Nucleodies by Li-, Na-, Mg-, and Ca-montmorillonite. **1968,** *16* 285.

60. Sparks, D.L. *Environmental soil chemistry.* Academic Press: San Diego, California, 2003.

61. MacKay, A.A. and Seremet, D.E. Probe compounds to quantify cation exchange and complexation interactions of ciprofloxacin with soils. *Environ. Sci. Technol.* **2008,** *42* (22), 8270-8276.

62. Jolin, W.; Sullivan, J.; Vasudevan, D.; MacKay, A.A. Column Chromatography to Obtain Organic Cation Sorption Isotherms. *Environ. Sci. Technol.* **2016,** *50* (15), 8196-8204.

63. Boek, E. Molecular dynamics simulations of interlayer structure and mobility in hydrated Li-, Na-and K-montmorillonite clays. *Mol. Phys.* **2014,** *112* (9-10), 1472-1483.

64. Hendricks, S.B.; Nelson, R.A.; Alexander, L.T. Hydration Mechanism of the Clay Mineral Montmorillonite Saturated with Various Cations. *J. Am. Chem. Soc.* **1940,** *62* (6), 1457-1464.

65. Chung, J. and Zasoski, R.J. Ammonium-potassium and ammonium-calcium exchange equilibria in bulk and rhizosphere soil. *Soil Sci. Soc. Am. J.* **1994,** *58* (5), 1368-1375.

66. Balek, V.; Beneŝ, M.; Ŝubrt, J.; Pérez-Rodríguez, J.; Sánchez-Jiménez, P.; Pérez-Maqueda, L.A.; Pascual-Cosp, J. Thermal characterization of montmorillonite clays saturated with various cations. *J. Therm. Anal. and Calor.* **2008,** *92* (1), 191-197.

67. Xu, W.; Johnston, C.T.; Parker, P.; Agnew, S.F. Infared Study of Water Sorption on Na-, Li-, Ca-, and Mg-Exchanged (SWy-1 and SAz-1) Montmorillonite. *Clays Clay Miner.* **2000,** *48* (1), 120-131.

68. Greathouse, J.A.; Refson, K.; Sposito, G. Molecular Dynamics Simulation of Water Mobility in Magnesium-Smectite Hydrates. *J. Am. Chem. Soc.* **2000,** *122* (46), 11459-11464.

69. Kostich, M.S.; Batt, A.L.; Lazorchak, J.M. Concentrations of prioritized pharmaceuticals in effluents from 50 large wastewater treatment plants in the US and implications for risk estimation. **2014,** *184* 354-359.

70. Heberer, T. Occurrence, fate, and removal of pharmaceutical residues in the aquatic environment: a review of recent research data. *Toxicol. Lett.* **2002,** *131* (1–2), 5-17.

71. Daughton, C.G. and Ternes, T.A. Pharmaceuticals and personal care products in the environment: agents of subtle change? *Environ. Health Perspect.* **1999,** *107 Suppl 6* 907-938.

72. Karickhoff, S.W. and Bailey, G.W. Protonation of organic bases in clay-water systems. *Clays Clay Miner.* **1976,** *24* (4), 170-176.

73. Ikhsan, J.; Angove, M.J.; Wells, J.D.; Johnson, B.B. Surface complexation modeling of the sorption of 2-, 3-, and 4-aminopyridine by montmorillonite. *J. Colloid Interface Sci.* **2005,** *284* (2), 383-392.

74. Skipper, N.; Refson, K.; McConnell, J. Computer simulation of interlayer water in 2: 1 clays. *J. Chem. Phys.* **1991,** *94* (11), 7434-7445.

75. Mikhail, R.S.; Brunauer, S.; Bodor, E. Investigations of a complete pore structure analysis: I. Analysis of micropores. *J. Colloid Interface Sci.* **1968,** *26* (1), 45-53.

76. Etzel, J.E. and Keramida, V. *Treatment of metal plating wastes with an unexpanded vermiculite cation exchange column.* Google Patents: 1980.

77. Sips, R. On the structure of a catalyst surface. *J. Chem. Phys.* **1948,** *16* (5), 490-495.

78. Sawhney, B. Potassium and cesium ion selectivity in relation to clay mineral structure. *Clays Clay Miner.* **1970,** *18* (1), 47-52.

79. Nir, S.; Hirsch, D.; Navrot, J.; Banin, A. Specific Adsorption of Lithium, Sodium, Potassium, and Strontium to Montmorillonite: Observations and Predictions. *Soil Sci. Soc. Am. J.* **1986,** *50* 40-45.

80. Dixon, J.B. and Weed, S.B. *Minerals in soil environments.* Soil Science Society of America Inc.: 1989.

81. Brown, G. and Brindley, G.W. *Crystal structures of clay minerals and their X-ray identification.* Oxford Univ Press: 1980.

82. Jones, A.D.; Bruland, G.L.; Agrawal, S.G.; Vasudevan, D. Factors influencing the sorption of oxytetracycline to soils. *Environ. Toxicol. Chem.* **2005,** *24* (4), 761-770.

83. Vasudevan, D.; Bruland, G.L.; Torrance, B.S.; Upchurch, V.G.; MacKay, A.A. pH-dependent ciprofloxacin sorption to soils: Interaction mechanisms and soil factors influencing sorption. *Geoderma* **2009,** *151* (3), 68-76.